Check for updates

Received: 28 March 2022 | Revised: 13 July 2022 | Accepted: 6 August 2022

DOI: 10.1002/er.8581

REVIEW PAPER

The role of power device technology in the electric vehicle powertrain

Endika Robles | Asier Matallana | Iker Aretxabaleta | Jon Andreu | Markel Fernández | José Luis Martín

Faculty of Engineering, University of the Basque Country (UPV/EHU), Bilbao, Spain

Correspondence
Endika Robles, Faculty of Engineering, University of the Basque Country (UPV/EHU), Plaza Ingeniero Torres Quevedo 1, Bilbao 48013, Spain.
Email: endika.robles@ehu.eus

Funding information
Eusko Jaurlaritza, Grant/Award Number: IT1440-22; Ministerio de Ciencia e Innovación, Grant/Award Number: PID2020-115126RB-I00

Summary

In the automotive industry, the design and implementation of power converters and especially inverters, are at a turning point. Silicon (*Si*) IGBTs are at present the most widely used power semiconductors in most commercial vehicles. However, this trend is beginning to change with the appearance of wide-bandgap (WBG) devices, particularly silicon carbide (SiC) and gallium nitride (*GaN*). It is therefore advisable to review their main features and advantages, to update the degree of their market penetration, and to identify the most commonly used alternatives in automotive inverters. In this paper, the aim is therefore to summarize the most relevant characteristics of power inverters, reviewing and providing a global overview of the most outstanding aspects (packages, semiconductor internal structure, stack-ups, thermal considerations, etc.) of *Si*, SiC, and *GaN* power semiconductor technologies, and the degree of their use in electric vehicle powertrains. In addition, the paper also points out the trends that semiconductor technology and next-generation inverters will be likely to follow, especially when future prospects point to the use of "800 V" battery systems and increased switching frequencies. The internal structure and the characteristics of the power modules are disaggregated, highlighting their thermal and electrical characteristics. In addition, aspects relating to reliability are considered, at both the discrete device and power module level, as well as more general issues that involve the entire propulsion system, such as common-mode voltage.

KEYWORDS

automotive, electric drive, IGBT, inverter, MOSFET, power electronics, power semiconductors, wide-bandgap materials

1 | INTRODUCTION

Power semiconductors are key components of any modern system of power electronics that contribute to energy conversion and efficient energy management. Today, there is a wide range of power semiconductor devices and technologies[1] with constant improvements in both their electro-thermal characteristics and their packages.

This is an open access article under the terms of the Creative Commons Attribution-NonCommercial-NoDerivs License, which permits use and distribution in any medium, provided the original work is properly cited, the use is non-commercial and no modifications or adaptations are made.
© 2022 The Authors. *International Journal of Energy Research* published by John Wiley & Sons Ltd.

1099114x, 2022, 15, Downloaded from https://onlinelibrary.wiley.com/doi/10.1002/er.8581 by Universidad Del Pais Vasco, Wiley Online Library on [17/01/2023]. See the Terms and Conditions (https://onlinelibrary.wiley.com/terms-and-conditions) on Wiley Online Library for rules of use; OA articles are governed by the applicable Creative Commons License

INTERNATIONAL JOURNAL OF ENERGY RESEARCH

The choice of one type of semiconductor over another is conditioned by the application for which it is intended. In this sense, the main criteria for selecting a device are voltage-current ranges, switching speed, power losses, maximum operating temperature, and cost, among others.

The predominant semiconductor technology in an electric vehicle powertrain converter is the silicon (*Si*) Insulated Gate Bipolar Transistor (IGBT).[2,3] Each generation of this device has significant electro-thermal improvements, achieving considerable technological maturity, for use in automotive traction inverters* (Figure 1). As silicon technology will dominate the semiconductor market in the short term,[4] and will probably account for approximately 85% of the market by 2025 (Figure 2A), understanding the development of these devices based on silicon technology and their improvements will provide useful insights into their future developments.

There are several publications that describe the advances of the IGBT structure,[5,6] combining the improvements that various manufacturers have added to semiconductor cathode and anode technologies,[7] which produce devices with better features such as SOA,[8,9] power density,[10] oscillations,[11] reliability,[12] and temperature.[13,14] There are also alternative developments that add additional characteristics to IGBTs (Reverse Blocking (RB) and Reverse Conducting (RC)).[15,16] However, it is difficult to obtain a clear classification based on IGBT internal structures, because there are multitude of variants and developments. Nevertheless, a general classification is prepared in this literature review, based on the advances relating to cell and vertical substrate technologies.[17] This classification is also complemented by the technological developments of some reference manufacturers such as Infineon, Fuji Electric, and Mitsubishi. In this way, an overview of the IGBT families is obtained, providing designers with additional information to better understand various comparative studies between *Si* IGBTs and wide-bandgap (WBG) technologies.[18,19]

In general, discrete devices alone do not meet the stringent current rating requirements that are applicable to automotive power inverters. To do so, manufacturers have developed different power module architectures,[1,3,20] where the bare dies are parallelized. The most widely used architectures to form the inverter (commonly known as

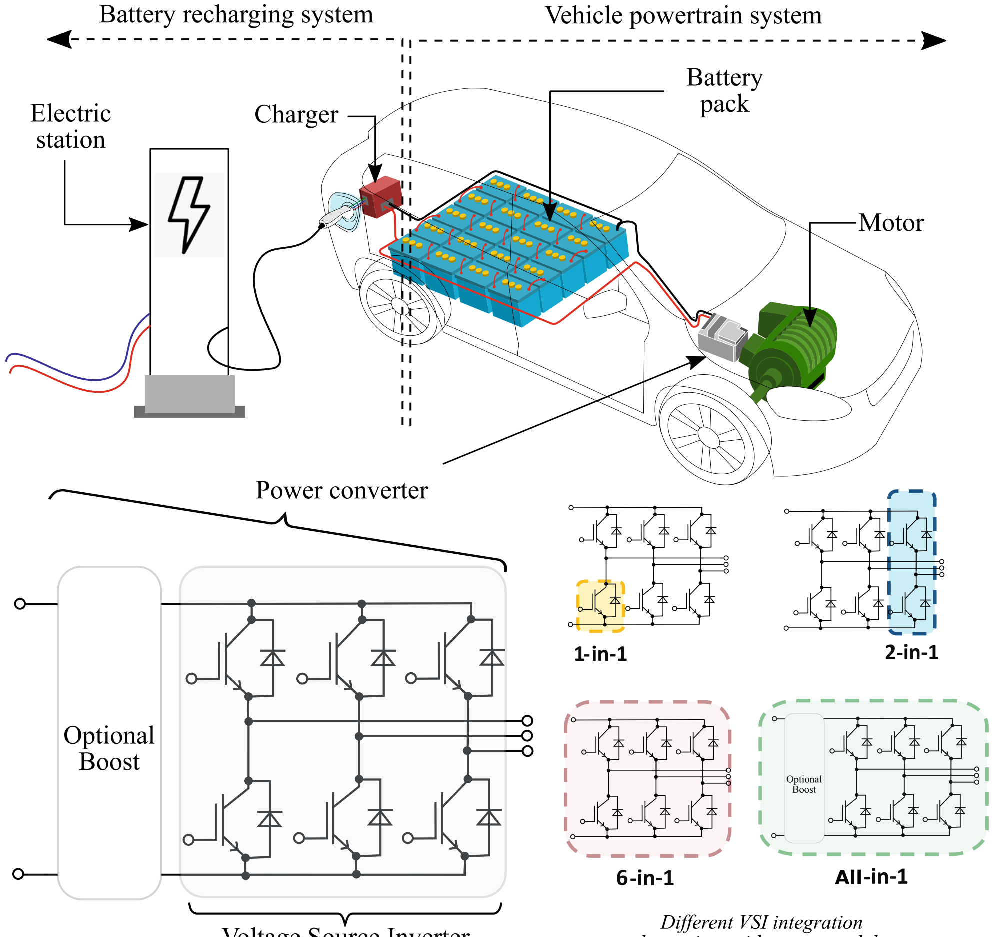

FIGURE 1 Electric vehicle powertrain, highlighting power converters, and their different forms of integration via power modules

1099114x, 2022, 15, Downloaded from https://onlinelibrary.wiley.com/doi/10.1002/er.8581 by Universidad Del Pais Vasco, Wiley Online Library on [17/01/2023]. See the Terms and Conditions (https://onlinelibrary.wiley.com/terms-and-conditions) on Wiley Online Library for rules of use; OA articles are governed by the applicable Creative Commons License

the Voltage Source Inverter [VSI]) of the electric vehicle powertrain are the 2-in-1 or half-bridge and the 6-in-1 or six-pack (Figure 1), although some manufacturers have also developed some other custom designs. For example, Fuji Electric has developed an all-in-1 module for the Honda Accord that consists of an Integrated Power Module (IPM) and includes a boost converter and two three-phase inverters. This module is packaged with conventional technology but it includes a direct-cooling heatsink with straight fins bonded to the substrate.[2] Other examples are the inverters of the Chevrolet Volt and the Tesla Model 3, the designs for which were based on 1-in-1 architectures. Some notable features of the Chevrolet Volt inverter are that wire bonds are replaced by a flip-chip soldering technique to improve the current distribution and the reliability of the die interconnection. In addition, ceramic substrates are included with a Coefficient of Thermal Expansion (CTE) equal to the CTE of silicon, so as to mitigate the thermal stress.[2] Instead, the Tesla Model 3 inverter has the notable feature of being the first inverter in a commercial vehicle to include silicon carbide devices.[3,21] Following the Tesla vehicle, other manufacturers have since included WBG technologies in the inverters of their own vehicles, specifically made of SiC materials. Likewise, other materials such as gallium nitride (*GaN*)[22] are also under consideration†.

Table 1 compares some converters, based on discrete devices or power modules, that are used in the powertrain of commercial electric vehicles‡. In general, most vehicle manufacturers, such as Nissan, BMW, Audi, Toyota, and Chevrolet use power modules with silicon IGBTs based on the aforementioned architectures (1-in-1, 2-in-1, etc.). However, there are also some commercial vehicles that include discrete IGBT devices in their inverters, as in the case of Tesla (Roadster, Model S, or Model X) models, which use International Rectifier semiconductors (AUIR family, TO-247 package) on a power Printed Circuit Board (PCB). In addition, some examples of vehicles already on the market that use SiC technology such as the BYD Han and the Lucid Air are also shown in Table 1.

Regarding the semiconductor market, Figure 2B shows the trend of the power modules between 2019-2025 where growth levels of 9.1% are expected.[26] The market for electric vehicles has experienced the greatest growth of power modules, and is projected to rise from some 1000 million units in 2019 to 3000 million units in 2025. In this context, the highest number of power-module sales corresponds to *Si* technology (US $19.13 million) while WBG technologies, especially SiC and *GaN*, are expected to represent around US$3.4 billion in 2025.[4] Both technologies are likely to lead to a

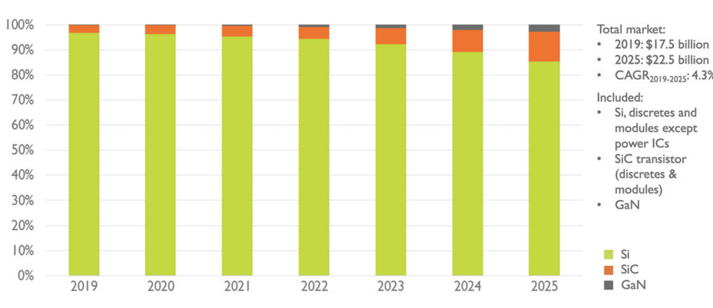

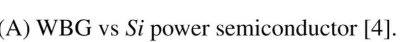
(A) WBG vs *Si* power semiconductor [4].

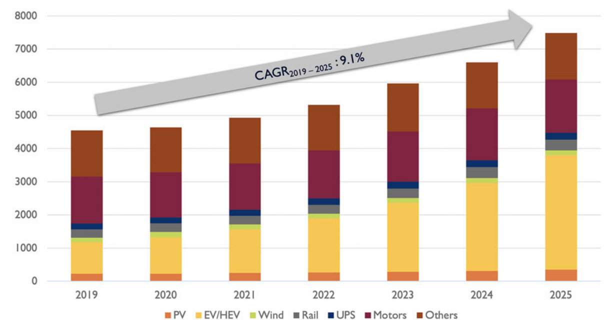

(B) Power module market size [26].

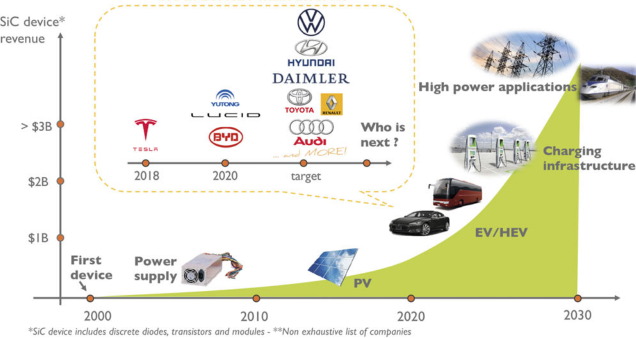

(C) Roadmap for power *SiC* devices [27].

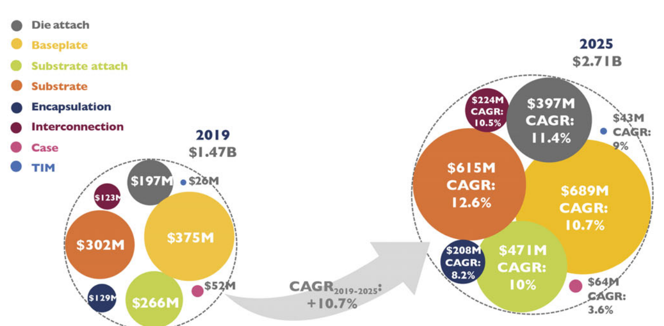

(D) Power module packaging market forecast [26].

FIGURE 2 Market trend for *Si*, wide-bandgap (WBG)semiconductors and power module packaging (*source*: *Yole Dévelopment*)

1099114x, 2022, 15, Downloaded from https://onlinelibrary.wiley.com/doi/10.1002/er.8581 by Universidad Del Pais Vasco, Wiley Online Library on [17/01/2023]. See the Terms and Conditions (https://onlinelibrary.wiley.com/terms-and-conditions) on Wiley Online Library for rules of use; OA articles are governed by the applicable Creative Commons License

TABLE 1 Features of power modules or discrete devices with the inverter fitted in some commercial vehicles (sorted by year and semiconductor technology)[2,3,28,29]

Vehicle	Brand	Model	Year	Inverter manufacturer	Used topology	Number modules/ discrete devices	Semiconductor technology[h]
	Nissan	Leaf	2012	Nissan	2-in-1	3	*Si* IGBT
	Renault	Zoe	2013	Continental/ Infineon	6-in-1	1	*Si* IGBT
	Mercedes-Benz	S550	2014	Hitachi	2-in-1	3	*Si* IGBT
	Honda	Accord[c]	2014	Fuji Electric	All-in-1	1	*Si* IGBT
	Tesla	Roadster[e]	2014	Infineon	TO-247 discrete	84	*Si* IGBT
	Tesla	Model S70 D[d]	2015	Infineon-	TO-247 discrete	36	*Si* IGBT
	Audi	e-Tron PHEV	2016	Bosch	2-in-1	3	*Si* IGBT
	BMW	i3	2016	Infineon	6-in-1	1	*Si* IGBT
	Cadillac	CT6[a]	2016	Hitachi	2-in-1	6	*Si* IGBT
	Chevrolet	Volt[a]	2016	Delphi	1-in-1	12	*Si* IGBT
	Tesla	Model X[e]	2016	Infineon	TO-247 discrete	84	*Si* IGBT
	Toyota	Prius4G[f]	2016	Denso/Toyota	2-in-1	6	*Si* IGBT
	Audi	e-Tron BEV[a]	2019	Hitachi	2-in-1	6	*Si* IGBT
	Volkswagen	ID.3	2020	Infineon	6-in-1	1	*Si* IGBT
	Tesla	Model 3	2018	ST Microlec.	1-in-1	24[i]	SiC MOSFET
	BYD	Han[b]	2020	BYD Semicond.	6-in-1	1	SiC MOSFET
	Lucid	Air	2020	[g]	[g]	[g]	SiC MOSFET

[a]Two motors and one inverter for each motor.
[b]Some models include two motors and therefore two inverters. Only the main inverter includes SiC MOSFETs.
[c]Two motors with a DC/DC and one inverter in a single custom module for each motor.

1099114x, 2022, 15, Downloaded from https://onlinelibrary.wiley.com/doi/10.1002/er.8581 by Universidad Del Pais Vasco, Wiley Online Library on [17/01/2023]. See the Terms and Conditions (https://onlinelibrary.wiley.com/terms-and-conditions) on Wiley Online Library for rules of use; OA articles are governed by the applicable Creative Commons License

[d]One inverter with six TO-247 discrete devices per switch.

[e]84 discrete T0-247, 36 for each inverter (one inverter for each motor), and 12 for the DC/DC (6 per switch).

[f]Classified as an all-in-one module, because it includes DC/DC and 2 inverters in its customized power control unit.

[g]Data not provided by the manufacturer.

[h]In most cases, manufacturers provide no reference to identify the semiconductor that they use in their inverters.

[i]Using many modules may require 1-in-1 module parallelization. The positive temperature coefficient (PTC) of SiC MOSFETs is responsible for increasing the resistance where the current is highest and the current is therefore reduced that makes parallelization easier.[30]

$CAGR_{2019–2025}$ (compound annual growth rate) in the sector of 4.3%.

According to this data, silicon will continue to dominate the market over coming years, although a WBG large-scale and sudden change will also be likely, especially in SiC technology. This trend change is shown in Figure 2C. In fact, *Yole Développement* states that the SiC power devices in electric vehicles are set to grow beyond US$1.5 Billion in 2025.[27] This growth in the demand for silicon and some WBG§ semiconductor technologies, and their use, and production, implicitly entails increased production of the various power-module technologies. Considering the above, Figure 2D shows the expected development of each layer of the power modules, leading to a $CAGR_{2019–2025}$ of 10.7%, which means going from US $1.47 billion in 2019 to US$2.71 billion in 2025.[26] However, although *GaN* inverter prototypes are also being tested,[36] short-term forecasts show that SiC will coexist with *Si* and that both will prevail over *GaN* in relation to electric vehicle inverter technologies.

A new paradigm is therefore emerging in the automotive powertrain industry,[37,38] making it necessary to identify the technological characteristics of WBG semiconductors compared to *Si*, thereby identifying their strengths and weaknesses.[39,40] In many research works, WBG devices,[41] substrate technology,[39] device operation mode,[42] conduction and switching losses,[43,44] reverse conduction capacity and operating ranges,[45] have been analyzed, among others. Such information is supplemented in this comprehensive literature review that is focused on WBG devices of electric vehicle powertrains and changing trends and usage over the medium-to-long-term,[1,46] highlighting the most suitable SiC and *GaN* alternatives for future electric vehicles. Moreover, changes within the automotive market are technically compared through an exhaustive analysis of WBG manufacturers.

Although the characteristics of WBG devices continue improving to reach their maximum theoretical performance, there is another great limitation linked to current package technology. The stray inductances (L_{stray}) introduced by the package have notable effects when attempting to operate at high switching frequencies with very fast switching transients.[47,48] For this reason, the leap from silicon technology to other semiconductors derived from WBG materials can cause some problems such as oscillations and electromagnetic interferences (EMI),[49,50] higher harmonic content,[51] cross-talk effects,[52] and the effect of overvoltages on semiconductor shutdown.[53,54] In the literature, many works can be found in which attempts to solve the aforementioned problems are described through solutions that are mainly based on reducing the negative effects of parasite inductances in discrete devices[55-58] or power modules (embedded bare dies).[59-62] Taking into account the new trends and technical requirements on this topic (in addition to others such as efficiency, losses, power density, cost, and size-weight ratio), the main features of power modules and discrete devices are explained in this review. At this point, the benefits of using power modules compared to discrete devices are highlighted, summarizing the main solutions for the electric vehicle.

The implementation of WBG technology not only presents challenges at an electrical level, but also at a thermal level. One of the most important is the heat evacuation capacity of power modules.[63] For this reason, the technical characteristics[64-66] of the main solutions (stack-up layers, assembly techniques, materials, packages, etc.) are presented in this work. In addition, the technical limitations are described and summarized (λ and CTE), pinpointing the main technical solutions adopted by the manufacturers and the trends arising from recent experimental innovations (overmold,[29,67,68] double-sided DBC,[69-72] IPM,[73-75] and 3D structure[65,76,77]). Likewise, the technical characteristics of the cooling systems are also addressed, indicating the proven technologies and the most advanced concepts to evacuate the heat from the power modules, essential to prevent overheating and device destruction.

It is moreover to be highlighted that a significant percentage of powertrain system failures are due to power electronic converter failures, which compromise system reliability. From the point of view of the designer of power converters, one of the main challenges to improve reliability is to understand the causes behind the failure of semiconductor devices and power modules. In this sense, this paper provides an overview of the latest developments that are being investigated to improve power electronic devices integrated into the vehicle powertrain, thereby covering the main aspects of switch

1099114x, 2022, 15, Downloaded from https://onlinelibrary.wiley.com/doi/10.1002/er.8581 by Universidad Del Pais Vasco, Wiley Online Library on [17/01/2023]. See the Terms and Conditions (https://onlinelibrary.wiley.com/terms-and-conditions) on Wiley Online Library for rules of use; OA articles are governed by the applicable Creative Commons License

reliability.[12,78-81] Moreover, complete operation of the inverter is considered, reviewing reliability aspects such as common-mode voltage.[82-84]

In summary, the main aim of this work is to provide a global vision of the trends and challenges of semiconductor devices and power modules that incorporate the inverter of the electric vehicle propulsion systems, emphasizing semiconductor technology, the device structure, different characteristics that influence the optimal operation of the inverter, as well as other aspects that affect the reliability of semiconductors and the powertrain system. Furthermore, it should be said that the exhaustive review carried out in this document is focused on the point of view of the electronic designer and engineer, while other works in the literature address some of these aspects from a more physical point of view. Bearing in mind the above, the structure of this paper is as follows.

Firstly, Section 2 focuses on the *Si* IGBT device technology, reviewing how its internal structure has evolved and why it has been necessary to exploit other technologies. In addition, the power modules for the electric vehicle market that include these devices are also analyzed. Subsequently, the highlights of WBG technology are reviewed in Section 3, analyzing the types of devices on the market, and focusing on devices that can compete directly with the *Si* IGBT, which are the most suitable for use in an electric vehicle. Then, the design aspects of power modules and discrete devices are reviewed in Section 4, such as packages, mechanical aspects, and thermal behavior, among others. Moreover, the main cooling technologies used for heat dissipation in semiconductor devices in electric vehicles are included. In Section 5, critical aspects of semiconductor devices and power modules are explained, such as the effect of stray inductances and other reliability problems. Finally, the most relevant conclusions of this study are presented in Section 6.

2 | SILICON TECHNOLOGY: SI IGBT

IGBTs are devices that combine Metal-Oxide-Semiconductor Field-Effect Transistor (MOSFET) gating characteristics with the high current carrying capability of the Bipolar Junction Transistor (BJT). This semiconductor is also characterized by low conduction voltages (low conduction losses) and short switching transients (low switching losses). Since its launch (around 1979 at General Electric), the device has undergone continuous development, to the point where it is now the main semiconductor used in medium power applications (eg, the electric vehicle powertrain). Throughout its development, each innovation was based on the parts that form the IGBTs, mainly the cell and the vertical structure (Figure 3).

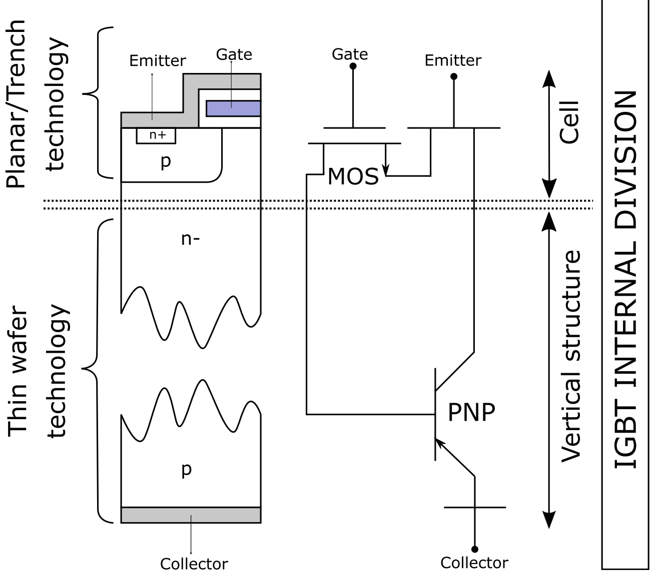

FIGURE 3 IGBT internal structure and equivalent Darlington circuit

2.1 | Cell and vertical IGBT structure technologies

The IGBT cell¶ or IGBT upper surface is where the emitter (E) and gate (G) terminals are located. The cell has undergone considerable improvements throughout its development, and four different cell types have now been advanced[85]:

1. *Planar cell*, Figure 4-①: the first IGBT cell structure, this conventional Planar cell had the limitation of obtaining a high conduction voltage drop (V_{CES}) and, therefore, higher conduction losses.[17] The dimensions of the cell structure and the doping profiles were optimized, to resolve this problem, thereby reducing the conduction losses.[86] However, these improvements were not sufficient and, as a result, new cell structures were proposed.
2. *Enhanced Planar cell*, Figure 4-②: to improve the cell technology, the IGBT was designed with a lightly doped *n*-layer, known as a hole barrier, so that the V_{CES} is further reduced. The result is a reduction of conduction losses of up to 30% compared to conventional technology.[86] In addition to increased robustness against overcurrents, as well as the ability to withstand short circuits. However, the main

1099114x, 2022, 15, Downloaded from https://onlinelibrary.wiley.com/doi/10.1002/er.8581 by Universidad Del Pais Vasco, Wiley Online Library on [17/01/2023]. See the Terms and Conditions (https://onlinelibrary.wiley.com/terms-and-conditions) on Wiley Online Library for rules of use; OA articles are governed by the applicable Creative Commons License

disadvantage of this cell alternative was the reduction in the blocking voltage of the IGBT.[86] Even so, manufacturers such as Hitachi in its HiGT device[87] and ABB with the SPT+[88] are committed to this technology, whose performance they expect to rival and eventually outperform other cell architectures with better performance, which is the case of the Trench cell and its respective developmental stages.[86]

3. *Trench cell*, Figure 4-③: this development broke with the main limitations of conventional Planar technology, with which the generation of sufficient carriers in the emitter to reduce the conduction voltage and power losses was not possible. For this purpose, a vertical MOS channel was integrated over the Planar cell structure, giving rise to the Trench cell. The main characteristic of this technology is that it reduces the forward voltage drop (V_{CES}) and, consequently, the conduction losses are as high as 30-40% compared to the original Planar cell devices.[89]
4. *Enhanced Trench cell*, Figure 4-④: current IGBT designs combine the concepts of the enhanced Planar cell and the Trench cell. This enhanced Trench cell architecture adds a carrier hole barrier to the Trench cell to improve the carrier store.[6,20] For example, the manufacturer Mitsubishi Electric uses this type of enhanced Trench cell in its CSTBT structure, achieving a 25% reduction in comparison with the turn-off losses of the conventional Planar cell.[90,91]

Besides, the vertical structure of the IGBT** encompasses the drift region, the buffer layers (optional), and the IGBT collector terminal (Figure 4). There are two

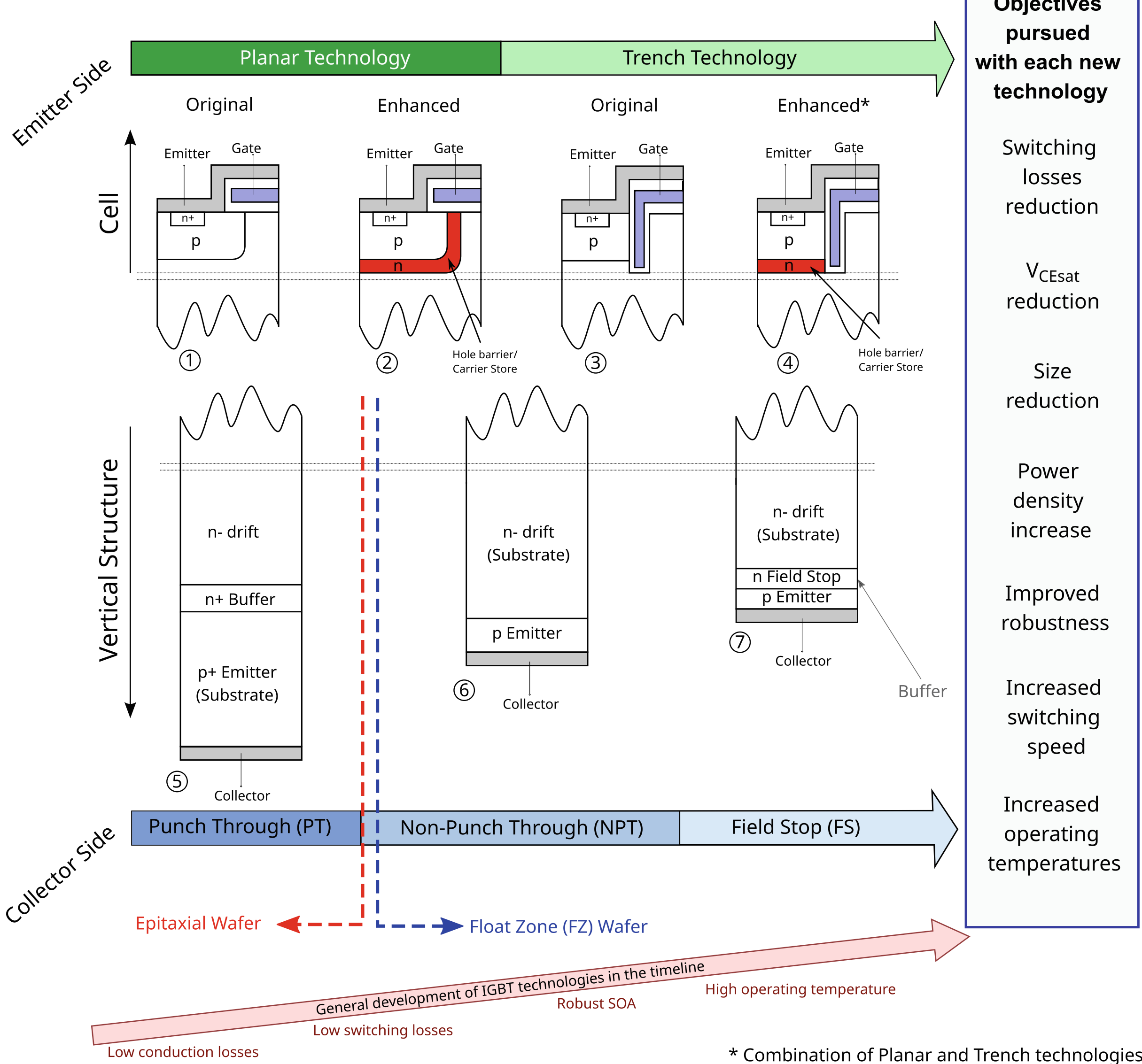

FIGURE 4 Development of the Insulated Gate Bipolar Transistor (IGBT) structure

1099114x, 2022, 15, Downloaded from https://onlinelibrary.wiley.com/doi/10.1002/er.8581 by Universidad Del Pais Vasco, Wiley Online Library on [17/01/2023]. See the Terms and Conditions (https://onlinelibrary.wiley.com/terms-and-conditions) on Wiley Online Library for rules of use; OA articles are governed by the applicable Creative Commons License

main alternatives during their fabrication: (i) using an epitaxial wafer or (ii) using a Float Zone (FZ) wafer††. These alternatives define the development stages that characterize the various IGBT vertical structures[85]:

1. *Punch Through* (*PT*), Figure 4-⑤: here the vertical structure is manufactured on an epitaxial substrate. The first IGBTs employed such a structure (along with Planar cells) and were characterized by having a buffer layer that controls the IGBT electric field. The technology was developed for 300 to 1700 V ranges, as it was complicated to obtain voltages above 2 kV due to the limitations introduced by the epitaxial substrate. In fact, the PT structure required a large amount of silicon, increasing the device size and price. In addition, this structure presented a high dependence on the temperature of its electrical parameters and problems with device parallelization.[5] Even so, PT-IGBTs dominated in up to 600 V blocking voltage applications for several years.[92]
2. *Non-Punch Through (NPT)*, Figure 4-⑥): this structure was developed by a division of Siemens that is now part of Infineon.[92] For that purpose, an FZ substrate was used, which improved short-circuit robustness and made it possible to control carrier life span.[5] Although NPT devices have higher conduction and switching losses than PT devices, semiconductors for ranges between 600-4500 V can be manufactured using a smaller amount of silicon, breaking with the limitations of PTs. Another benefit of this structure is the lower dispersion of its electrical parameters between devices in the same batch, which is not the case with PTs. Likewise, this structure has a positive temperature coefficient, which makes its parameters more stable when facing temperature variations, facilitating the device parallelization (an absolutely necessary condition in medium power applications such as the electric vehicle powertrain).
3. *Field Stop (FS)*, Figure 4-⑦: this structure is the result of combining the advantages of PT and NPT technologies with the aim of improving conduction and switching losses. Depending on the manufacturer, the FS structure is also known by other names: Soft Punch Through (SPT)[86] and Light Punch Through (LPT), from ABB and Mitsubishi respectively.[20] The optimization of the *n*-type layer is fundamental for the FS structure, as well as the implementation of the buffer layer to reduce the thickness of the device. This minimizes conduction resistance without affecting the blocking voltage. In addition, the turn off speed is also improved, reducing switching losses, which therefore permits higher switching frequencies.[86]

Recent IGBT developments are focused on combining variants of the enhanced Trench cell with the most recent evolutions of the FS vertical structure.[85] For example, the Micro Pattern Trench (MPT) technology,[97,98] developed by Infineon, attempts to implement a further increase in the width of the IGBT channel, which can be achieved by narrow parallel trenches‡‡. It is of enormous benefit for applications requiring no short-circuit withstand capability, since a higher channel width directly lowers the on-state voltage drop. Another relevant enhanced Trench FS solution is the Carrier Stored Trench Gate Bipolar Transistor (CSTBT),[99,100] developed by Mitsubishi, which reduces turn-off losses and provides greater tolerance to short-circuits, due to LPT§§ technology and the insertion of the enhanced Trench cell with the CS layer.

Although the main research and evolution lines of IGBTs consist of obtaining improvements from the enhanced Trench FS structure, there are also other research lines to integrate new features, such as Reverse Blocking (RB) and Reverse Conducting (RC). In this sense, the IGBTs work together with an anti-parallel diode, called a FreeWheeling Diode (FWD), which protects the IGBT and permits the flow of reverse current. It is a totally necessary condition in applications such as electric vehicles, because a path is needed for inductive currents when the IGBT is turned-off and, in addition, it facilitates battery recharching from the motor during regenerative braking. As an example, Figure 5 shows the incorporation of the diode inside the Trench FS IGBT,¶¶ forming a RC IGBT device.[20] This solution, which integrates the FWD into the IGBT structure, consists of dividing the anode *p* of the diode into several sections and the cathode *n* is integrated in the IGBT emitter. In this way, the antiparallel diode uses the same silicon wafer as the IGBT,[101] although there is no possibility of optimizing the diode independently of the IGBT. There is also the

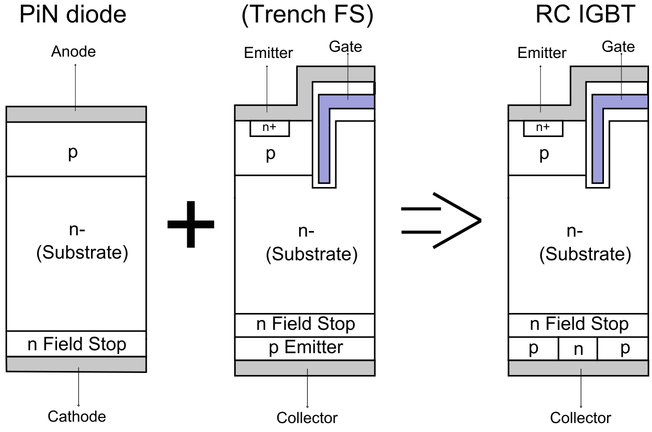

FIGURE 5 Structure of the RC-IGBT technology

1099114x, 2022, 15, Downloaded from https://onlinelibrary.wiley.com/doi/10.1002/er.8581 by Universidad Del Pais Vasco, Wiley Online Library on [17/01/2023]. See the Terms and Conditions (https://onlinelibrary.wiley.com/terms-and-conditions) on Wiley Online Library for rules of use; OA articles are governed by the applicable Creative Commons License

FIGURE 6 Development stages of Infineon 1200 V @75 A IGBT generations[20,93-96]

possibility of integrating the diode by placing both structures, the IGBT and FWD, in parallel within the same wafer (pilot diode[102]). A technique that improves the performance of the FWD, although it also increases the surface of the RC IGBT.[103,104]

Manufacturing costs also depend on the bare die size. In this sense, the reduction of their size has also been an objective in recent years, leading to the different IGBT generations. During the stages of their development, along with the increase in power density, the maximum operating temperatures have also increased at the same time as the conduction voltage drop has been reduced. An example is shown in Figure 6, which represents the stages and trends of bare die sizes for the different IGBT generations of 1200 V/75 A from Infineon. As can be seen, there has been a reduction in saturation voltage of approximately 55% and a 6-fold increase in power density. However, it should be noted that the reduction in device size reduces their robustness and short-circuit capability,[105] so a compromise must be reached between power losses, price, and robustness at each stage of its development.

Each stage in the development of IGBT technology, in which there has been an improvement in the device features (reduction of chip size and better usage of the silicon surface, reduction of conduction voltage and therefore reduction of conduction losses, improvement of the shutdown process and reduction of the tail current (I_{tail}), increase of the maximum blocking voltages and increase of the operating temperatures, among others) has undoubtedly been driven by the requirements of one particular application or another. In the specific case of electric vehicles, manufacturers have been demanding increasing power densities, operating temperatures, efficiencies, and better reliability characteristics. All these developments have the aim of improving such aspects as robustness, power ratings, dynamic response, and vehicle autonomy. For this reason, among others, most manufacturers opt to use power modules in their vehicles, as higher power densities are provided from systems that are, generally speaking, increasingly optimized. All these aspects are analyzed in greater detail in the following sections.

2.2 | IGBT-based power modules

The range of products on the market is very wide (both in discrete devices and power modules) and multiple variants of IGBT technologies may be found. In addition, these variants are embedded in very diverse packages (Section 4) and there is no specific regulation that determines the housing of each device/module. Although there are a large number of manufacturers, as an example and in order to understand their differences, this work reviews the information provided by some of the major power semiconductor manufacturers, including Infineon, Fuji Electric, and Mitsubishi Electric. In this sense, Figures 7 and 8 show each main stage in the development of the *Si* IGBTs that have been incorporated into

1099114x, 2022, 15, Downloaded from https://onlinelibrary.wiley.com/doi/10.1002/er.8581 by Universidad Del Pais Vasco, Wiley Online Library on [17/01/2023]. See the Terms and Conditions (https://onlinelibrary.wiley.com/terms-and-conditions) on Wiley Online Library for rules of use; OA articles are governed by the applicable Creative Commons License

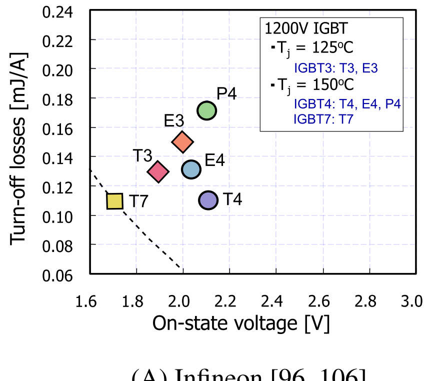

(A) Infineon [96, 106].

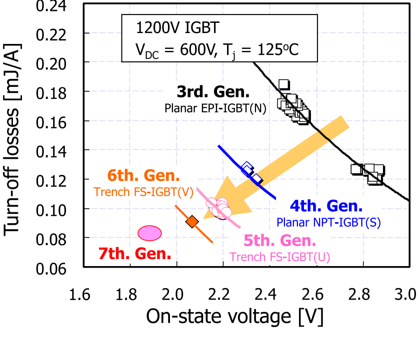

(B) Fuji Electric [96,107,108].

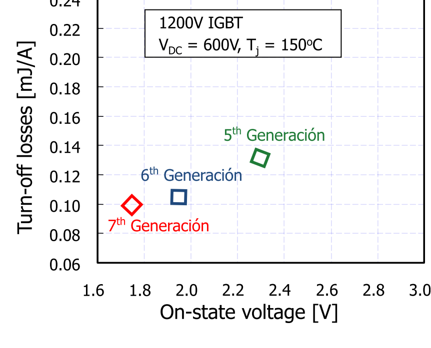

(C) Mitsubishi Electric [96,109-111].

FIGURE 7 Development stages of turn-off energy in relation to conduction voltage for different generations of Insulated Gate Bipolar Transistor (IGBT) modules (based on information from Manufacturers)

their power modules. The main differences between each manufacturer's technologies are set out below:

- *Infineon*, Figure 8A: the IGBT technology that Infineon is currently using for its power modules is based on Trench cell variants with FS vertical structure (Section 2.1). This manufacturer has named the power modules according to their main characteristics (power range, losses, switching speed, etc.) Some examples of these names are: E3 for its standard series, T3 for low loss devices, or T4, E4, and P4 for low, medium, and high power series respectively. In this regard, Figure 7A shows the trend and evolution (in terms of turn-off losses and conduction voltages) of some current modules. It is important to highlight the T7 technology, which uses MPT technology (inside the category enhanced Trench FS), as considerable improvements have been achieved, reducing the losses by approximately 40% and the conducting voltage by 20% compared to the P4 series. Moreover, other developments are also presented such as the Reverse Conducting Drives Automotive-Insulated Gate Bipolar Transistor (RCDA-IGBT), which includes the FWD within the same substrate, thereby reducing the total area of the IGBT and diode assembly by more than 60%.
- *Fuji Electric*, Figure 8B: this manufacturer has labeled its power modules technologies with letters for each series as each IGBT generation was innovated. As with Infineon, the commercial power modules consist of the Trench cell combination with the FS vertical structure (Section 2.1), as these have lower power losses, as shown in Figure 7B through the fifth, sixth, and seventh S Trench Cell device generations, using an MPT-like technology for the combination of the Trench cells with the vertical FS structure. In fact, looking at the graph, some seventh generation modules improve upon the characteristics of third generation modules by up to 35% for conducting voltage and by up to 55% for turn-off losses. The manufacturer also incorporates RC IGBT developments based on Trench FS (X series) technology. In this case, the pilot diode technique is implemented to achieve the union between the IGBT and FWD in the same substrate device.
- *Mitsubishi Electric*, Figure 8C: the fifth generation of power modules from this manufacturer, the vertical LPT structure (equivalent to Infineon's FS), is implemented together with the enhanced Trench cell, yielding the CSTBT device (Section 2.1). This device, also considered as an enhanced Trench FS solution, achieves a significant reduction in power losses compared to previous generations. In addition, as with the power modules from Infineon and Fuji Electric, the latest CSTBT generations also have lower switching losses and conduction voltage. In fact, according to Figure 7C, the seventh generation is superior to the fifth generation by, approximately, 25% in both conducting and switching losses. In addition, it also has RC IGBT developments, using the pilot diode technique on a CSTBT device (seventh generation) that optimizes the FWD and improves the thermal performance of the device.

Regarding the operating ranges of the available power modules that the above-mentioned manufacturers are currently marketing, Figure 9 shows the series/generations (classified by voltage -V_{CES}- and current -$I_{c_{nom}}$- ranges***) of the power modules (2-in-1 and 6-in-1) marketed by some of the leading semiconductor manufacturers (Infineon, Fuji Electric, Mitsubishi Electric, and Semikron).

Figure 9 also indicates the modules that are classified as "automotive grade"††† (rounded technologies) or that are otherwise recommended by the manufacturer for use

1099114x, 2022, 15, Downloaded from https://onlinelibrary.wiley.com/doi/10.1002/er.8581 by Universidad Del Pais Vasco, Wiley Online Library on [17/01/2023]. See the Terms and Conditions (https://onlinelibrary.wiley.com/terms-and-conditions) on Wiley Online Library for rules of use; OA articles are governed by the applicable Creative Commons License

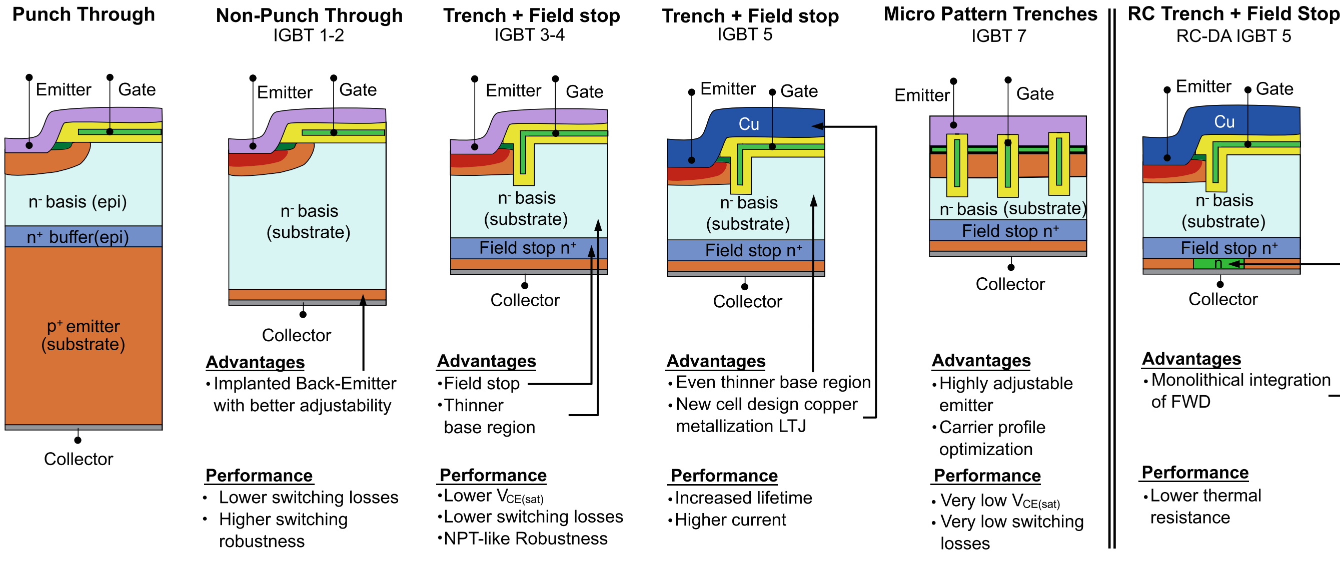

(A) Infineon IGBT modules [104, 106, 120–124]

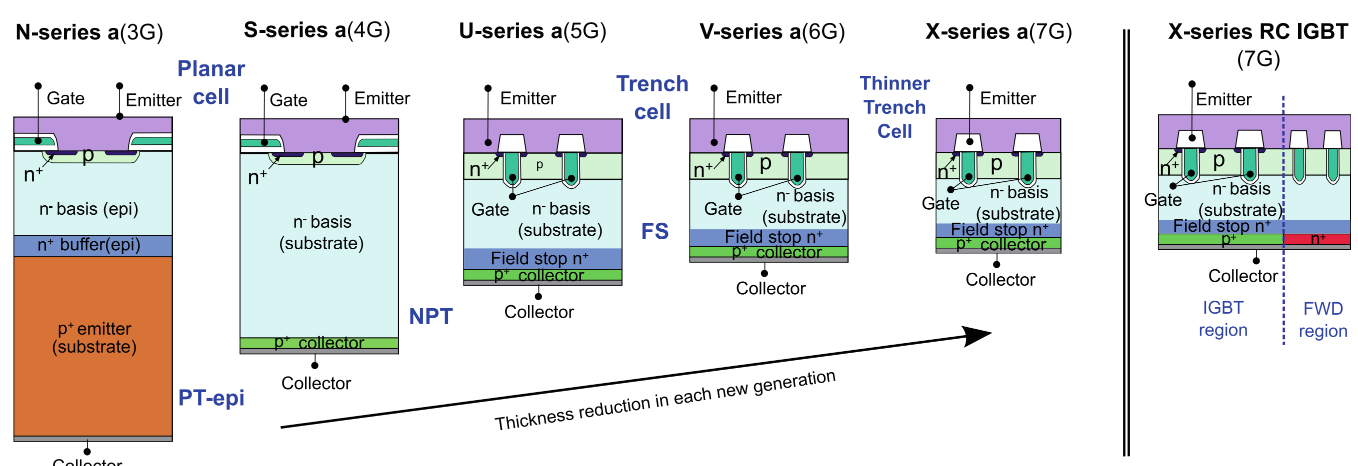

(B) Fuji Electric IGBT modules [104, 108, 125–128].

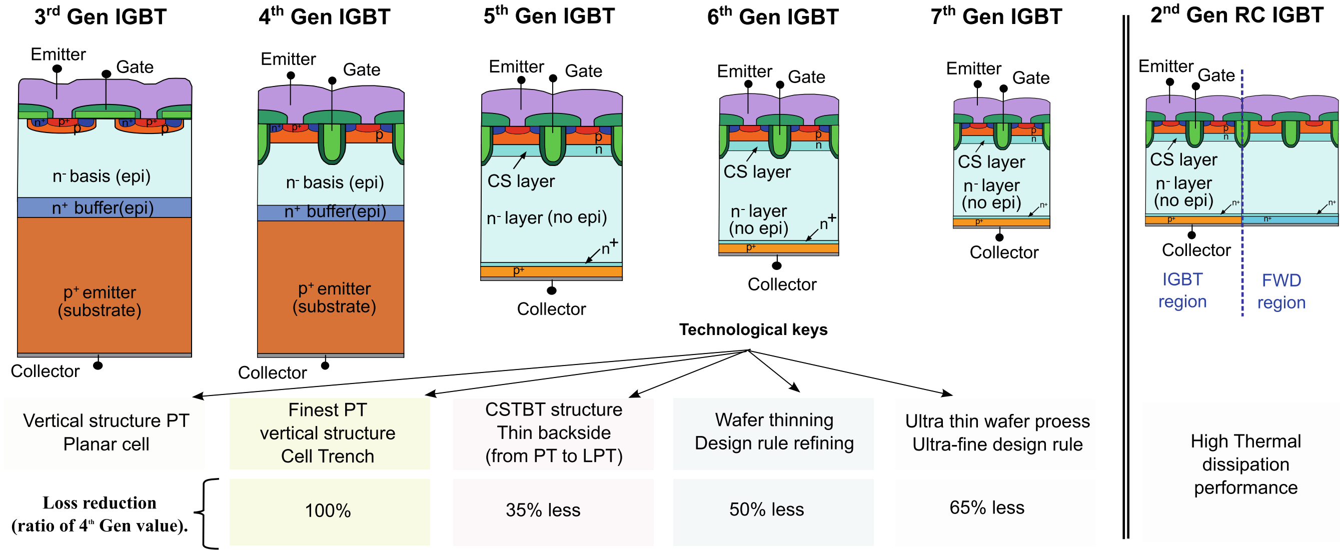

(C) Mitsubishi Electric IGBT modules [129–134].

FIGURE 8 Development of the IGBTs used in various power modules according to the manufacturer

1099114x, 2022, 15, Downloaded from https://onlinelibrary.wiley.com/doi/10.1002/er.8581 by Universidad Del Pais Vasco, Wiley Online Library on [17/01/2023]. See the Terms and Conditions (https://onlinelibrary.wiley.com/terms-and-conditions) on Wiley Online Library for rules of use; OA articles are governed by the applicable Creative Commons License

1099114x, 2022, 15, Downloaded from https://onlinelibrary.wiley.com/doi/10.1002/er.8581 by Universidad Del Pais Vasco, Wiley Online Library on [17/01/2023]. See the Terms and Conditions (https://onlinelibrary.wiley.com/terms-and-conditions) on Wiley Online Library for rules of use; OA articles are governed by the applicable Creative Commons License

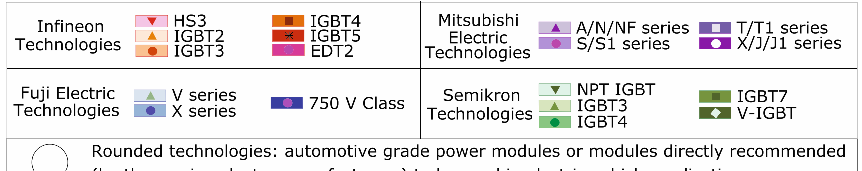

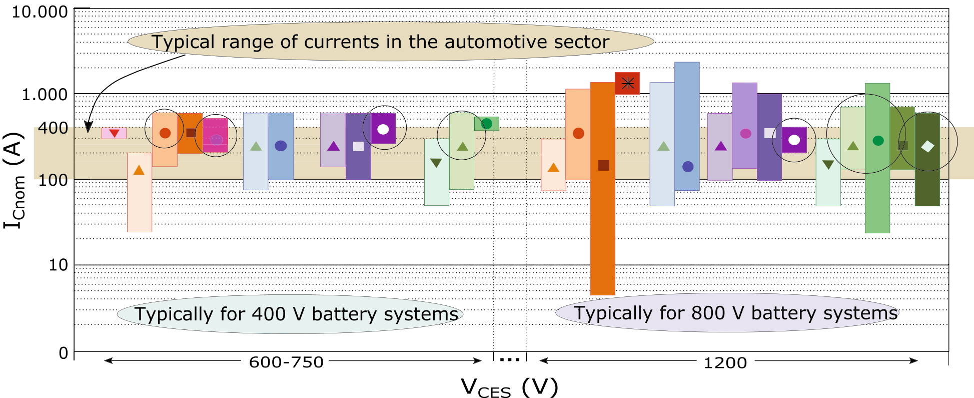

(A) Modules for the Half-Bridge topology (2-in-1).

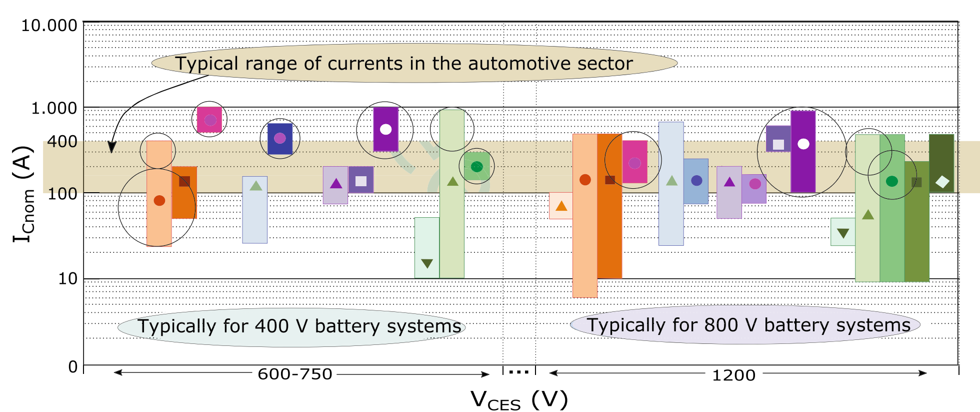

(B) Modules for the Voltage Source Inverter topology (6-in-1).

FIGURE 9 Operating range of the IGBT module technologies offered by the manufacturers Infineon, Fuji Electric, Mitsubishi Electric, and Semikron, considering the nominal current and the blocking voltage

in electric vehicle applications. As can be seen, all manufacturers offer solutions intended for electric mobility in the “400 V" and the “800 V" ranges and for 2-in-1 and 6-in-1 configurations. Besides, this figure shows how most of the power modules on offer reach the typical current ranges (100 to 400 A) required by electric vehicles.[2,3] In this context, several examples confirming the latter can be found on the market: (i) vehicle manufacturers such as Toyota with 650 V-180 A modules, Honda Insight with 600 V-300 A, Chevrolet Volt with 430 V-325 A, Nissan Leaf with 600 V-340 A, and Mercedes Benz with 700 V-325 A[2]; and (ii) automotive traction inverter manufacturers such as Cascadia-Rinehart[112] with their products in the “400 V" (PMX100DX 400 V-300 A; CM200DX 480 V-300 A) and “800 V" range (PM100DZ 820 V-150 A; CM200DZ 840 V-200 A); and BorgWarner manufacturer (Gen4-Size10 800 V-200 A).[113]

Conidering the classification of power module voltages, (600 to 750 V and 1200 V, Figure 9), the wide range of modules (regardless of the automotive grade) that cover the demand for vehicles categorized as “400 V" and “800 V" systems can be seen (most light electric vehicles are generally equipped with battery packs with a nominal voltage range between 250 V and 450 V, known as “400 V" systems; whereas in heavy electric vehicles where most vehicles operate with nominal voltages close to 600-650 V and, in some sports cars, the voltage may slightly exceed 900 V, in which case they are known as “800 V" systems).[1,114-119] Thus, 600 to 750 V rated modules are suitable for “400 V" systems, while 1200 V rated modules‡‡‡ are suitable for “800 V" systems.

On the other hand, Figure 9 shows that manufacturers continue to rely on silicon technology (unlike SiC technology where solutions for the automotive sector

tend mainly to respond to the "800 V" systems), to cover the range of "400 V" and "800 V".

Finally, no notable trends are observed with regard to the topology of the modules (2-in-1 and 6-in-1). Thus, topologies in relation to both silicon technology (Figure 9) and SiC (Figure 14) have been designed for the inverter of the electric vehicle powertrains. Vehicle manufacturers usually opt for the three-phase inverter (m = 3), in which case one 6-in-1 or three 2-in-1 topologies should be used. At this point, it is worth mentioning that multiphase machine technology (m > 3) brings with it a series of advantages§§§ that make it attractive for next-generation electric vehicles. In this case, and depending on the number of phases of the machine, multiphase inverters should normally be formed from 2-in-1 topologies, in order to optimize the number of semiconductors.

3 | WIDE-BANDGAP (WBG) TECHNOLOGIES: SIC AND GAN SEMICONDUCTORS

WBG devices have been improving their performance thanks to innovations in their designs and manufacturing techniques.[32,135] As a result of these advances, lower conduction voltage drops, higher operating temperatures, and better stability of all parameters may be achieved with respect to temperature.

Today, SiC devices are an alternative to *Si* for medium-power applications (ie, electric vehicles powertrain),[136] as the physical characteristics of SiC material (Figure 10) can be used to manufacture smaller devices capable of withstanding high blocking voltages, which switch more quickly, thus reducing switching losses.[137]

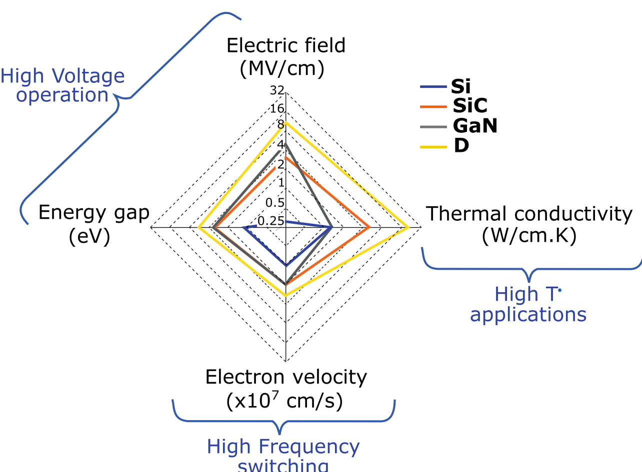

FIGURE 10 Physical properties of silicon and WBG materials based semiconductors[32,34,35,138-140]

Devices based on *GaN* have also improved their performance in recent years. *GaN* material has higher electron mobility than SiC, which means that *GaN* devices are better suited for high-frequency switching operations. In general, although most parameters of *GaN* technology show superior characteristics to SiC devices (Figure 10), although the lower thermal conductivity of SiC technology makes it more challenging for the high power density applications,[141] used in electric vehicles. Furthermore, unlike SiC devices, *GaN* technology is manufactured on other substrates such as *Si*, SiC and, even, *sapphire*, due to difficulties and low quality materials for pure *GaN* substrates. Various *GaN* layers are epitaxially grown on these substrates (Figure 11A), resulting in lateral devices (current flows laterally) instead of vertical devices (current flows vertically) as with SiC devices¶¶¶.

Commercially speaking, there are different SiC and *GaN* devices,[1] whose main characteristics are summarized in Table 2. However, among all these devices, semiconductor manufacturers have mainly focused their efforts on SiC MOSFET and *GaN* High-Electron-Mobility Transistor (HEMT) devices as alternatives to the *Si* IGBT.

3.1 | WBG alternatives to Si IGBT: SiC MOSFET and GaN HEMT

At present, there are no commercial solutions for IGBT devices based on SiC and *GaN* materials. In the case of

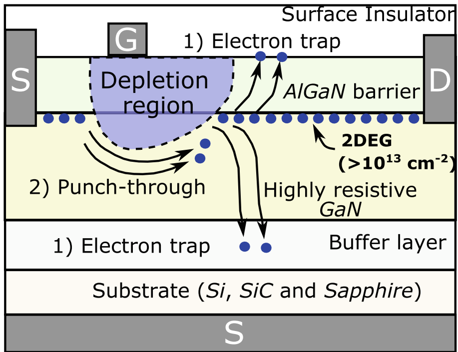

(A) *GaN* HEMT internal structure.

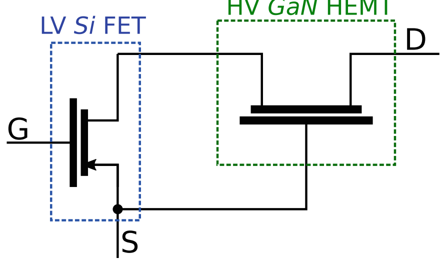

(B) *GaN* HEMT cascode configuration.

FIGURE 11 Layer structure and cascode configuration of *GaN* HEMT for normally-*off* operation[144-146]

1099114x, 2022, 15, Downloaded from https://onlinelibrary.wiley.com/doi/10.1002/er.8581 by Universidad Del Pais Vasco, Wiley Online Library on [17/01/2023]. See the Terms and Conditions (https://onlinelibrary.wiley.com/terms-and-conditions) on Wiley Online Library for rules of use; OA articles are governed by the applicable Creative Commons License

1099114x, 2022, 15, Downloaded from https://onlinelibrary.wiley.com/doi/10.1002/er.8581 by Universidad Del Pais Vasco, Wiley Online Library on [17/01/2023]. See the Terms and Conditions (https://onlinelibrary.wiley.com/terms-and-conditions) on Wiley Online Library for rules of use; OA articles are governed by the applicable Creative Commons License

TABLE 2 Advantages and disadvantages of SiC and *GaN* devices[1,32,144,150,155-161]

Device		Main advantages	Main disadvantages
SiC diodes		Lower reverse recovery charge than *Si*.	
		Lower switching losses than *Si*.	
		Positive temp. Coefficient[a]	
	PiN	High Voltage (>3,3 kV).	High reverse recovery current
		Low leakage current (Temp. independent)	High reverse recover charge
		Low conduction resistance	
	SBD	Typical voltage about 600 V	Higher leakage current
		Low reverse recovery current	High variation with temperature
		Low reverse recovery charge	
	JBS	Hybrid device (SBD and PiN) 600 V-3.3 kV	
SiC BJT		Normally-*off*	Current controlled
		Low conduction voltage drop	Complexity of the driver[b]
		Gate-emitter low conduction voltage	
		Fast switching dynamics	
SiC JFET (lateral, vertical)		High operation temp.	Lateral JFET normally-*on*[c]
		Threshold voltage no temp. dependency	$V\ T_{JFET}$ normally-*on*[d]
		Vertical JFET without parasitic diode[e]	
		Low conduction resistance	
SiC MOSFET		Normally-*off*.	Low robustness (gate reliability)
		Gate charge similar to *Si* IGBTs	
		Same drivers as for *Si* IGBTs can be used[f]	
		Ratings similar to *Si* IGBTs[g]	
		Higher switching frequencies	
		Positive temperature coefficient[a]	
		Higher thermal conductivity	
GaN HEMT		Conduction of current in both directions	Normally-*on*
		Active freewheeling diode	Lateral structure (lower voltage blocking capacity)
		Low conduction resistance	Lower thermal dissipation than SiC
			There are no *GaN* homogeneous substrates[h]
	Cascode	Normally-*off* (serial *Si* MOSFET)	Conduction resistance increase (*Si* MOSFET)
		Lower power losses than *Si*.	Optimization of *Si* MOSFET cascode in each application
		Conventional MOSFET gate drivers	
	p-HEMT	Normally-*off*	Reliability issues[i]
		(No dielectric (insulator) issues	Very complex gates, less voltage isolation
		(Low resistance under the gate (channel)	
	MIS-HEMT	Normally-*off*	Critical impact of dielectric on device performance[j]
		Large forward breakdown	Very complex gates, less voltage isolation
			High conduction resistance

[a]Required for easy device parallelization.
[b]Compared with the voltage controlled devices.
[c]Compromising converter safety under transistor firing control malfunctions. Junction-Gate Field-Effect Transistors (JFET) devices are vertical. The term lateral or vertical refers to the formation of the channel within the device.
[d]VTJFET normally-*on* appears in cascode configuration to be normally-*off*.
[e]Such parasitic diodes exhibit low performance, including high conduction losses.
[f]Simplifying the migration from *Si* to WBG power conversion technology.
[g]Taking into account that the SiC MOSFET is compared with the IGBT structure.
[h]High quality of *GaN* substrates for vertical devices is under research (*GaN*-on-*GaN* technology[159]).
[i]Optimization of p-GaN etching needed for low-access resistance and to prevent critical leakage current.[158,159]
[j]New developments are necessary to optimize the gate dielectric interface, which affects conduction resistance and device reliability.[160,161]

SiC, IGBT developments based on this technology are in early research stages.[147] In this context, the manufacturers of semiconductors have committed themselves to the use of SiC MOSFETs and *GaN* HEMTs as competitors and alternatives to *Si* IGBTs. The highlights of these devices are reviewed below:

1. SiC *MOSFET*: these semiconductors are turned off by default (normally-*off*) and provide a good balance between conduction and switching losses,[137] mainly due to their low conduction resistance and gate charge (Q_g). Their introduction in power converters is interesting, as they reduce power losses compared to *Si* IGBTs (Figure 12). In addition, similar driver circuits can be used as for *Si* IGBTs, which facilitate the transition between both technologies. On the other hand, they can work without an external anti-parallel diode, because they incorporate an intrinsic diode (body diode) in their structure.[137,148,149] However, the use of this diode must be analyzed for each application, as the incorporation of external Junction Barrier Schottky (JBS) diodes can offer better performance, due to a more highly optimized design and manufacture.[150] In fact, SiC power modules generally include anti-parallel JBS SiC diodes to improve power module properties.

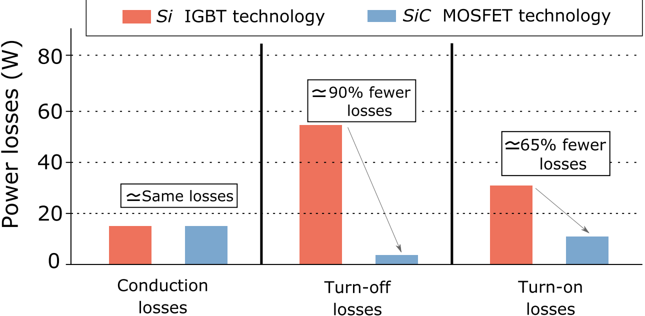

(A) Power losses at 30 kHz of *SiC* MOSFET and *Si* IGBT [151, 152].

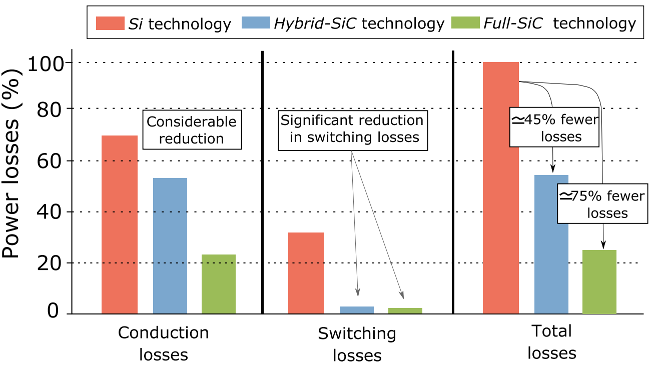

(B) HB power modules, in *Si*, Hybrid-*SiC* and All-*SiC* (V_{cc}=800 V, I_o=450 A_{pk}, 5 kHz, M=1 and P.F=0.85) [153, 154].

FIGURE 12 Comparison of power losses of *Si* technology vs SiC technology

2. *GaN HEMT*: these devices are based on *Si* wafers[142,143,162] (*GaN*-on-*Si* technology)**** on which their *AlGaN/GaN* thin layers are placed (Figure 11A). Unlike previous devices, *GaN* HEMTs are turned on by default (normally-*on*). In electric vehicles, as well as in other power applications, it is very important, in terms of safety, to use normally-*off* devices.[163] For this reason, the following two techniques are used, in order to obtain normally-*off GaN* HEMT devices:In general, the low conduction resistance (eg, 25 $m\Omega$ @650 V-60 A is the lowest value of an available 650 V single package) and fast switching speed achieved by the *GaN* devices make them good candidates for certain electric vehicle applications. However, HEMTs are lateral devices with very narrow gates to ensure their blocking ability (either for devices *on* and *off* by default, or for p-HEMT and MIS-HEMT). These structural characteristics determine the behaviour of *GaN* HEMT. Firstly, narrow gates, lateral current conduction, and low thermal conductivity mean that these semiconductors cannot evacuate heat as efficiently (higher thermal resistance) in comparison with vertical devices.[170] Secondly, the blocking voltage must be supported between the drain and the source, located on the same surface (not within the volume of the semiconductor, as with vertical devices).[164] Significant research is therefore underway to achieve high quality *GaN* substrates, for developing *GaN*-on-*GaN* technology.[171-174] Besides, the current range of *GaN* HEMT devices is at present insufficient for electric vehicle applications. A large number of paralleled devices will be required to achieve those current ranges, assuming a higher cost, due to the use of more devices and greater complexity in the design of the circuit, in order to balance all the semiconductors.
   a. Within the same encapsulation, connect the *GaN* HEMT with a low voltage *Si* MOSFET (*off* by default) in cascode configuration (Figure 11B).[145,164,165] This solution offers good results, however, the maximum operating temperature of the *Si* MOSFET, lower than the *GaN* device, limits the temperature of the cascode configuration. In addition, it increases the conduction resistance of the structure, as the resistivity of both devices must be considered.
   b. Include additional gate structures within the *GaN* HEMT device to make it *off* by default. Today, manufacturers are working and commercializing devices based on this trend, avoiding the cascode solution.[166] To do so, there are two different technological approaches: (i) use of a p-n junction

1099114x, 2022, 15, Downloaded from https://onlinelibrary.wiley.com/doi/10.1002/er.8581 by Universidad Del Pais Vasco, Wiley Online Library on [17/01/2023]. See the Terms and Conditions (https://onlinelibrary.wiley.com/terms-and-conditions) on Wiley Online Library for rules of use; OA articles are governed by the applicable Creative Commons License

structure between the gate and the source of the transistor (p-HEMT[157,167,168]), a solution that is commercialized by companies such as EPC and Panasonic[158,159]; and (ii) the introduction of a Metal-Insulating-Semiconductor (MIS) structure in the gate (MIS-HEMT[144,156,169]), as some developments at NEC have done.[158]

In short, and considering the above, although the direct alternatives of the IGBT device are the SiC MOSFET and the *GaN* HEMT, it is worth reviewing other more general aspects, such as other alternatives of WBG devices and power modules that are based on these technologies.

3.2 | WBG discrete devices and power modules for the electric vehicle

3.2.1 | WBG discrete devices

Regarding SiC devices, JBS diodes are preferred among the diodes available for the electric vehicle powertrain, because they carry higher voltages and present lower leakage currents than Schottky Barrier Diodes (SBD) (Table 2). Furthermore, SiC PiN diodes are not suitable for blocking voltages below 3.3 kV and their reverse recovery current causes greater power losses.[46] Similarly, as for SiC power transistors, MOSFETs are preferred over BJTs or JFETs, because they can switch at high frequencies, they are *off* by default, and they also require relatively simple driver circuits.[175,176] As an example, Figure 13 shows the voltage and current levels of the SiC JBS diodes and the SiC MOSFETs, considering discrete devices in this case. It should be noted that all the semiconductors taken into account for the figure data are encapsulated in TO-247 or D3PACK packages whose junction-to-case thermal resistance is equivalent. Taking into account the latter, the typical voltage and current ranges of SiC JBS are shown in Figure 13A, highlighting 4 voltage levels: 600 V, 650 V, 1200 V, and 1700 V, with current ranges between 10 A and 50 A. Similarly, the voltage and current ranges of the SiC MOSFETs are shown in Figure 13B. These devices have a voltage range between 650 V and 1700 V, with a higher number of devices for 1200 V. The usual current ranges of these SiC MOSFETs are between 2-90 A.

With regard to *GaN* devices, *GaN* Schottky diodes are in an experimental phase, presenting a lateral or quasi-vertical structure. The quality of the material is crucial in the design of this semiconductor, because defects affect the Schottky barrier and, therefore, the maximum

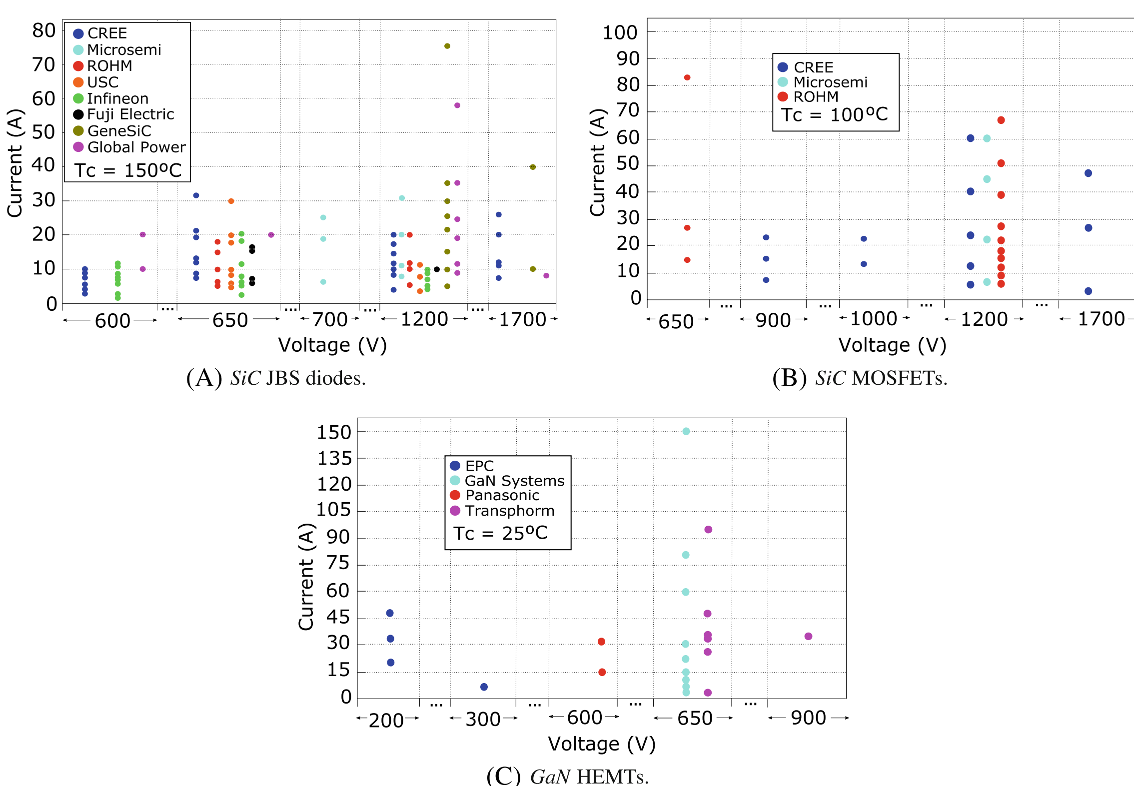

(A) *SiC* JBS diodes.

(B) *SiC* MOSFETs.

(C) *GaN* HEMTs.

FIGURE 13 The most widely marketed WBG devices and their current and voltage ranges, based on information from the manufacturers

1099114x, 2022, 15, Downloaded from https://onlinelibrary.wiley.com/doi/10.1002/er.8581 by Universidad Del Pais Vasco, Wiley Online Library on [17/01/2023]. See the Terms and Conditions (https://onlinelibrary.wiley.com/terms-and-conditions) on Wiley Online Library for rules of use; OA articles are governed by the applicable Creative Commons License

blocking capacity. The breaking voltages of the lateral *GaN* diodes on *sapphire* substrates are around 9.7 kV, but the forward voltage drop is still high. Moreover, *GaN* (Hydride Vapour Phase Epitaxy, HVPE) substrates have been used to start up experimental 600 V *GaN* Schottky diodes that could compete in the market with SiC diodes††††.

Consequently, the main device on the market, is the HEMT (Table 2).[1] This device uses a *Si* substrate to implement the 2DEG conduction layer with a low conduction resistance. In fact, its null reverse recovery makes it possible to manufacture transistors with bidirectional blocking and conduction voltage.[144,155] There are several companies that develop discrete devices of *GaN* material for energy applications, such as EPC, Exagan, GaN Systems, ST Microelectronics through Leti CEA, NTT, Panasonic, and Transphorm, among others.[1] Figure 13C shows the most common voltage ranges of the *GaN* HEMT technology, between 600 and 650 V with current levels of 3-150 A‡‡‡‡. As some specific examples, EPC offers discrete semiconductors with 350 V@6.3 A; and 90 V@90 A; the discrete semiconductors in the GaN Systems reach 650 V@150 A; the Panasonic discrete transistors reach 600 V@10 A; and, finally, the Transphorm discrete transistors reach 600 V with a drain current of 20 A.

3.2.2 | WBG power modules

As the current ratings of discrete semiconductors are, in many cases, not high enough for the needs of power applications, parallelization of discrete devices and bare dies is necessary to obtain high current levels. In this sense, as with *Si* technology, power module manufacturers are developing module solutions based on SiC technology. In relation to Mitsubishi HB modules, Figure 12B shows the advantages of using SiC semiconductors compared to conventional *Si* semiconductors, which represent a significant improvement in switching losses of approximately 75%.

Conducting the same comparative study as for *Si* power modules, in addition to the information from the manufacturers that is compared in Section 2.2, CREE/Wolfspeed, Global Power, Microsemi, and ROHM manufacturers have been reviewed, which are specialized in WBG semiconductors, as shown in Figure 14. This figure classifies the available options for *All*-SiC and *Hybrid*-SiC power modules according to voltage and current ranges for HB and VSI topologies§§§§. From this figure, it is observed that some manufacturers such as Infineon, CREE, or ROHM offer 100% SiC material solutions, but only for some topologies. For example, for the VSI topology only *full*-SiC solutions can be seen. However, this topology can be implemented using three HB modules, which a priori can lead to an increase in stray inductances, due to a lower level of integration. Other manufacturers have started to introduce hybrid configurations by incorporating the SiC antiparallel diode, although the predominant device is still the *Si* IGBT. In any case, typical operating ranges for automotive power modules containing SiC devices are usually 100-400 A, but with voltages of 1200 V. It can be understood from this analysis that the number of available modules is not even close to the number of modules using *Si* technology. However, it can be seen that manufacturers are starting to offer converter topology solutions based on this material, using SiC MOSFETs together with SiC JBS diodes. In addition, it can be seen that the 1200 V modules are the alternative used by vehicle manufacturers. As previously mentioned in the analysis of silicon modules, practically all light vehicles were running off "400 V" battery packs systems. However, they are now beginning to migrate to "800 V" battery packs.

With this change, a substantial reduction in the conductive wire weight will be achieved, as half the current will be handled for the same power.[114] Increasing the voltage of the battery pack will also reduce quadratic conduction losses ($P = I_{rms}^2 R$). The efficiency of the electric vehicle will therefore be improved with this change in battery voltage. 1200 V SiC power modules fit into this range and may be more suitable for use in conjunction with "800 V" batteries. On the other hand, it should be noted that the options in SiC with automotive grade are less than those of *Si*. Although it is true that several manufacturers propose their modules for the powertrain of electric vehicles, most of them do not meet this grade. Infineon's FF08MR12W1MA1_B11 is an example of an automotive-grade full-SiC module.

Another aspect to consider is the Power (P) of the motor, expressed in the following equation:

$$P = T \cdot n, \tag{1}$$

where the Torque (T) is a function of the motor current and the Speed (n) is a function of the frequency (f_{mod}) of the modulating voltage synthesized by the converter. In the case of SiC technology, which operates at significantly higher switching frequencies (f_{sw}) than silicon, the f_{mod} can be increased (maintaining an adequate frequency modulation ratio and with reduced switching losses), so that the machine can operate at high speeds (eg, n $\simeq$ 15.000 rpm[46,178]). This increase in speed means that the inverter can be sized to operate at lower currents maintaining the same power ratings. In this way, the rating of the currents of the SiC power modules will never be as critical as the silicon modules (lower currents).

1099114x, 2022, 15, Downloaded from https://onlinelibrary.wiley.com/doi/10.1002/er.8581 by Universidad Del Pais Vasco, Wiley Online Library on [17/01/2023]. See the Terms and Conditions (https://onlinelibrary.wiley.com/terms-and-conditions) on Wiley Online Library for rules of use; OA articles are governed by the applicable Creative Commons License

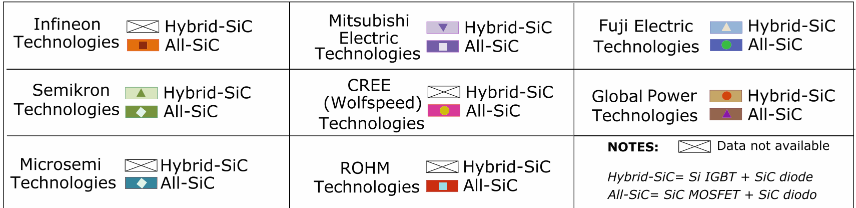

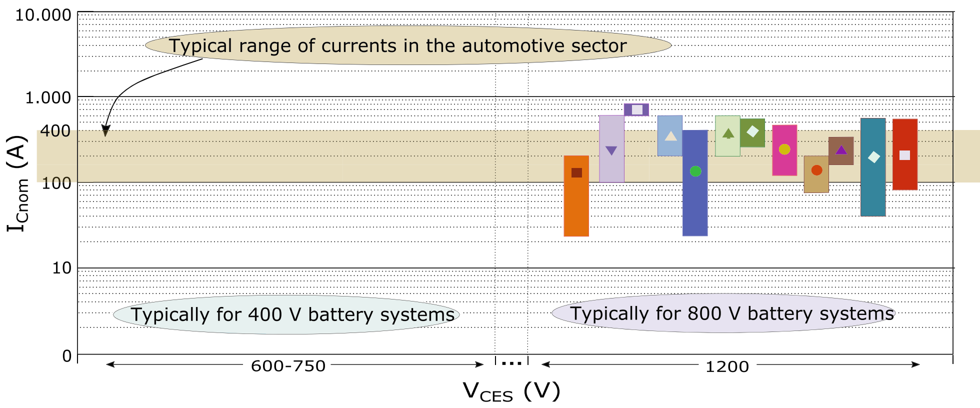

(A) Modules for the Half-Bridge topology (2-in-1).

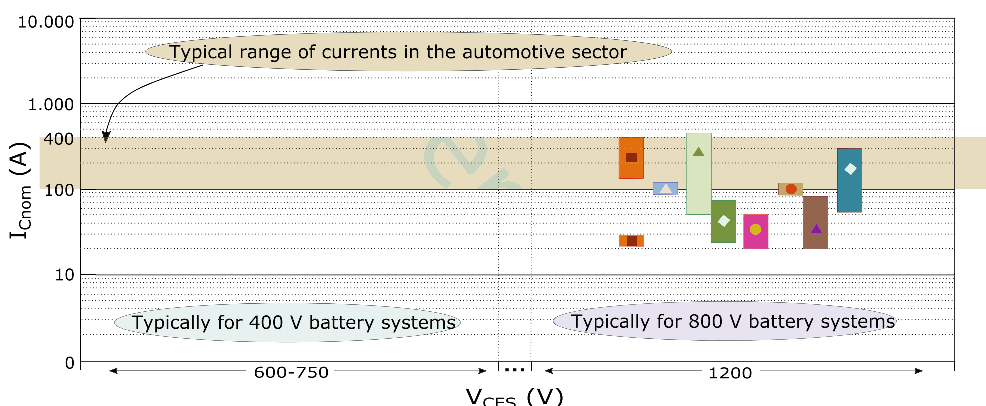

(B) Modules for the Voltage Source Inverter topology (6-in-1).

FIGURE 14 Operating range of power modules incorporating SiC technologies based on information from the manufacturer, considering the nominal current and the blocking voltage

According to the scientific literature[143,187-190] on *GaN* technology, this technology is expected to be competitive against *Si* and SiC in future automotive and high power density applications, which will require higher switching frequencies for medium voltages. However, with regard to *GaN* power modules for the powertrain of the electric vehicle, at the moment there is no catalog of commercial solutions (in general, there are only prototypes in the experimental phase). Therefore, the same comparative analysis cannot be performed as in the case of *Si* and SiC. As an example, the manufacturer of *GaN* Systems has presented a prototype of a *GaN* module made by Silver-micro (GS-EVM-3PH-650V300A-SM1). The module consists of a three-phase traction inverter—75 kW, 650 V, and 300 A per - using 12 GS-065-150-1-D devices from GaN Systems that theoretically permit a 99% reduction in switching losses compared to *Si* IGBT modules for automotive purposes.[36]

As there is a wide range of discrete devices and power modules technologies, in the following, a review of different design aspects for power semiconductor technologies will be performed. Among these aspects, the most important alternatives of packages and housings are shown, the different constituent layers of the power modules are analyzed (interconnection, substrate, base-plate, etc.), the most important cooling types are reviewed and, finally, parasitic effects such as stray inductances are analyzed.

4 | INTERNAL STRUCTURE AND CHARACTERISTICS OF POWER MODULES

Power semiconductors (bare dies) have to be integrated in packages to form a power converter, either in power modules or discrete semiconductors. Usually, with some

1099114x, 2022, 15, Downloaded from https://onlinelibrary.wiley.com/doi/10.1002/er.8581 by Universidad Del Pais Vasco, Wiley Online Library on [17/01/2023]. See the Terms and Conditions (https://onlinelibrary.wiley.com/terms-and-conditions) on Wiley Online Library for rules of use; OA articles are governed by the applicable Creative Commons License

TABLE 3 Examples of some automotive power modules

Topology	Manufacturer	Technology	Part	Package (Tables 4 and 5)	V_{block} (V)	$I_{@Tc\,25^oC}$ (A)	L_{Stray} (nH)	R_{th} (K/W)[b] IGBT/MOSFET	R_{th} (K/W)[b] Diode
6-in-1	Fuji Electric	*Si*	6MBI800XV-075 V-01	-	750	800	15	JF = 0.141	-
	GaN Systems	*GaN*	GSEVM3PH650V300ASM1	①	650	300	[a]	JC = 0.200	-
	Hitachi	*Si*	MBB400TX12A	②	1200	400	40	JW = 0.138	JW = 0.168
		Si	MBB500TX7B	②	750	500	30	JW = 0.216	JW = 0.275
		Si	MBB600TV6A	②	650	600	30	JW = 0.145	JW = 0.210
		Si	MBB800TV7A	②	700	800	30	JW = 0.135	JW = 0.165
		Si	MBB900TX7B	②	750	900	30	JW = 0.138	JW = 0.165
	Infineon	*Si*	FS650R08A4P2	-	750	650	15	JF = 0.170	JF = 0.230
		Si	FS75R07W2E3-B11A	-	650	95	35	JC = 0.500	JC = 0.700
		Si	FS820R08A6P2B	③	750	820	8	JF = 0.120	JF = 0.175
	Microsemi	Full-SiC	APTMC120TAM12CTPAG	④	1200	220	[a]	JC = 0.135	JC = 0.450
	Mitsubishi	*Si*	CT600CJ1A060	⑤	650	600	[a]	[a]	[a]
		Si	SEMiX151GD066HDs	-	600	150	20	JC = 0.210	JC = 0.360
		Si	SEMiX151GD126HDs	-	1200	100	20	JS = 0.092	JS = 0.155
		Si	SKiM459GD12E4V2	⑥	1200	450	10	JS = 0.092	JS = 0.155
	Semikron	Hybrid-SiC	SKiM459GD12F4V4	⑥	1200	450	10	JS = 0.099	JS = 0.172
	ST	Full-SiC	ADP300120W2-L	-	1200	290	10	JF = 0.120	-
2-in-1	Cree	Full-SiC	CAB011M12FM3	⑦	1200	105	11.4	JC = 0.553	-
		Full-SiC	CAB450M12XM3	⑧	1200	450	6.7	JC = 0.110	-
		Full-SiC	CAB530M12BM3	-	1200	530	11.1	JC = 0.065	-
		Full-SiC	CAB760M12HM3	⑨	1200	760	4.9	JC = 0.068	-
	Hitachi	Si	Customized	⑩	700	325[c]	[a]	[a]	[a]
	Infineon	*Si*	FF450R08A03P2	⑪	750	450	15	JC = 0.090	JC = 0.145
		Full-SiC	FF8MR12W2M1-B11	-	1200	150	8	JH = 0.346	-
	Microsemi	*Si*	APTGTQ200A65T3G	⑫	650	200	[a]	JC = 0.310	JC = 0.350
		Full-SiC	MSCSM120AM02CT6LIAG	-	1200	947	3	JC = 0.040	JC = 0.109
	Mitsubishi	*Si*	CT600DJH060	⑬	650	600	[a]	[a]	[a]

1099114x, 2022, 15, Downloaded from https://onlinelibrary.wiley.com/doi/10.1002/er.8581 by Universidad Del Pais Vasco, Wiley Online Library on [17/01/2023]. See the Terms and Conditions (https://onlinelibrary.wiley.com/terms-and-conditions) on Wiley Online Library for rules of use; OA articles are governed by the applicable Creative Commons License

TABLE 3 (Continued)

Topology	Manufacturer	Technology	Part	Package (Tables 4 and 5)	V_{block} (V)	$I_{@Tc\ 25°C}$ (A)	L_{Stray} (nH)	R_{th} (K/W)[b] IGBT/MOSFET	Diode
	ROHM	Full-SiC	BSM300D12P2E001	⑭	1200	300	13	JC = 0.080	
		Full-SiC	BSM600D12P3G001	⑭	1200	576	10	JC = 0.061	JC = 0.080
	Semikron	Hybrid-SiC	SKM200GB12T4SiC2	⑮	1200	200	15	JS = 0.014	JS = 0.210
		Full-SiC	SKM500MB120SC	⑮	1200	485	15	CS = 0.013	-
1-in-1	Toyota/Denso	Si	Customized	⑯	650	180[c]	[a]	[a]	[a]
	Cree/Delphi	Si	Customized	⑰	650	285[c]	[a]	[a]	[a]
	ST	Si	Customized	⑱	650	100[c]	[a]	[a]	[a]

[a]Data not provided by the manufacturer.
[b]CS, case to sink; JC, junction to case; JF, junction to fluid; JH, junction to heatsink; JS, junction to sink; JW, junction to wind.
[c]The current data are provided in rms values. However, it is not very precise, as it may in some cases be the nominal current and, in other cases, the maximum current.

exception, power modules are used instead of discrete elements in electric vehicles. In this context, SiC devices are also rapidly gaining prominence, while *GaN* devices are hardly used; smaller devices are being manufactured gaining power density; heat extraction is being optimized and, at the same time, stray inductances reduced; manufacturers are likewise developing customized power-module designs to adapt to the needs of each manufacturer.

Table 3 shows examples of some outstanding power modules from different manufacturers, identifying the module architecture, semiconductor technologies, and operating ranges, as well as stray inductance and thermal resistance coefficients of the modules. Likewise, Tables 4 and 5 show some examples of the most relevant power module packages where *Si*, SiC, and *GaN* semiconductors are used. Lastly, Figure 15 shows (including information about the voltage and current ranges of each package, as well as the stray inductances[179-186] and the thermal characteristics) some examples of discrete semiconductor packages to be used for the electric vehicle powertrain. Thermal resistance (R_{th}) is within the range of 0.2 K/W and 0.4 K/W for power modules and for discrete devices, respectively, and stray inductances within the range of around 10 to 15 nH and 15 to 25 nH for power modules and TO-247 packages respectively. Likewise, although the highlights and the main innovations of each package are shown in the above-mentioned tables and figures, all these aspects are analyzed in greater depth in this section and in the following one.

Taking into account the importance of the power modules, their internal structure and the parameters that most affect their performance are exhaustively analyzed below.

4.1 | Power module vertical structures (stack-up)

Power modules have some structural advantages when compared with discrete devices, mainly due to the incorporation of inorganic substrates (usually DBCs).[206,207] As a result, they generally have the ability to conduct high currents¶¶¶¶. The highly integrated components provide a high power density.[208] In addition, their robustness and mechanical stability make them an ideal solution for the use of bare dies, as they can withstand thermal cycle variations and evacuate heat flows efficiently. These attributes are due to their high thermal conductivity (low thermal resistance, R_{th}) and their high capacity to dissipate the heat generated by the semiconductors throughout the substrate*****,[208] mainly vertically. Moreover, they can be easily assembled with cooling systems, since

1099114x, 2022, 15, Downloaded from https://onlinelibrary.wiley.com/doi/10.1002/er.8581 by Universidad Del Pais Vasco, Wiley Online Library on [17/01/2023]. See the Terms and Conditions (https://onlinelibrary.wiley.com/terms-and-conditions) on Wiley Online Library for rules of use; OA articles are governed by the applicable Creative Commons License

TABLE 4 Examples of some standardized and customized electric vehicle power module housings and their main innovations (1/2)

No.	Photo of package	Manufacturer and package	Main innovations of the modules of each package	Refs.
①		GaN Systems HybridPack	The novelty of this power module is the use of *GaN* technology, as there are not many commercial modules of this material. It has the advantage of ultra-low switching losses, zero QRR, and ultra-high $^{dV}/_{dt}$ ruggedness. The package is a modified well-known HybridPACK, although it includes such features as press-fit pins for ease of assembly and high thermal conductivity base-plates (Figure 16-⑥)	191
②		Hitachi Suijin Series	This package provides high function 6-in-1 modules incorporating direct water-cooling with pin-fins (Figure 18). Modules in the series use the same package, so that the common mechanical design can be reused with converters of different ratings. It includes the latest generation Hitachi IGBT (≈MPT), which reduces energy losses and improves controllability compared to conventional trench IGBT. Likewise, it uses copper sintering to improve die attach (Figure 16-③)	192
③		Infineon HybridPack Drive	This package is commonly used in electric vehicles and has been optimized for this purpose It provides low stray inductance (Section 5.1), heatsink with pin-fins (Figure 18) and press-fit signal terminals to avoid additional time-consuming selective soldering processes. There are a lot of different *Si*-based and SiC-based (semiconductor technologies) solutions using this package	196
④		Microsemi SP6-P	This alternative is one of the most compact 6-in-1 configurations (reduced size), in addition to having a low thermal resistance. It includes SiC technology with an *AlN* substrate (Table 6-④b) to improve thermal behavior. The terminals, both for power and for control signals, are solderable for easing the connection with a PCB	194
⑤		Mitsubishi J1-Series	The power modules of this package use the 7th-generation CSTBT chip technology (Figure 4-④). The package includes Direct Lead Bonding (DLB) (wirebond-less) which ensures high reliability (Figure 16-①). It also includes a direct water-cooling structure with aluminum cooling fins to prevent the devices from overheating. It also stands out because of its reduced size compared to other packages, which improves its power density	195
⑥		Semikron Skim 93	This type of power module is insulated in so far as it uses a Al_2O_3 DBC ceramic substrate (Table 6-④b). It implements solderless sinter technology (Figure 16-③), pressure contact technology for terminals and has a spring contact system to attach the PCB driver to the control terminals. Likewise, it has a reduced stray inductance compared to other power modules	196
⑦		Cree FM 3	This module package is a 2-in-1 with reduced size and high power density. It includes SiC technology with ultra-low losses and high-frequency operation. Thermally speaking, there is no baseplate layer for this option, so the module needs to include a Thermal Interface Material (TIM) for its indirect cooling systems	197

1099114x, 2022, 15, Downloaded from https://onlinelibrary.wiley.com/doi/10.1002/er.8581 by Universidad Del Pais Vasco, Wiley Online Library on [17/01/2023]. See the Terms and Conditions (https://onlinelibrary.wiley.com/terms-and-conditions) on Wiley Online Library for rules of use; OA articles are governed by the applicable Creative Commons License

1099114x, 2022, 15, Downloaded from https://onlinelibrary.wiley.com/doi/10.1002/er.8581 by Universidad Del Pais Vasco, Wiley Online Library on [17/01/2023]. See the Terms and Conditions (https://onlinelibrary.wiley.com/terms-and-conditions) on Wiley Online Library for rules of use; OA articles are governed by the applicable Creative Commons License

TABLE 4 (Continued)

No.	Photo of package	Manufacturer and package	Main innovations of the modules of each package	Refs.
⑧		Cree XM 3	An outstanding aspect of this package is its reliability. It provides greatly reduced stray inductance with a dedicated drain Kelvin pin that enables direct voltage sensing for gate driver overcurrent protection (Section 5.1). It also includes a Si_3N_4 insulator and a copper baseplate that provides small thermal resistance (Table 6-④b and ⑥)	198
⑨		Cree HM 3	This package stands out for its high reliability. The stray inductance is optimized more than the XM 3 package (Table 3-⑧) and its thermal resistance is also reduced. It includes a lightweight *AlSiC* baseplate (Figure 16-⑥) and a high-reliability Si_3N_4 insulator (Table 6-④b). Furthermore, the SiC technology in use provides very low power losses compared to other modules	199

TABLE 5 Examples of some standardized and customized electric vehicle power module housings and their main innovations (2/2)

No.	Photo of package	Manufacturer and package	Main innovations of the modules of each package	Refs.
⑩		Hitachi DSC package used in Audi e-Tron	This 2-in-1 module consisting of a trench silicon IGBT/diode significantly increases both the power density and the cooling efficiency of the module, due to double-sided cooling (Figure 17). By removing heat from both the top and bottom side and eliminating thermal grease and the baseplate, a better heat dissipation is achieved. Cooling efficiency is also improved by using resin and isolation sheets of high thermal conductivity between the copper lead frame (Figure 16-①) and the heatsink with pin-fins	2
⑪		Infineon Hybrid Pack DSC	HybridPACK DSC is a very compact 2-in-1 package targeting electric vehicles. The innovative and small package is designed for double-sided cooling (Figure 17, double-sided DBC) with superior thermal performance. Compared to other single side solutions, the thermal resistance of modules with this package is therefore reduced	200
⑫		Microsemi SP3F	One of the main characteristics of this type of package is its small size and reduced volume, as well as the fact that it includes solder terminals for easing the connection of both power and control signals with PCB substrates for power and driver connections	201
⑬		Mitsubishi J-Series T-PM	This type of module stands out as a very compact solution that can increase power density. It has a high-reliability Direct Lead Bonding (DLB) structure which reduces wire resistance and inductance (Figure 16-①). Likewise, semiconductor devices of modules with this package also have a low collector-emitter saturation voltage which improves conduction losses	202
⑭		Rohm E and G series	This solution consists of 2-in-1 SiC half-bridge power modules with fewer losses than *Si* IGBT modules (Figure 12(B)), achieving switching frequencies of 50 kHz and parasitic inductance of 10 to 13 nH (Table 3). The baseplate is connected to the heatsink with a TIM layer, applying a constant torque over the module. Likewise, the control terminals can be soldered to a PCB or connected via pressure contact	203

(Continues)

TABLE 5 (Continued)

No.	Photo of package	Manufacturer and package	Main innovations of the modules of each package	Refs.
⑮		Semikron Semitrans 3	The novelty of this series of power module is linked to SiC technology: both hybrid and full-SiC solutions. Furthermore, it is optimized to switch at higher frequencies and reduce power losses. This solution uses screw terminals which facilitate the interconnection with external busbars	204
⑯		Toyota & Denso Prius fourth gen.	This module is mainly targeted at improving power densities and reducing parasitic inductance. The module features double-sided cooling (Figure 17) with isolated sheets and its dimensions improve modularity. Instead of using wirebonds, the die is attached thanks to the flip-chip soldering technique (Figure 16-①) to a nickel (*Ni*) electrode. Likewise, another interesting characteristic is the reduction of conduction losses	2
⑰		Delphi & Cree Chevrolet Volt	This 1-in-1 IGBT/diode module uses the flip-chip soldering technique instead of wirebonds to improve the current distribution and the lifetime of the die interconnection (Figure 16-①). The *AlSiC* baseplate layer is removed (Table 6-④b and ⑥) and the cooling system is directly connected to the ceramic substrate, whose materials have a CTE of greater similarity to the die to mitigate thermal stress. Moreover, fewer layers between the die and the coolant reduce the thermal resistance	2
⑱		STMicroelectronics Tesla Model 3	The main novelty of the module was the incorporation of SiC device. With a 1-in-1 custom design that includes pin-fins as the heatsink. The package is produced with silver sintering technology (Figure 16-③) to improve the module reliability (<thermal resistance) and wirebonds are replaced by copper lead (ribbon bonding, Figure 16-①), which improves heat dissipation and power capability	205

the substrate provides electrical insulation without the need to incorporate additional insulating layers.[209,210]

The conventional power module structure, also known as the vertical structure, is mainly defined by the following layers (Figure 16A[1] and Table 6):

- *Layer 1: Interconnection* (Figure 16A-①). It establishes the connection between the top layer of the dies and the top layer of the substrate (Figure 16④a). The most commonly used technology is aluminium wirebonding (around 300 μm in diameter).[211] There are also alternatives to wirebondings, such as flip-chip, ribbon bonding, direct lead bonding (DLB), and copper posts and areas,[1,206] which increase the contact surface with the dies, increasing the current carrying capacity, and reducing the thermal path R_{th}.[212] However, the use of these new solutions requires the modification of the metallization layers (Figure 16②a), which increases the manufacturing costs.[213]
- *Layer 2: Semiconductors* (Figure 16A-②). Dies (Figure 16②b) have metallization layers††††† (Figure 16②a) on both surfaces to connect the top surface of the semiconductors to the wirebondings and the bottom surface of the semiconductor to the top layer of the substrate.[1]
- *Layers 3 and 5: Attach-solder joint* (Figure 16A-③ and ⑤). A series of metallic alloys are placed between the dies (Figure 16②b) and the top layer of the substrate (Figure 16④a), and between the bottom layer of the substrate (Figure 16④c) and the base-plate (Figure 16A-⑥), employing sintering or brazing processes,[214] to provide the necessary mechanical, thermal, and electrical bonding between these surfaces. In this way, these layers bond the semiconductors to the substrate and the

1099114x, 2022, 15, Downloaded from https://onlinelibrary.wiley.com/doi/10.1002/er.8581 by Universidad Del Pais Vasco, Wiley Online Library on [17/01/2023]. See the Terms and Conditions (https://onlinelibrary.wiley.com/terms-and-conditions) on Wiley Online Library for rules of use; OA articles are governed by the applicable Creative Commons License

Package	SOT-227	TO-247	TO-220	TO-263	TO-LL	GaNPX
Technology	Si - SiC	Si - SiC	Si - SiC	Si - SiC	Si - SiC	GaN
V_{range} a)	600 V - 1200 V	600 V - 1700 V	600 V - 1200 V	600 V - 650 V	600 V - 650 V	600 V - 650 V
$I_{@Tc=25^{\circ}C}$ b)	200 A	160 A	120 A	35 A	30 A	60 A
R_{th}	0.10 K/W - 0.5 K/W	0.10 K/W - 1.1 K/W	0.10 K/W - 0.5 K/W	0.4 K/W - 0.6 K/W	0.46 K/W - 1.2 K/W	0.3 K/W - 4.0 K/W
L_{paras}	~ 5 nH	15 nH - 25 nH	8 nH - 12 nH	5 nH - 8 nH	1 nH - 2 nH	0.2 nH - 2 nH

a) V_{range} blocking voltage: collector-emitter (IGBT); drain-source (MOSFET); reverse blocking voltage (diode).
b) Maximum currents are limited by packages and leads. The silicon die can withstand even greater current limits.

FIGURE 15 Some of the most widely used packages in power converters and some of their most important characteristics[179-186]

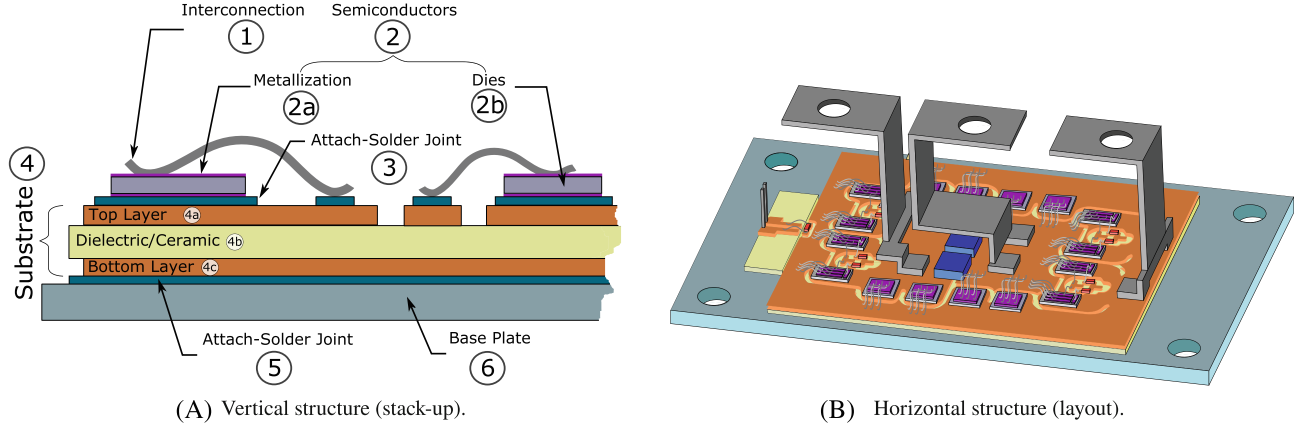

FIGURE 16 General vertical and horizontal structure for a typical power module[1]

substrate to the base-plate. The conventional materials in the *Si* modules have to date been *SnPb* and *SnAgPb* (Table 6),[206] which withstand temperatures within the range of 150°C to 175°C.[137] However, alternatives are emerging to improve this performance based on gold alloys (>280°C)‡‡‡‡‡ and silver-indium alloys (206°C).[206,217] Although the main advances toward achieving better thermal conductivities and higher reliability against thermal fatigue are associated with silver sintering technique (>220°C),[218,219] and the sintering of nano-copper materials.[220]

- *Layer 4: Substrate* (Figure 16A-④). The inorganic structure is formed of two conductive layers (Figure 16④a and ④c) separated by either a dielectric or a ceramic plate (Figure 16④b). The top conductive layer provides a surface for electrical connections to power semiconductors and other components (mainly passive elements and power and control terminals), and to provide good thermal conductivity to spread heat to the ceramic substrate and to the bottom conductive layer. The most common solution is based on Direct Bonded Copper (DBC) substrate§§§§§.[221] In terms of innovations, Insulated Metal Substrate (IMS) has better thermal performance than PCB and lower manufacturing costs than traditional DBC substrate.[223,224] New substrates are also evolving toward thinner structures, for both conductive layers (leadframe technology)[225] and ceramics (thin-film insulation technology),[226] thus improving the thermal behavior of the structure and facilitating component integration.
- *Layer 6: Base-plate* (Figure 16A-⑥). A metallic (copper or aluminum alloy) surface, whose main function is to provide mechanical support to the rest of layers, as well as to absorb and homogeneously to distribute heat over the entire surface of the inorganic substrate, so as to transmit it to the cooling liquid.[137,206]

All these layers (Figure 16A) determine the thermal behavior between the power semiconductors and the

1099114x, 2022, 15, Downloaded from https://onlinelibrary.wiley.com/doi/10.1002/er.8581 by Universidad Del Pais Vasco, Wiley Online Library on [17/01/2023]. See the Terms and Conditions (https://onlinelibrary.wiley.com/terms-and-conditions) on Wiley Online Library for rules of use; OA articles are governed by the applicable Creative Commons License

TABLE 6 Power modules vertical structures and cooling systems: main features[1,85,206,215,216]

Figure 16A	Layer	Material	Thickness (mm)	Conductivity λ (W/m·K)	CTE (ppm/°C)	Role
①	Interconnection	Al		205–230	23.8–26.4	
		Cu	0.075 -	386–398	17.8	Connect the top terminals of the dies
		Au	0.500	310	14	to the substrate top layer.
		Ag		429	19	
②a	Metallization	Al	0.004 -	205–230	23.8–26.4	Coating dies with alloys for
	(Semiconductors)	Ni/Ag	0.008	-	-	proper connection with other layers
②b	Dies	*Si*	0.250 -	170	2.6–3.3	Permit current blocking or
	(Semiconductors)	SiC		300–400	4–6	conduction according to polarization
		GaN	0.380	130	3–6	
③	Attach solder	*Sn*96.5/*Ag*3.5	0.050 -	33	30	Provide electrical connection and
	joint	*Sn*10/*Pb*88/*Ag*2		27	29	mechanical joint between ②b and ④a
		*Sn*10/*Pb*9	0.127	25	29	
④a	Top conductor	*Cu*		386 ∼ 398	17.8	Provide horizontal electrical
	(Vertical)	*Al*	0.127 -	205 ∼ 230	23.8 ∼ 26.4	connection and vertical thermal
		*Cu*50/*Mo*50	0.600	250	10	conduction
		*Cu*30/*Mo*70		195	7.5	
④b	Ceramics	Al_2O_3		33	7.2	Provide electrical insulation
	(Substrate)	*AlN*	0.250 -	170	4.5	and vertical thermal conduction
		BeO	1.000	270	7	
		Si_3N_4		60	2.7	
④c	Bottom conductor	Same as the layer ④a				Provide thermal conduction
	(Substrate)					and mechanical support
⑤	Attach solder	Same as layer ③				Provide thermal connection
	joint					and mechanical join between ④c y ⑥
⑥	Base-plate	*Cu*	2.000	386 ∼ 398	17.8	Provide mechanical support and
		Al		205 ∼ 230	23.8 ∼ 26.4	temperature diffusion over the entire
		*Mo*85/*Cu*15		165	6.8	surface (heat-spreading)
		AlSiC		180 ∼ 200	7 ∼ 12	
⑦	TIM[a]	*Standard*	0.050	-	-	Improve thermal transmission
		ZnO		-	-	between layers ⑥ and ⑧ (as long as
		Dow Corning SE4422		-	-	this layer is necessary)
⑧	Cold-plate	*Al*	>2.000[b]	-	-	Cooling the power module
		CoolPoly E5101		-	-	when in contact with
		Graphite		-	-	the coolant
		AlSiC		-	-	

Notes: Layers 7 and 8 are not part of the power module in Figure 16A. They are the cooling system layers of the module.
[a]In some cases, such as direct cooling by means of pin-fins, this layer is unnecessary.
[b]The thickness of this layer is determined by the power-module cooling system.

coolant, so materials with high thermal conductivity (λ) are therefore essential to achieve a low thermal resistance (R_{th}).[96] Usually, *Si* power modules are limited to a R_{th} per area unit of 0.3-0.4 K·cm^2/W (70 KVA modules).[206] In the case of WBG devices, especially SiC devices, the smallest die sizes appear in the most compact designs

1099114x, 2022, 15, Downloaded from https://onlinelibrary.wiley.com/doi/10.1002/er.8581 by Universidad Del Pais Vasco, Wiley Online Library on [17/01/2023]. See the Terms and Conditions (https://onlinelibrary.wiley.com/terms-and-conditions) on Wiley Online Library for rules of use; OA articles are governed by the applicable Creative Commons License

1099114x, 2022, 15, Downloaded from https://onlinelibrary.wiley.com/doi/10.1002/er.8581 by Universidad Del Pais Vasco, Wiley Online Library on [17/01/2023]. See the Terms and Conditions (https://onlinelibrary.wiley.com/terms-and-conditions) on Wiley Online Library for rules of use; OA articles are governed by the applicable Creative Commons License

requiring a R_{th} around 0.2 K·cm^2/W.[206] Such a reduction in size also limits the number of wirebondings that can be placed on the die surface (Figure 16②a), which affects the current that can circulate through the module¶¶¶¶¶.

Regarding mechanical aspects, the thermal expansion coefficient (CTE or α) of a material is particularly relevant, as it indicates the expansion/contraction they may undergo due to temperature variations. In the case of power modules, these CTEs (Table 6) should be as similar as possible to avoid mechanical fatigue between layers[20,96] that causes reliability problems and reduces the module's lifetime******.[227,228] This problem is especially relevant in soldered and interconnection layers.[229] The main power-module innovations have been focused on new designs and materials,[230,231] to improve design reliability, to introduce WBG technology (mainly SiC) into new designs, and to take advantage of their technological benefits (high temperature operation, etc.). The main power-module innovations are focused on new designs and materials.[230,231] These can be divided into four categories (Figure 17[206]):

1. Overmold: this technology employs lead-frame and thin-film insulation substrates that directly bind the semiconductors, thus increasing the connection surface of the dies.[29] Generally, modules using this technology have lower stray inductances and the R_{th} is considerably reduced compared to the conventional DBC structure. The latter structure ensures that the temperature will be more evenly distributed over the surfaces. Even so, it still uses wirebonding for the control terminals.[235]
2. Double-sided DBC: this structure is very similar to the overmold, in this case, the interconnecting wirebondings are replaced by copper areas on conventional DBC†††††† substrates.[236] These areas expand the contact surface with the die, which results in a homogeneous distribution on both sides, while the cooling system reduces any thermal peaks.[237]
3. Integrated Power Module (IPM): this architecture integrates the control driver and snubber capacitors of power semiconductors within the same module.[238] As a result, there are fewer stray inductances of the switching loops and the switching speeds are therefore higher. However, these components are subjected to higher operating temperatures‡‡‡‡‡‡[239] and the limited space of the module limits the incorporation of these capacitors.
4. 3D structure: a structure that integrates various substrates in a vertical structure, such as inorganic substrates, gate driver ICs, and heatsinks.[206,240] In this way, stray inductances are reduced and the design is endowed with great flexibility.[241] However, thermal management is much more complex, due to the different propagation paths and non-uniformity of temperature in each of the substrates.[215]

4.2 | Cooling technologies

The introduction of new devices, assembly methods, and manufacturing techniques is contributing to the increase in power density.[232] Generally speaking, the effects of constant heating/cooling cycles required by the electric vehicle application need to be mitigated to meet power-density and system-reliability requirements making it necessary to use liquid cooling

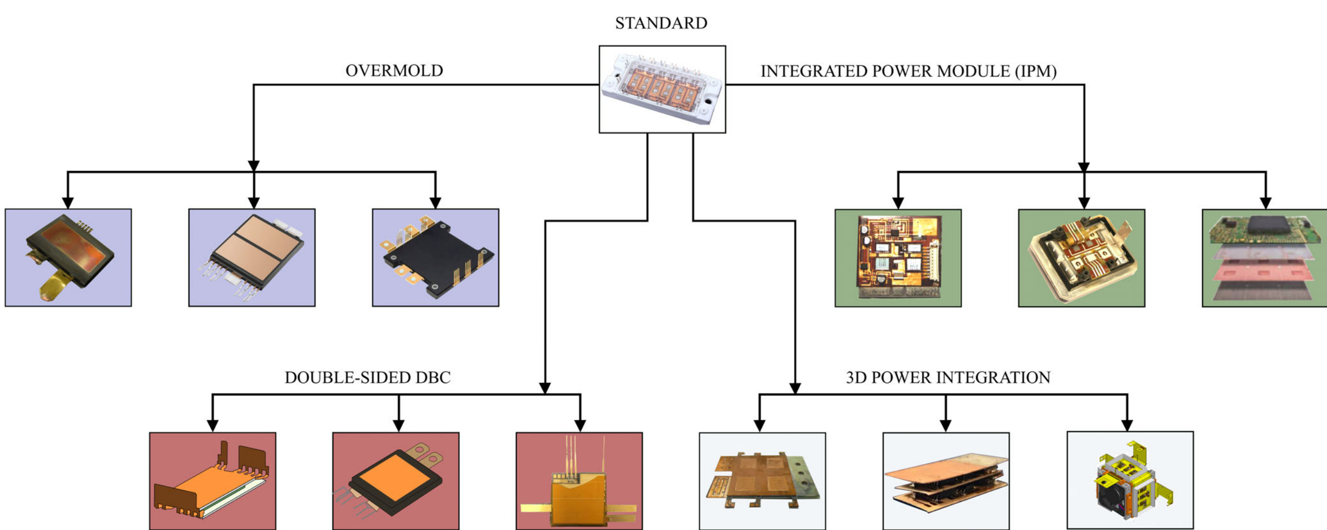

FIGURE 17 New vertical designs for power modules[206]: Overmold[29,67,68]; Double-sided DBC[69-72]; IPM[73-75]; 3D integration[65,76,77]

systems. Despite being more complex solutions compared to air cooling§§§§§§ due to the greater number of components, volume, and weight that reduces the overall power density, they are the most appropriate solution, as the heat transfer capacity of liquid is much greater compared to air. The main liquid cooling methods (Figure 18) that are in use are described below[209,233,242]:

- Indirect liquid cooling[243]: compared to natural and forced air cooling, indirect liquid cooling reduces the R_{th}. The cold-plates[244] (Figure 18-②), a system where there is no direct contact between the semiconductors and the coolant, stand out. In this structure there is a Thermal Interface Material (TIM, Table 6) layer that simplifies the assembly process, although it increases the R_{th} (it can contribute up to 30% of the total thermal resistance[245]) and makes direct cooling methods, in which this intermediate element is not used, more efficient.
- Direct liquid cooling[246]: this technique eliminates the TIM layer, so that the coolant is in direct contact with the surface to be cooled (Figure 18-③a). Direct liquid cooling is the technique of choice in electric vehicle applications,[247] as R_{th} is ostensibly reduced, resulting in high energy density solutions. Several technologies are available:
- Direct cooling via pin-fins[247-249] (Figure 18-③b): a series of pin-fins of various geometries (diamond, circular, elliptical, etc.) are incorporated on the back of a base-plate. The pin-fins increase the contact surface between the coolant and the module, resulting in greater heat exchange. This type of cooling is the solution employed by Infineon's HybridPACK family of

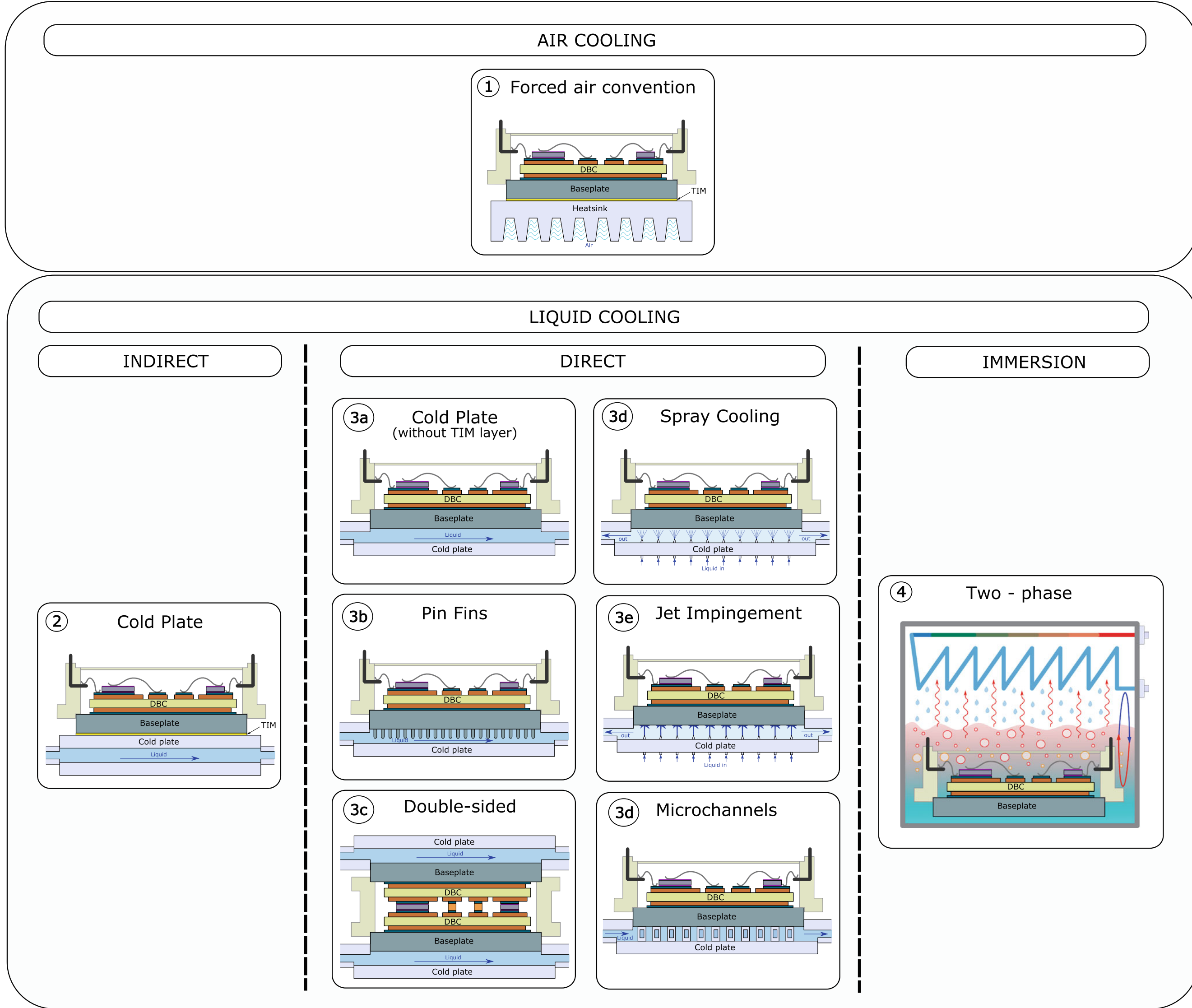

FIGURE 18 Active cooling systems for power modules[209,232-234]

1099114x, 2022, 15, Downloaded from https://onlinelibrary.wiley.com/doi/10.1002/er.8581 by Universidad Del Pais Vasco, Wiley Online Library on [17/01/2023]. See the Terms and Conditions (https://onlinelibrary.wiley.com/terms-and-conditions) on Wiley Online Library for rules of use; OA articles are governed by the applicable Creative Commons License

power modules widely used in electric vehicle applications.

- Double-sided direct cooling[243,250,251] (Figure 18-③c): heat is dissipated from both sides of the semiconductors, which are assembled between two substrates (the double-sided DBC module structure described above is mandatory). Assembly becomes more complex due to the need for new interconnection techniques, the availability of semiconductors suitable for sintering on both sides, insulation requirements, mechanical stability requirements (fatigue), thermo-mechanical mismatches (CTE) between the materials involved, etc. Even so, this technology is quickly developing, due to the increment in power density and cost reductions.[252]
- There are other cooling methods such as spray cooling[209,253] (Figure 18-③d), jet impingement cooling[209,254] (Figure 18-③e), and the use of microchannels[255,256] inside cold-plates (Figure 18-③d), although they are much more complex to implement in electric vehicle applications.
- Two-phase immersion cooling[209,253] (Figure 18-④): a cooling system that involves the immersion of the semiconductors in a container of dielectric liquid. It offers a high heat transfer coefficient¶¶¶¶¶¶ and considerably reduces (compared to previous techniques) the thermal resistance between the semiconductor and the fluid. Despite these advantages, this technique requires somewhat unconventional designs, limiting its use in the electric vehicle powertrain.

5 | OTHER DESIGN AND OPERATIONAL CONSIDERATIONS RELATED TO RELIABILITY

Apart from the vertical stack-ups and the cooling systems that are related to the thermal overstress, other reliability-related aspects of discrete semiconductors and power modules need to be considered. It is worth mentioning that the reliability enhancement of general-purpose power converters and those particular inverters of the automotive industry is usually based on multi-disciplinary approaches, among which stand out physics-of-failure, design-for-reliability, accelerated testing, and condition monitoring.[79] These aspects are fundamental for reliable systems and there are many studies on their advances.[12,78-81]

The reliability methods are usually focused on evaluating failure mechanisms,[12,80,81] analyzing data and testing methods,[78,80] accumulated damage modeling and lifetime prediction,[12,81,257] and the implementation of efficient maintenance and reliability improvement schemes.[78,81] In any case, and regardless of the approach toward reliability, power semiconductors usually fail because they operate under conditions that stress beyond their maximum ratings. Moreover, there are many factors affecting reliability such as electrical faults, heat, chemicals, radiation, and mechanical stresses[80] which can occur in different layers of discrete devices******* and power modules[258,259] (Section 4):

1. Interconnection - Figure 16A-①: In general, when a wire-bond connection fails, the device may cause severe failure and, even, open circuit faults.[260] In fact, wire-bond degradation is one of the most common failure modes for power modules.[252] In an overcurrent condition, the wire temperature might rise to reach the melting point, at which point the wire bond at one of its two ends usually breaks. In view of the above, there has been significant research over the past few years to move away from wire bonding as an interconnection method and to introduce other alternative interconnection technologies, especially in WBG devices where the space for the wire bonds is considerably reduced.[1,261] Likewise, there are several publications that analyze how to improve reliability in relation to this topic where the main causes that can produce a failure mechanism of this type are, among others, thermal fatigue due to high current flow, mechanical stress in the bond wire due to improper bonding, and cracks at the interface between the bond wire and die.[78,257,262]
2. Metallization - Figure 16②a: these faults arise due to the electromigration of the material (usually aluminum) in the direction of current flow, due to high electric fields; alloy breakdown, due to electrical overvoltage caused by high currents; metal corrosion and wear caused by welding; and improper deposition, and mounding and cracking of the metal at the contact surfaces.[263,264]
3. Semiconductor - Figure 16②b: in addition to stress-related failures when operating above the maximum ratings of current, voltage, and temperature, the main causes of failure of the semiconductor device can be diffusion problems during its manufacturing process, defects in the semiconductor crystal, or the presence of impurities and contaminants in the material.[265,266] Moreover, there are other problems related to the formation of semiconductor junctions, doping, and temperature, for example, avalanche breakdown and latch-up effects.[267-269] Other aspects should not be overlooked such as high electric fields, transients, gate-oxide degradation, and body diode degradation, which can also cause malfunction and

1099114x, 2022, 15, Downloaded from https://onlinelibrary.wiley.com/doi/10.1002/er.8581 by Universidad Del Pais Vasco, Wiley Online Library on [17/01/2023]. See the Terms and Conditions (https://onlinelibrary.wiley.com/terms-and-conditions) on Wiley Online Library for rules of use; OA articles are governed by the applicable Creative Commons License

the destruction of discrete devices and power modules.[78,79]

4. Attach-solder joint - Figure 16A-③: Usually, this failure occurs when the die overheats due to inadequate contact between the die and the substrate, which lowers the thermal conductivity between both elements and leads to stress and cracking and, finally, device failure.[78,270] The novel improvements are focused on obtaining new Ag sintering solutions with higher λ, and CTEs similar to adjacent layers.[271] In addition, the stabilization of silver microstructures, adding nanoparticles of other materials (eg, copper), is fundamental to increase the service life of these joints.[272]
5. Substrate - Figure 16A-④: The conductor and ceramic layers typically have different shapes and/or thicknesses. Moreover, the CTE of each material varies greatly†††††††; these problems generate asymmetrical distributions of stress/strain resulting in overall warpage. Warpage variations can induce mechanical fatigue during the lifetime and represent a limiting factor for reliability.[274,275] In addition, they can even cause cracking of the substrate and rupture of power devices.

Many of the problems of each layer are technological limitations due to current materials and manufacturing techniques. However, when dealing with the design of power modules, certain improvements can be made through their electrical design. In this sense, it is important to reduce stray inductances as much as possible, and to increase both the reliability and the durability of power semiconductors.[181,182,276,277] This critical design aspect, and its implication in both discrete devices and power modules, is discussed below. Later, other aspects that are not so well known, related to inverter reliability and automotive propulsion systems are discussed. Specifically, the problems derived from the common-mode voltage together with the switching of the devices are analyzed in this document.[82-84]

5.1 | Oscillations during commutation and stray inductances

Power converters (Figure 16B) operate at switching frequencies (f_{sw}) within the range of 10-18 kHz[46] when silicon IGBTs are used, and higher frequencies when SiC MOSFET converters are used, which can go above 100 kHz.[278-280] Among other improvements, increasing the switching frequency makes it possible to improve the total harmonic distortion of the currents flowing through the motor phases of the electric vehicle. In consequence, the fundamental frequency is increased without losing signal quality, which also increases the electric motor speed. This relationship can be seen in (1). Considering such an expression, the faster the motor runs, the more power it can deliver for the same amount of torque, which is a function of current, and the latter determines, to a large extent, the size of the motor.

In addition to the switching frequency (f_{sw}), the switching speed (di/dt and dv/dt) of the semiconductor also plays a crucial role in the behavior of the converter. In electric vehicles, this speed value is within the range of 5 $KA/\mu s$, which depends on several factors, including the semiconductor gate characteristic (Q_g), the driver circuit performance, and the stray inductance of the semiconductor current commutation path. In power converters, (2) is critical, which quantifies the overvoltage peak in a semiconductor switching. The total inductance (L_{loop}) that is formed in the power loop (Figure 19) is the sum of the values of all the inductances (3) that are in the commutation path where the current flows. It must be taken into account that the different converter components (Figure 19A) such as the capacitor (L_{ESL}), the busbar (L_{bb_T}, L_{bb_B}), and the power module (L_{stray}) can all add stray inductances.

In the case of power modules, the terms related to the MOSFET drain and source ($L_{d_T}, L_{s_T}, L_{d_B}, L_{s_B}$) shown in Figure 19B can be determined by the stray inductance (L_{stray}) of the power module, given by the manufacturer. L_{stray} represents the sum of all the inductance from the positive terminal to the negative terminal (Figure 19A$\bigoplus - \ominus$). In the particular case of design with discrete semiconductors, both the stray inductances of packages (Figure 15) and the PCB paths must be taken into consideration.

$$V_L = L_{loop}\, di/dt. \tag{2}$$

$$L_{loop} = \sum L_x = L_{ESL} + L_{bb_T} + L_{bb_B} + L_{d_T} + + L_{s_T} + L_{d_B} + L_{s_B}. \tag{3}$$

The existence of these inductances causes other unwanted effects, such as overvoltages, oscillations, increased converter losses, and EMI, which can cause the failure of a power semiconductor. Indeed, there are several solutions related to reliability that are introduced and discussed to improve the power device robustness.[207,276,277,281,282] In the particular case of a MOSFET, the peak voltage (Figure 19B) is given by (4), which is directly related to the DC-bus capacitor voltage (V_C), the power loop inductances (L_{loop}), and the switching speed (di/dt).

1099114x, 2022, 15, Downloaded from https://onlinelibrary.wiley.com/doi/10.1002/er.8581 by Universidad Del Pais Vasco, Wiley Online Library on [17/01/2023]. See the Terms and Conditions (https://onlinelibrary.wiley.com/terms-and-conditions) on Wiley Online Library for rules of use; OA articles are governed by the applicable Creative Commons License

(A) Current commutation path vs internal power module layout (4 parallelized semiconductors per switch).

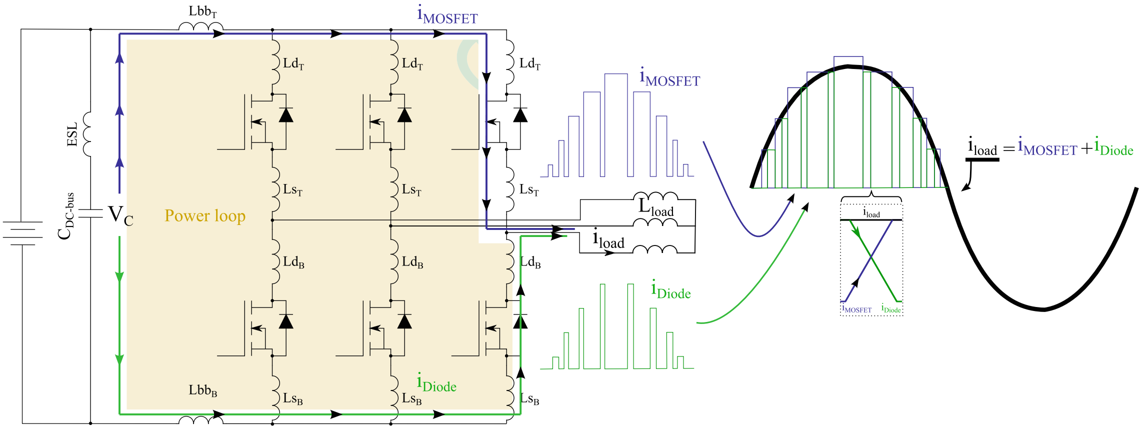

(B) Power layout commutation loops for power modules or discrete-based converters.

FIGURE 19 Commutation loops and stray inductances on power converters

$$V_{DS} \simeq V_C + V_L \simeq V_C + L_{loop}\, di/dt. \tag{4}$$

As an example, Figure 20 shows the results obtained for a specific case with a 600 V source and a 10 A load current. On the one hand, the oscillations that are created in the voltage during a switching in the case of an L_{loop} of 10 nH result in a 50 V overshoot (8.33% of the nominal voltage). On the other hand, it can be seen that when the switching is carried out in a converter with a 40 nH L_{loop} (ie, a typical value when TO-247 packages are used), the overshoot considerably increases up to 120 V (20% of the nominal voltage). Compared to a power module with a good layout design (eg, an Infineon FS820R08A6P2B power module with an 8 nH stray inductance), the additional inductance introduced by the encapsulation of the discrete semiconductors will worsen the inverter performance. A fact that explains why manufacturers are creating very low inductance discrete packages (Figure 15) to rival the behavior of the power modules. Even so, it is observed that the majority of manufacturers continue to opt for power modules instead of converters based on discrete semiconductors (Tables 3–5).

There are several techniques to prevent the aforementioned adverse effects. One of the best ways to proceed is to try to reduce stray inductances acting on the power loop (L_{loop}), for example, by adding snubber capacitors to reduce the power loop,[276,287] using low inductance bus bars,[184,277,288,289] or using low inductance packages when employing discrete semiconductors. Another technique in

1099114x, 2022, 15, Downloaded from https://onlinelibrary.wiley.com/doi/10.1002/er.8581 by Universidad Del Pais Vasco, Wiley Online Library on [17/01/2023]. See the Terms and Conditions (https://onlinelibrary.wiley.com/terms-and-conditions) on Wiley Online Library for rules of use; OA articles are governed by the applicable Creative Commons License

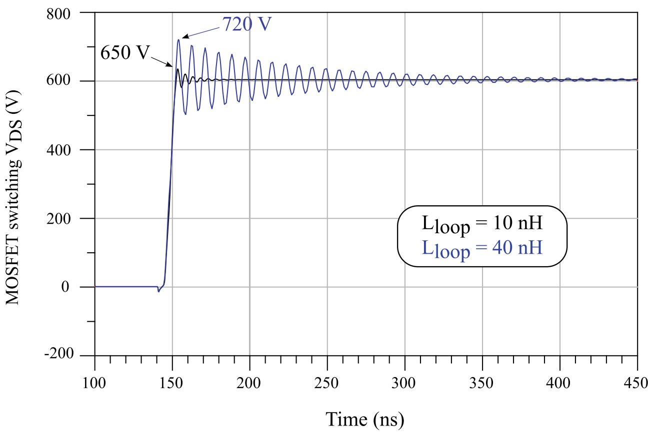

FIGURE 20 MOSFET V_{DS} voltage oscillations for 10 nH and 40 nH stray inductance power loops

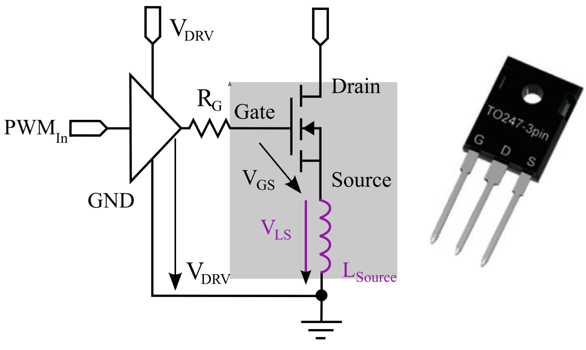

(A) Standard TO-247-3 package.

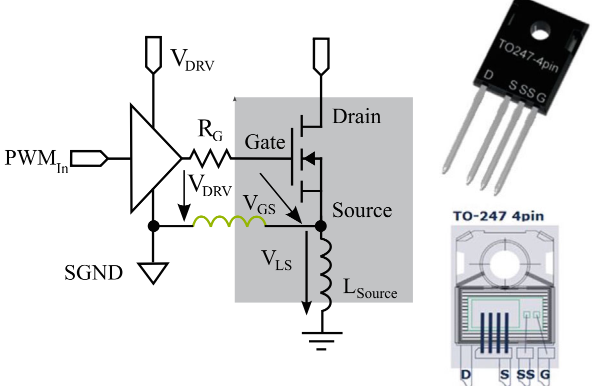

(B) Kelvin connection TO-247-4 package.

FIGURE 21 TO-247 package variants: with and without the Kelvin auxiliary connection[283-285]

use is to slow down the system (lower di/dt and dv/dt) by increasing the gate resistances (Figure 21—R_G) in the gate driver circuit.[290-292] In addition, there are some oscillation attenuation methods that act on the gate loop, such as the use of either ferrite beads[293] or RLC filters.[53] Otherwise, there are Active Gate Drivers (AGD)[294] circuits, a solution that has proven to be very useful. Yet another example of improvement in this regard is the Kelvin connection (Figure 21), a technique that allows the power loop to be decoupled from the gate loop. In this context, an example of two devices can be seen: one without a Kelvin connection (Figure 21A) and another with a Kelvin connection (Figure 21B).[283] Some of the best known examples in this sense are the SOT-227, TO-247-4, and TO-263-7 packages (Figure 22), which significantly improve the inductances that appear in the gate loop, and therefore the switching losses.[286] Kelvin connections can reduce common source stray inductances for multichip power modules, but they cannot totally decouple the gate-source loop and the drain-source loop, because they are still in the loop of drain currents, moreover, auxiliary-source connections are able to mitigate the transient MOSFETs current imbalances.[284] In any case, whether a Kelvin connection is or is not used, it is necessary to design the discrete device or the power module considering the parasitic phenomenon of inductances. Nevertheless, this aspect is already being optimized to a great extent with each new power module or discrete semiconductor solution that is launched on the market.

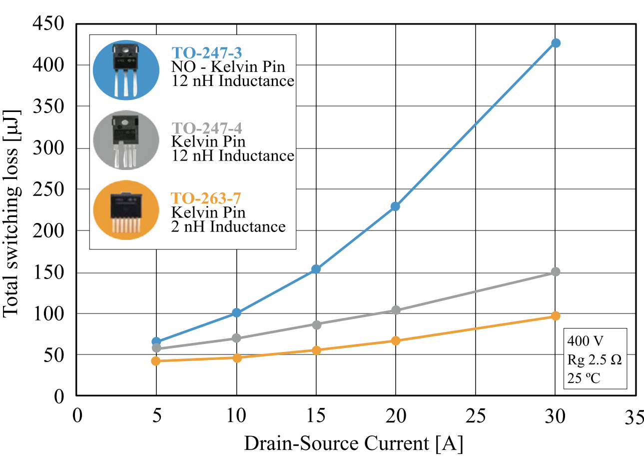

FIGURE 22 Kelvin connection switching loss comparison for TO-247-3, TO-247-4, and TO-263-7 packages[286]

5.2 | Common-mode voltage issue

Another major reliability issue with electric vehicle propulsion systems is the Common-Mode Voltage (CMV) issue.[83,84] Specifically, the switching of semiconductor devices produces common-mode voltage patterns that create several problems for both the inverter and the entire propulsion system. Figure 23 represents these problems in a simplified way. Among them, the main ones are the bearing currents, the deterioration of the stator winding insulation, and both the radiated and the

1099114x, 2022, 15, Downloaded from https://onlinelibrary.wiley.com/doi/10.1002/er.8581 by Universidad Del Pais Vasco, Wiley Online Library on [17/01/2023]. See the Terms and Conditions (https://onlinelibrary.wiley.com/terms-and-conditions) on Wiley Online Library for rules of use; OA articles are governed by the applicable Creative Commons License

FIGURE 23 Common-mode voltage problems exacerbated by switching due to the high slew rates and high frequencies with WBG devices

conducted EMI that are derived from this voltage pattern.[295-298] Increasing the switching frequency of discrete semiconductor devices and power modules, that is, migrating towards new semiconductor technologies such as SiC and *GaN*, will cause CMV problems to become more habitual.[84] The reason is because, if the frequency increases, then the number of variations increases accordingly. In addition, as discussed in Section 2.2, migrating battery systems to “800 V" systems and therefore using power modules with higher operating voltages (1200 V in the short term), also aggravates these waveforms, increasing the amplitude of the CMV variations.[83,114,299]

Typically, a large number of solutions have been proposed in the industry to minimize the undesirable effects arising from CMV, but mainly from the mechanical and electric motor point of view. Among these, ceramic bearings, isolated bearings, grounding straps, and shaft grounding rings have often been mentioned.[83] However, these types of solutions do not solve the problem from the origin, that is, from the point of view of semiconductor switching. Although at the device level there are few possible alternative solutions, in recent decades a large number of modulation techniques[83,297,300] and alternative topologies to the conventional inverter[82,301,302] have been investigated to reduce or to eliminate these reliability problems.

For example, multilevel converters improve the CMV-derived problems. However, to date, their use in electric vehicles has not been viable, mainly due to the high numbers of devices and their greater “complexity”. The semiconductor devices, due to the architecture of the multilevel converters, can block lower voltages more easily than a conventional two-level inverter.[303-305] This observation brings with it two potential benefits for using these converters in electric vehicles and for reducing CMV. The first is that they can facilitate the introduction of other types of semiconductors that block lower voltages, such as *GaN* HEMT, which could justify their use and increase several of the benefits of the propulsion system. The second is that conventional *Si* devices of approximately 600 V blocking voltage can also be used in newer “800 V" battery systems, which could allow for a smooth migration, rather than replacing all *Si* converters with WBG devices.[299]

On the other hand, as mentioned in Section 2.2, multiphase converters are a promising alternative in electric vehicles‡‡‡‡‡‡‡ as they increase power density and provide fault tolerance, an aspect that improves the reliability of the electric vehicle propulsion systems.[300,306] Specifically, the power system must be designed and dimensioned in a way that the Mean Time Between Failures (MTBF) is maximized.[1] However, as fault-free operation cannot be 100% guaranteed, fault tolerance can be

1099114x, 2022, 15, Downloaded from https://onlinelibrary.wiley.com/doi/10.1002/er.8581 by Universidad Del Pais Vasco, Wiley Online Library on [17/01/2023]. See the Terms and Conditions (https://onlinelibrary.wiley.com/terms-and-conditions) on Wiley Online Library for rules of use; OA articles are governed by the applicable Creative Commons License

considered crucial and, therefore, due to the additional degrees of freedom of multiphase topologies, various problems can be solved, in addition to the CMV.[296]

6 | CONCLUSIONS

The silicon IGBT has been the preferred choice among automotive manufacturers for the development of their inverters, (using both discrete devices and power modules) over past decades. The main reason is that it is a mature technology that offered adequate performance levels for the first generations of electric vehicle powertrains, facilitating switching at "high" frequencies (10-18 kHz) and withstanding high power levels (hundreds of amps and voltages within the range 600-1200 V). Over the years, IGBTs have passed through different stages of technological and structural development (Planar, Trench, PT, NPT, FS, etc.), which has made it possible to achieve higher power densities, operating temperatures, and efficiencies, as well as better reliability characteristics. The latest trends followed by manufacturers converge toward the same solution: to combine enhanced Trench cell technology with optimized vertical FS structure. These devices have over previous IGBT generations reduced switching losses to approximately 55% and the conduction voltage up to 35%, in addition to the innovation, in some cases, of new functionalities such as RB and RC. However, in the short term, these devices are not expected to provide the high performance levels required by automotive manufacturers and various international programs such as Horizon Europe, USCAR, DOE, and UN ESCAP, among others. In fact, in comparison with previous technologies, this performance requires improvements of between 30 and 50% in size, power density, thermal management, converter losses, costs, etc.

Considering the above, in recent years WBG devices have emerged as an alternative to *Si* IGBTs, principally due to the improved performance and great potential of these materials. Specifically, the *GaN* material has a high potential. However, the manufacture of *GaN* transistors for the propulsion system of electric vehicles has not, to date, reached the performance levels required by automotive manufacturers. The difficulty of developing semiconductors based on *GaN-on-GaN* technology has led to these semiconductors being manufactured as lateral devices, with reduced voltage (600-650 V) and current (10-60 A) ratings, and lower thermal conductivity. Besides, the development of normally-*on GaN* HEMT devices requires modifying the internal structure of these semiconductors, which deteriorates their initial performance. In addition, the analysis carried out shows that there are no commercial *GaN* devices intended for the electric drives for vehicles. Contrarily, SiC technology represents a real solution for electric vehicle drives, and a significant variety of relatively mature vertical devices can be found in the market. Among them, the MOSFET is the most suitable for this sort of application and is a potential rival that might one day replace *Si* IGBTs. The reduced power losses and higher operating temperatures stand out among their benefits. Likewise, the ability to block higher voltages (1200 V) makes them suitable for "800 V" battery systems. It can therefore be stated that *Si* and SiC technologies will continue in the short term to be part of electric vehicle power converters. In this sense, it is likely that the use of SiC technology will have expanded 15% in 2025.

In terms of the design aspects, there are several criteria that must be considered when choosing a discrete device or a power module (packages, insulation, stray inductances, cooling, connection terminals, etc.). In general, power modules have more advantages than discrete devices. In fact, practically all manufacturers have chosen the option of installing power modules within their vehicles. One of the main parameters that affects robustness is inductance. In this sense, parasitic inductance in power modules (≈10 *nH*) is observably lower than in discrete semiconductors (≈40 *nH* in the case of the TO-247). In addition, from the point of view of current ratings, the high current conductivity of power modules must be taken into account, resulting in high power density. Likewise, the enhanced thermal behavior of the modules, lower thermal resistance and impedance, and higher thermal mass are all favorable points. It must not be forgotten thatpower modules are also subject to heat spreading, which favors an even distribution of substrate temperature.

New interconnection techniques such as ribbon bond, flip-chip, and copper posts are also being used to improve power module reliability and, to take advantage of WBG technology, as well as new attach-solder joint techniques based on improved *Ag* sintering techniques and nanocopper materials. Likewise, one of the main goals of the substrate is to improve thermal conductivity (as well as to maximize the CTE mismatch), for which reason, the new developments are attempts to reduce the thickness of the conductive layers (lead-frame technology) and of the ceramics (technology thin-film insulation). In addition, new stack-up designs are also appearing such as overmold and double-sided DBC that no longer use wire bondings, making interconnections through copper areas and cooling the module on both sides. Moreover, IPM (which integrates the control circuits within the power

1099114x, 2022, 15, Downloaded from https://onlinelibrary.wiley.com/doi/10.1002/er.8581 by Universidad Del Pais Vasco, Wiley Online Library on [17/01/2023]. See the Terms and Conditions (https://onlinelibrary.wiley.com/terms-and-conditions) on Wiley Online Library for rules of use; OA articles are governed by the applicable Creative Commons License

module) and 3D structures (which combine substrates of various technologies within the same package) are also under development.

Finally, as far as reliability is concerned, the main failure mechanisms are produced in interconnections and the attach-joint layers, due to the electro-thermal behavior of the power modules. The technical aspects and consequences of parasitic elements must be considered, given the importance of operating at high frequency with WBG technology, thus achieving the long-term objectives of the electric vehicle. The new trends consist of switching at higher frequencies ($\simeq$100 kHz) and blocking higher voltages (1200 V) to reduce Joule effect losses, gradually increasing battery systems from "400 V" to "800 V". Some techniques for reducing the harmful effects of switching at high frequencies should therefore be used such as adding snubber capacitors, signal filtering (ferrite beads and RLC), active gate drivers, and Kelvin connections. In addition, new advances in the automotive inverter will bring with them multiphase converter topologies and specific modulation techniques to augment the reliability of electric vehicle propulsion systems, thereby increasing both power density and efficiency, as well as solving various CMV-related problems.

ACKNOWLEDGEMENTS

This work has been supported in part by the Government of the Basque Country through the fund for research groups of the Basque University System IT1440-22 and the Ministerio de Ciencia e Innovación of Spain as part of project PID2020-115126RB-I00 and FEDER funds. Finally, the collaboration of *Yole Développement* (Yole) is appreciated for providing updated data on its resources.

ORCID

Endika Robles https://orcid.org/0000-0003-4720-496X
Asier Matallana https://orcid.org/0000-0002-3588-4147
Iker Aretxabaleta https://orcid.org/0000-0001-5651-3786
Jon Andreu https://orcid.org/0000-0003-2367-5513
Markel Fernández https://orcid.org/0000-0002-7280-5196
José Luis Martín https://orcid.org/0000-0002-5738-6376

ENDNOTES

* Generally, the power converter is an inverter, although sometimes it also includes a DC/DC converter between the battery pack and the inverter (Figure 1).

† Alternatively, there are other semiconductor materials under investigation, such as gallium oxide (Ga_2O_3) and diamond (*D*), which could be part of the next generation of devices.[22-25] However, their technological development is at present immature, so it will be some time before they can be used in commercial power devices.

‡ Table 1 only provides some examples of commercial vehicles. It should be noted that there are probably more vehicle solutions under development that use SiC in their vehicles, however, it is not usual for vehicle manufacturers to share this type of data.

§ WBG-related improvements are mainly linked to the physical properties of these semiconductor materials.[31-35]

¶ This part of the device is also often referred to as cathode technology.

** The layers that are part of this area of the IGBT are also called anode technology.

†† Chapter 4 of[92] describes semiconductor fabrication processes using epitaxial and Float Zone techniques.

‡‡ The initial enhanced Trench FS developments implement the trench cells on the semiconductor surface following a square arrangement.

§§ Similar to FS technology, except that the epitaxial wafer material is removed and a positive temperature coefficient is provided that simplifies the parallelization.

¶¶ Many manufacturers offer this technology under different names: ABB builds the Bi-mode Insulated Gate Transistor (BIGT), Infineon has the variant for resonant RC IGBT and hard switching RC-D IGBT applications, and Mitsubishi uses the name RC IGBT to refer to this technology.

*** The current ratings provided by each manufacturer are a function of case temperature (T_c), typically measured in the ranges of 50°C to 120°C. Therefore, the power modules shown in the operating ranges of Figure 9 are not fully comparable. For specific information, each manufacturer's information should be reviewed.

††† The automotive-grade ensures the quality, performance, and safety of the product under stringent automotive operating conditions. As an example, the Automotive Electronics Council has developed the AEC Q101 (Stress Test Qualification for Discrete elements) standard, which establishes common part-qualification and quality-system standards for automotive power semiconductors in terms of life-cycle, operating temperature, humidity, and vibrations.

‡‡‡ Manufacturers often also offer 900 V modules, however, these voltages are sometimes not suitable for "800 V" vehicles.

§§§ Multiphase systems provide several advantages over three-phase configurations, such as improved fault tolerance, lower conduction losses, and smoother DC-bus and torque ripples.

¶¶¶ Furthermore, the 2DEG layer may be highlighted, because it is the conductive layer, which is placed between the *AlGaN* and *GaN* layers, within the internal structure of this lateral type of device on heterogeneous *GaN* substrates.[142,143]

**** There are other substrates to grow GaN devices, such as SiC and *sapphire*.[158]

†††† It is also expected that the *GaN* JBS diodes will improve the behaviour of power rectifiers within the range of 600 V to 3.3 kV.[177]

‡‡‡‡ Devices with BGA, DFN-8, GaNPX, PQFN56, PQFN88, and TO-247 packages have been taken into account, all of which were evaluated at 25°C.

§§§§ The values provided are indicative based on the data manufacturer. Sometimes a manufacturer groups its modules in the

1099114x, 2022, 15, Downloaded from https://onlinelibrary.wiley.com/doi/10.1002/er.8581 by Universidad Del País Vasco, Wiley Online Library on [17/01/2023]. See the Terms and Conditions (https://onlinelibrary.wiley.com/terms-and-conditions) on Wiley Online Library for rules of use; OA articles are governed by the applicable Creative Commons License

same current range but different temperatures are used (T_c), therefore these variations must be considered when selecting the module.

¶¶¶¶ Assuming conventional refrigeration, there is a temperature increment of 17°C within the top conductive layer, a 1 mm wide and 0.3 mm *thick* Al_2O_3 ceramic plate, when 100 A flow through it.[208]

***** The heat is also distributed horizontally over the surface of the substrate resulting in an homogeneous heat distribution.

††††† Generally, Al is used for the top surface of the die and Ni/Ag for the bottom surface.

‡‡‡‡‡ They are only used in designs of small-sized dies; large dies such as power semiconductors have mechanical stiffness problems.

§§§§§ There are also other variants such as Direct Bonded Aluminum (DBA) and Active Metal Brazing (AMB).[221,222]

¶¶¶¶¶ Reducing the number of parallel wires means that the semiconductor current must flow through a number of conducting wires, producing thermal peaks that affect the reliability of the junctions. Moreover, these thermal peaks slightly increase the partial stray inductance of the interconnection.

****** The life-cycle requirements of the automotive industry are around 10 to 15 years with no operational failures.[227,228]

†††††† Several copper poles, equal in height to the semiconductors, are inserted between the dies to connect to the upper DBC.

‡‡‡‡‡‡ Most capacitors and magnetic components show instability and loss of properties at high temperatures (>200°C).[206]

§§§§§§ Forced air cooling (Figure 18-①) stands out because of its simplicity and low implementation costs. However, the airflow generated to dissipate the heat is insufficient for electric vehicles. Although with the new SiC solutions, their theoretical high-temperature ranges and the heat flow dissipation capacity of their power devices begin to make certain developments viable.

¶¶¶¶¶¶ This technology operates at lower flow rates and pumping powers than traditional single-phase water/glycol systems.

******* The discrete devices present a vertical structure similar to the power modules. There are interconnections with wire-bonding (or equivalent technology), metallizations, a substrate and attach-solder joints.[258]

††††††† Likewise, these CTE differences can also negatively affect the package, and induce other problems such as thermo-mechanical creep, corrosion, and material migration.[79,273]

‡‡‡‡‡‡‡ As of today mainly heavy vehicles, such as buses and trucks, use these technologies.

REFERENCES

1. Matallana A, Ibarra E, Lápez I, Andreu J, Garate JI, Jord ÃX, Rebollo J. Power module electronics in HEV/EV applications: new trends in wide-bandgap semiconductor technologies and design aspects. *Renew Sustain Energy Rev*. 2019;113:1-33.
2. Yang Y, Dorn-Gomba L, Rodriguez R, Mak C, Emadi A. Automotive power module packaging: current status and future trends. *IEEE Access*. 2020;8:160126-160144.
3. Reimers J, Dorn-Gomba L, Mak C, Emadi A. Automotive traction inverters: current status and future trends. *IEEE Trans Vehicul Technol*. 2019;68:3337-3350.
4. *Status of the Power Electronics Industry Report* (Technical Report). France: Yole Developpment; 2020.
5. Iwamuro N, Laska T, History IGBT. State-of-the-art, and future prospects. *IEEE Trans Electron Devices*. 2017;64:741-752.
6. Jordá X, Flores D, Godignon P, Vellvehi M, Millan J. Present and future of IGBTs. *Mundo Electrónico*. 1999;42-47.
7. Laska T. Progress in Si IGBT technology—as an ongoing competition with WBG power devices. *International Electron Devices Meeting (IEDM)*, San Francisco, CA: IEEE; 2019:1-4.
8. Buitrago E, Schneider N, Vitale W, Gupta G, De-Michielis L. Rugged LV Trench IGBT with extreme stability in continuous SOA operation: next generation LV Technology at Hitachi ABB Powergrids. *International Exhibition and Conference for Power Electronics, Intelligent Motion, Renewable Energy and Energy Management*. VDE (Germany); 2021:1-7.
9. Wang H, Su M, Sheng K. Theoretical performance limit of the IGBT. *IEEE Trans Electron Devices*. 2017;64:4184-4192.
10. Hao X, Ma K, Jia Z. 7th Generation IGBT technology enables highest power density stack in solar application. *International Power Electronics and Motion Control Conference (ECCE)*, Nanjing, China: IEEE; 2020:2056-2060.
11. Saito K, Miyoshi T, Kawase D, Hayakawa S, Masuda T, Sasajima Y. Simplified model analysis of self-excited oscillation and its suppression in a high-voltage common package for Si-IGBT and SiC-MOS. *IEEE Trans Electron Devices*. 2018;65:1063-1071.
12. Wang H, Blaabjerg F. Power electronics reliability: state of the art and outlook. *IEEE Trans Emerg Sel Topics Power Electron*. 2021;9:6476-6493.
13. Gregorio M, Stella F, Bojoi R, Pagani F. Estimation of the internal junction temperatures of resin encapsulated IGBT power modules. *Energy Conversion Congress and Exposition (ECCE)*, Detroit, MI, USA: IEEE; 2020:3253-3260.
14. Tiwari AK, Udrea F, Lophitis N, Antoniou M. Operation of ultra-high voltage (>10kV) SiC IGBTs at elevated temperatures: benefits & constraints. *International Symposium on Power Semiconductor Devices and ICs (ISPSD)*, Shanghai, China: IEEE; 2019:175-178.
15. Tran QT, Niedernostheide F-J, Pfirsch F, Mauder A, Baburske R, Eckel H-G. RC-GID IGBT—a novel reverse-conducting IGBT with a gate voltage independent diode characteristic and low power losses. *International Symposium on Power Semiconductor Devices and ICs (ISPSD)*. Nagoya, Japan: IEEE; 2021:347-350.
16. Saito K, Mori M, Miyoshi T, Furukawa T, Watanabe S. Innovative silicon increases output power of inverters. *International Exhibition and Conference for Power Electronics, Intelligent Motion, Renewable Energy and Energy Management*. Online conference: VDE; 2021:1-7.
17. Liu G, Ding R, Luo H. Development of 8-inch key processes for insulated-gate bipolar transistor. *Engineering*. 2015;1:361-366.
18. Fuentes CD, Kouro S, Bernet S. Comparison of 1700-V SiC-MOSFET and Si-IGBT modules under identical test setup conditions. *IEEE Trans Ind Appl*. 2019;55:7765-7775.

1099114x, 2022, 15, Downloaded from https://onlinelibrary.wiley.com/doi/10.1002/er.8581 by Universidad Del Pais Vasco, Wiley Online Library on [17/01/2023]. See the Terms and Conditions (https://onlinelibrary.wiley.com/terms-and-conditions) on Wiley Online Library for rules of use; OA articles are governed by the applicable Creative Commons License

19. Ning P, Yuan T, Kang Y, Han C, Li L. Review of Si IGBT and SiC MOSFET based on hybrid switch. *Chin J Electr Eng*. 2019; 5:20-29.
20. Volke A, Hornjamp M. *IGBT Modules—Technologies, Driver and Application*. Munich: Infineon Technologies AG; 2012.
21. Barbarini E. *STMicroelectronics SiC Module* (Technical Report). France: Tesla Model 3 Inverter; 2018.
22. Ballestín-Fuertes J, Muñoz-Cruzado-Alba J, Sanz-Osorio J, Laporta-Puyal E. Role of wide bandgap materials in power electronics for smart grids applications. *Electronics*. 2021;10: 1-26.
23. Godignon P, Soler V, Cabello M, Montserrat J, Rebollo J, Knoll L, Bianda E, Mihaila A. New trends in high voltage MOSFET based on wide band gap materials. *Proceedings of the International Semiconductor Conference (CAS)*. Sinaia: IEEE; 2017:3-10.
24. Godignon P, Rius G, Cabello M, Soler V, Montserrat J. Gallium Oxide as the next semiconductor for power devices. *Actas del Seminario Anual de Automática, Electrónica Industrial e Instrumentación (SAAEI)*, Barcelona, Spain: SAAEI; 2018:1-6.
25. Chow TP, Omura I, Higashiwaki M, Kawarada H, Pala V. Smart power devices and ICs using GaAs and wide and extreme bandgap semiconductors. *IEEE Trans Electron Devices*. 2017;64:856-873.
26. *Status of the Power Module Packaging Industry Report* (Technical Report). France: Yole Developpement; 2020.
27. *Power SiC: Materials, Devices and Applications Report* (Technical Report). France: Yole Developpement; 2020.
28. Cai W, Wu X, Zhou M, Liang Y, Wang Y. Review and development of electric motor systems and electric powertrains for new energy vehicles, automotive. *Innovation*. 2021;4:3-22.
29. Lu M-C. Comparative study on power module architectures for modularity and scalability. *J Electron Packag*. 2020;142: 1-10.
30. Bertelshofer T, März A, Bakran M-M. Limits of SiC MOSFETs' parameter deviations for safe parallel operation. *Proceedings of the European Conference on Power Electronics and Applications (EPE'18 ECCE Europe)*, Riga, Latvia: IEEE; 2018:1-9.
31. Araujo S, Kazanbas M, Wendt M, Kleeb T, Zacharias P. Prospects of GaN devices in automotive electrification. *Proceedings of the International Exhibition and Conference for Power Electronics, Intelligent Motion, Renewable Energy and Energy Management (PCIM)*, Nuremberg, Germany: VDE; 2014:1-8.
32. Millan J, Godignon P, Perpina X, Perez-Tomas A, Rebollo J. A survey of wide bandgap power semiconductor devices. *IEEE Trans Power Electron*. 2014;29:2155-2163.
33. Balda JC, Mantooth A. Power-semiconductor devices and components for new power converter developments: a key enabler for ultrahigh efficiency power electronics. *IEEE Power Electron Mag*. 2016;3:53-56.
34. Shenai K. The figure of merit of a semiconductor power electronics switch. *IEEE Trans Electron Devices*. 2018;65:4216-4224.
35. Abdelrahman AS, Erdem Z, Attia Y, Youssef MZ. Wide bandgap devices in electric vehicle converters: a performance survey. *Can J Elect Comput Eng*. 2018;41:45-54.
36. P. E. Europe. *POWER GAN—Power GaN Can Revolutionize the Industrial World* (Technical Report). The European Journal for Power Electronics and Technology, Nuremberg, Germany: VDE; 2019.
37. Henn J, Lüdecke C, Laumen M, et al. Intelligent gate drivers for future power converters. *IEEE Trans Power Electron*. 2022; 37:3484-3503.
38. Kumar S, Usman A, Rajpurohit BS. Battery charging topology, infrastructure, and standards for electric vehicle applications: a comprehensive review. *IET Energy Syst Integration*. 2021;3: 381-396.
39. Cittanti D, Vico E, Bojoi IR. New FOM-based performance evaluation of 600/650 V SiC and GaN semiconductors for next-generation EV drives. *IEEE Access*. 2022;10:51693-51707.
40. Li K, Evans P, Johnson M. SiC/GaN power semiconductor devices: a theoretical comparison and experimental evaluation under different switching conditions. *IET Electri Syst Transport*. 2018;8:3-11.
41. Yadlapalli RT, Kotapati A, Kandipati R, Koritala CS. A review on energy efficient technologies for electric vehicle applications. *J Energy Storage*. 2022;50:104212.
42. Dai H, Torres RA, Jahns TM, Sarlioglu B. Analysis and suppression of conducted common-mode EMI in WBG-based current-source converter systems. *IEEE Trans Transport Electrific*. 2022;8:2133-2148.
43. Parvez M, Pereira AT, Ertugrul N, Weste NHE, Abbott D, Al-Sarawi SF. Wide bandgap DC–DC converter topologies for power applications. *Proc IEEE*. 2021;109:1253-1275.
44. Ansari SA, Davidson JN, Foster MP. Evaluation of silicon MOSFETs and GaN HEMTs in soft-switched and hard-switched DC-DC boost converters for domestic PV applications. *IET Power Electron*. 2021;14:1032-1043.
45. Zhang C, Wang J, Qu K, et al. WBG and Si hybrid half-bridge power processing toward optimal efficiency, power quality, and cost tradeoff. *IEEE Trans Power Electron*. 2022;37:6844-6856.
46. López I, Ibarra E, Matallana A, Andreu J, Kortabarria I. Next generation electric drives for HEV/EV propulsion systems: technology, trends and challenges. *Renew Sustain Energy Rev*. 2019;114:1-23.
47. Dong Z, Wu X, Sheng K. Suppressing methods of parasitic capacitance caused interference in a SiC MOSFET integrated power module. *IEEE Trans Emerg Sel Topics Power Electron*. 2019;7:745-752.
48. Dutta A, Ang SS. Electromagnetic interference simulations for wide-bandgap power electronic modules. *IEEE Trans Emerg Sel Topics Power Electron*. 2016;4:757-766.
49. Zare F, Kumar D, Lungeanu M, Andreas A. Electromagnetic interference issues of power, electronics systems with wide band gap, semiconductor devices. *Proceedings of the IEEE Energy Conversion Congress and Exposition (ECCE)*, Montreal, QC, Canada: IEEE; 2015:5946-5951.
50. Yuan X. Application of silicon carbide (SiC) power devices: Opportunities, challenges and potential solutions. *Proceedings of the IEEE Industrial Electronics Society Conference (IECON)*, Beijing, China: IEEE; 2017:893-900.
51. Shi Y, Zhang Y, Wang L, Li H. Reduction of EMI noise due to nonideal interleaving in a 100 kW SiC PV converter. *IEEE Trans Power Electron*. 2019;34:13-19.
52. Zhang Z, Wang F, Tolbert LM, Blalock BJ, Costinett D. Understanding the limitations and impact factors of wide

1099114x, 2022, 15, Downloaded from https://onlinelibrary.wiley.com/doi/10.1002/er.8581 by Universidad Del Pais Vasco, Wiley Online Library on [17/01/2023]. See the Terms and Conditions (https://onlinelibrary.wiley.com/terms-and-conditions) on Wiley Online Library for rules of use; OA articles are governed by the applicable Creative Commons License

bandgap devices' high switching-speed capability in a voltage source converter. *Proceedings of the IEEE Workshop on Wide Bandgap Power Devices and Applications (WiPDA)*, Knoxville, TN, USA: IEEE; 2014:7-12.
53. Aretxabaleta I, Martínez de Alegría I, Garate JI, Matallana A, Andreu J. Wide-bandgap semiconductor HF-oscillation attenuation method with tuned gate *RLC* filter. *IEEE Trans Power Electron*. 2020;35:8025-8033.
54. Wang JH, Chung S-H. Impact of parasitic elements on the spurious triggering pulse in synchronous buck converter. *IEEE Trans Power Electron*. 2014;29:6672-6685.
55. Ke J, Zhao Z, Zou Q, Peng J, Chen Z, Cui X. Device screening strategy for balancing short-circuit behavior of paralleling silicon carbide MOSFETs. *IEEE Trans Device Mater Reliab*. 2019; 19:757-765.
56. Zhang B, Wang S. A survey of EMI research in power electronics systems with wide-bandgap semiconductor devices. *IEEE Trans Emerg Sel Topics Power Electron*. 2020;8:626-643.
57. Chen J, Peng H, Cheng Z, et al. A novel power loop parasitic extraction approach for paralleled discrete SiC MOSFETs on multilayer PCB. *IEEE Trans Emerg Sel Topics Power Electron*. 2021;9:6370-6384.
58. Tiwari S, Basu S, Undeland TM, Midtgård O-M. Efficiency and conducted EMI evaluation of a single-phase power factor correction boost converter using state-of-the-art SiC Mosfet and SiC diode. *IEEE Trans Ind Appl*. 2019;55:7745-7756.
59. Qi Z, Pei Y, Wang L, Yang Q, Wang K. A highly integrated PCB embedded GaN full-bridge module with ultralow parasitic inductance. *IEEE Trans Power Electron*. 2022;37:4161-4173.
60. Alizadeh R, Alan Mantooth H. A review of architectural design and system compatibility of power modules and their impacts on power electronics systems. *IEEE Trans Power Electron*. 2021;36:11631-11646.
61. Li J, Liang Y, Mei Y, Tang X, Lu G-Q. Packaging design of 15 kV SiC power devices with high-voltage encapsulation. *IEEE Trans Dielectr Electr Insul*. 2022;29:47-53.
62. Zhou Y, Jin Y, Chen Y, Luo H, Li W, He X. Graph-model-based generative layout optimization for heterogeneous SiC multichip power modules with reduced and balanced parasitic inductance. *IEEE Trans Power Electron*. 2022;37:9298-9313.
63. Hu Z, Hu B, Ran L, et al. Monitoring power module solder degradation from heat dissipation in two opposite directions. *IEEE Trans Power Electron*. 2022;37:9754-9766.
64. Montazeri M, Huitink DR, Wallace A, et al. Vertically stacked, Flip-Chip wide bandgap MOSFET co-optimized for reliability and switching performance. *IEEE Trans Emerg Sel Topics Power Electron*. 2021;9:3904-3915.
65. Chen C, Huang Z, Chen L, Tan Y, Kang Y, Luo F. Flexible PCB-based 3-D integrated SiC half-bridge power module with three-sided cooling using ultralow inductive hybrid packaging structure. *IEEE Trans Power Electron*. 2019;34:5579-5593.
66. Li X-D, Lu G-Q, Mei Y-H. Reliable aluminum wire-bonded SiC/Si diodes with laminated Al/Cu stress buffers. *IEEE Trans Power Electron*. 2022;37:10149-10153.
67. Kawase T, Ishihara M, Miyamoto N, Hiyama K, Godo S. J1-Series Modules with Integrated Cooler for Electric and Hybrid Vehicles. *International Exhibition and Conference for Power Electronics, Intelligent Motion, Renewable Energy and Energy Management*, Nuremberg, Germany: VDE; 2017:1-4.
68. Ghannam A, van Haare N, Bravin J, Brandl E, Brandstatter B, Klingler H, Auer B, Meunier P, Kersjes S. Ultra-thin QFN-like 3D package with 3D integrated passive devices. *Electronic Components and Technology Conference (ECTC)*, Las Vegas, NV, USA: IEEE; 2019:1789-1795.
69. Mantooth HA, Ang SS. Packaging architectures for silicon carbide power electronic modules, in. *International Power Electronics Conference (IPEC-ECCE)*, Niigata, Japan: IEEE; 2018: 153-156.
70. Brinkfeldt K, Ottosson J, Otto A, Mann A, Zschieschang O, Frankeser S, Andersson D. Thermal simulations and experimental verification of power modules designed for double sided cooling, in. *Electronic Components and Technology Conference (ECTC)*, Las Vegas, NV, USA: IEEE; 2016:1415-1422.
71. Double side cooled module FF400R07A01E3 S6, technical report, *Inf Dent*, 2020.
72. Yang F, Liang Z, Wang ZJ, Wang F. Design of a low parasitic inductance SiC power module with double-sided cooling. *IEEE Applied Power Electronics Conference and Exposition (APEC)*, Tampa, FL, USA: IEEE; 2017:3057-3062.
73. Mouawad B, Espina J, Li J, Empringham L, Johnson CM. Novel Silicon Carbide Integrated Power Module for EV application. *Wide Bandgap Power Devices and Applications in Asia (WiPDA Asia)*, Xi'an, China: IEEE; 2018:176-180.
74. Dutta A, Ang SS. A module-level spring-interconnected stack power module. *IEEE Trans Compon Packag Manuf Technol*. 2019;9:88-95.
75. Tsukizawa M, Sasaki H, Lee J, Jeong J, Bae H. A new single in-line package of intelligent power modules for low power motor drive applications. *Conference on Electric Power and Energy Conversion Systems (EPECS)*, Kitakyushu, Japan: IEEE; 2018:1-4.
76. Ning P, Liu J, Wang D, Zhang Y, Li Y. Assessing the fatigue life of SiC power modules in different package structures. *IEEE Access*. 2021;9:12074-12082.
77. Zhang Y, Nee HP, Hammam T, Belov I, Ranstad P, Bakowski M. Multiphysics characterization of a novel SiC power module. *IEEE Trans Compon Packag Manuf Technol*. 2019;9:489-501.
78. Nguyen H, Kwak S. Enhance reliability of semiconductor devices in power converters. *Electronics*. 2020;9:2068.
79. Abuelnaga A, Narimani M, Bahman A. Power electronic converter reliability and prognosis review focusing on power switch module failures. *J Power Electron*. 2021;21:1-16.
80. Luo Y, Xiao F, Wang B, Liu B. Failure analysis of power electronic devices and their applications under extreme conditions. *Chin J Electr Eng*. 2016;2:91-100.
81. Wang B, Cai J, Du X, Zhou L. Review of power semiconductor device reliability for power converters. *CPSS Trans Power Electron Appl*. 2017;2:101-117.
82. Robles E, Fernandez M, Ibarra E, Andreu J, Kortabarria I. Mitigation of common mode voltage issues in electric vehicle drive systems by means of an alternative AC-decoupling power converter topology. *Energies*. 2019;12:1-27.
83. Robles E, Fernandez M, Andreu J, Ibarra E, Ugalde U. Advanced power inverter topologies and modulation techniques for common-mode voltage elimination in electric

1099114x, 2022, 15, Downloaded from https://onlinelibrary.wiley.com/doi/10.1002/er.8581 by Universidad Del Pais Vasco, Wiley Online Library on [17/01/2023]. See the Terms and Conditions (https://onlinelibrary.wiley.com/terms-and-conditions) on Wiley Online Library for rules of use; OA articles are governed by the applicable Creative Commons License

motor drive systems. *Renew Sustain Energy Rev*. 2021;140: 1-26.

84. Han Y, Lu H, Li Y, Chai J. Analysis and suppression of shaft voltage in sic-based inverter for electric vehicle applications. *IEEE Trans Power Electron*. 2019;34:6276-6285.
85. Matallana A. *Contributions to the Design of Power Modules for Electric and Hybrid Vehicles: Trends, Design Aspects and Simulation Techniques* (Ph.D. thesis). Basque Country: University of The Basque Country (UPV/EHU); 2020.
86. Rahimo M, Kopta A, Linder S. Novel Enhanced-Planar IGBT Technology Rated up to 6.5kV for Lower Losses and Higher SOA Capability. *Proceedings of the International Symposium on Power Semiconductor Devices and ICs (ISPSD)*, Naples, Italy, USA: IEEE; 2006:1-4.
87. Mori M, Oyama K, Arai T, et al. A planar-gate high-conductivity IGBT (HiGT) with hole-barrier layer. *IEEE Trans Electron Devices*. 2007;54:1515-1520.
88. Wu R, Wen J, Wu J, Chen Z, Peng C, Wang Y. Analysis of power losses in voltage source converter with new generation IGBTs. *Proceedings of the Computer Science and Automation Engineering (CSAE)*, Zhangjiajie, China: IEEE; 2012:674-678.
89. Selgi L, Fragapane L. Experimental evaluation of a 600 V super-junction planar PT IGBT prototype; Comparison with planar PT and trench gate PT technologies. *Proceedings of the European Conference on Power Electronics and Applications (EPE ECCE Europe)*, Lille, France: IEEE; 2013:1-7.
90. Motto E, Donlon J, Nakagawa T, Ishimura Y, Satoh K, Yamada J, Yamamoto M, Kusunoki S, Nakamura H, Nakamura K. A 1700 V LPT-CSTBT with low loss and high durability. *Proceedings of the Applied Power Electronics Conference (APEC)*, Dallas, TX, USA: IEEE; 2002:173-178.
91. Kang X, Lu L, Wang X, Santi E, Hudgins JL, Palmer PR, Donlon JF. Characterization and modeling of the LPT CSTBT-the 5th generation IGBT. *Proceedings of the Industry Applications (IAS)*, Salt Lake City, UT, USA: IEEE; 2003:982-987.
92. Lutz J, Schlangenotto H, Scheuermann U, Doncker RD. *Semiconductor Power Devices Physics, Characteristics, Reliability*. Germany: Springer; 2011.
93. *Application Note AN-983* (Technical Report). California, United States: International IR Rectifier; 2012.
94. *TRENCHSTOP™ 5: A Breakthrough in IGBT Innovation* (Technical Report). Germany: Infineon; 2020.
95. Chiola D, Hüsken H. *1200V HighSpeed 3 IGBT A New IGBT Family Optimized for High-Switching Speed* (Technical Report). Germany: Infineon; 2013.
96. Qian C, Gheitaghy AM, Fan J, et al. Thermal management on IGBT power electronic devices and modules. *IEEE Access*. 2018;6:12868-12884.
97. Jaeger C, Philippou A, VeIlei A, Laven JG, Härtl A. A new sub-micron trench cell concept in ultrathin wafer technology for next generation 1200 V IGBTs. *International Symposium on Power Semiconductor Devices and IC's (ISPSD)*, Sapporo, Japan: IEEE; 2017:69-72.
98. Imperiale I, Baburske R, Arnold T, et al. Opportunities and challenges of a 1200 V IGBT for 5 V gate voltage operation. *International Symposium on Power Semiconductor Devices and ICs (ISPSD)*, Vienna, Austria: IEEE; 2020:505-508.
99. Kamibaba R, Konishi K, Fukada Y, Narazaki A, Tarutani M. Next generation 650V CSTBT™ with improved SOA fabricated by an advanced thin wafer technology. *International Symposium on Power Semiconductor Devices & IC's (ISPSD)*, Hong Kong, China: IEEE; 2015:29-32.
100. Zhang J, Xiao X, Zhu R, Zhao Q, Zhang B. Low loss and Low EMI noise CSTBT with Split gate and recessed emitter trench. *IEEE J Electron Devices Soc*. 2021;9:704-712.
101. Sheikhian I, Kaminski N, VoB S, Scholz W, Herweg E. Optimisation of the reverse conducting IGBT for zero-voltage switching applications such as induction cookers. *IET Circuits Devices Syst*. 2014;8:176-181.
102. Lexow D, Tran QT, Eckel H-G. Comparison of reverse conducting IGBT concepts regarding reverse-recovery behavior and gate drive requirements. *European Conference on Power Electronics and Applications (EPE'21 ECCE Europe)*, Ghent, Belgium: IEEE; 2021:1-8.
103. Osawa A, Nakayama T, Ogawa E, et al. RC-IGBT power module for xEV powertrain with fast and accurate on-chip temperature sensor. *European Conference on Power Electronics and Applications (ECCE)*, Genova, Italy: IEEE; 2019:1-5.
104. Findlay EM, Udrea F. Reverse-conducting insulated gate bipolar transistor: a review of current technologies. *IEEE Trans Electron Devices*. 2019;66:219-231.
105. Mauder A, Laska T, Lorenz L. Dynamic behaviour and ruggedness of advanced fast switching IGBTs and diodes. *Proceedings of the Conference Record of the IEEE Industry Applications Society Annual Meeting (IAS)*, Salt Lake City, UT, USA: IEEE; 2003:995-999.
106. *AN2018-14: TRENCHSTO™ 1200 V IGBT7 Application Note* (Technical Report). Tokyo, Japan: Infineon; 2018.
107. *Introduction to Fuji Power Modules—Innovating Energy Technology* (Technical Report). Tokyo, Japan: Fuji Electric Co., Ltd.; 2016.
108. Kawabata J, Momose F, Onozawa Y. 7th-generation 'X series' IGBT module. *Fuji Elect Rev*. 2015;61:237-241.
109. Takahashi T, Yoshiura Y. *The 6th-Generation IGBT & Thin Wafer Diode for New Power Modules* (Technical Report). Germany: Mitsubishi Electric; 2011.
110. Miyazawa M, Radke T, Lakshmanan N. 7th generation 1700V IGBT modules: loss reduction and excellent system performance. *Bodo's Power Syst*. 2018;52-55.
111. *7th Generation IGBT Module T/T1-Series* (Technical Report). Tokyo, Japan: Mitsubishi Electric; 2018.
112. *PM and CM inverters* (Technical Report). Oregon, USA: Cascadia; 2021.
113. *BorgWarner power electronics solutions* (Technical Report). Michigan, USA: BorgWarner; 2021.
114. Jung C. Power up with 800-V systems: the benefits of upgrading voltage power for battery-electric passenger vehicles. *IEEE Electrific Mag*. 2017;5:53-58.
115. Fischer HM. *Voltage Casses for Electric Mobility* (Technical Report). Germany: ZVEI—German Electrical and Electronic Manufacturers Association; 2013.
116. Aretxabaleta I, Martínez De Alegía I, Andreu J, Kortabarria I, Robles E. High-voltage stations for electric vehicle fast-charging: trends, standards, charging modes and comparison of unity power-factor rectifiers. *IEEE Access*. 2021;9:102177-102194.
117. Meintz A, Zhang J, Vijayagopal R, et al. Enabling fast charging - vehicle considerations. *J Power Sources*. 2017;367: 216-227.

1099114x, 2022, 15, Downloaded from https://onlinelibrary.wiley.com/doi/10.1002/er.8581 by Universidad Del Pais Vasco, Wiley Online Library on [17/01/2023]. See the Terms and Conditions (https://onlinelibrary.wiley.com/terms-and-conditions) on Wiley Online Library for rules of use; OA articles are governed by the applicable Creative Commons License

118. Reber V. New possibilities with 800-volt charging. *Porsche Eng Mag*. 2020;1:10-15.
119. Engstle A, Deiml M, Angermaier A, Schelter W. 800 volt for electric vehicles voltage level suitable for calibration. *ATZ Worldwide*. 2013;115:38-43.
120. TRENCHSTOP™. *5 S5 Infineon's Low VCE(Sat) High-Speed Soft-Switching IGBT* (Technical Report). Germany: Infineon; 2015.
121. Volke A, Baessler M, Umbach F, Hille F, Rusche W, Hornkamp M. The new power semiconductor generation: 1200V IGBT4 and EmCon4 Diode. *India International Conference on Power Electronics*, Chennai, India: IEEE; 2006:77-82.
122. Wang J, Najmi V, Burgos R, Boroyevich D. Reliability-oriented IGBT selection for high power converters. *IEEE Applied Power Electronics Conference and Exposition (APEC)*, Charlotte, NC, USA: IEEE; 2015:2500-2503.
123. Yeon J, ul ain Akbar SQ. A reverse-conducting IGBT enabling high switching frequency up to 60 kHz for PFCs in home appliances. *European Conference on Power Electronics and Applications (ECCE)*, Ghent, Belgium: IEEE; 2021:1-9.
124. *Reverse Conducting RC-DA IGBT according to AEC-Q Standard High Intensity Discharge Lighting Applications (HID)* (Technical Report). Germany: Infineon; 2015.
125. *Sixth-Generation V-Series IGBT Module* (Technical Report). Tokyo, Japan: Fuji Electric Co., Ltd; 2011.
126. *Fuji 7th Generation IGBT Module X Series* (Technical Report). Tokyo, Japan: Fuji Electric Co., Ltd; 2018.
127. Kleingrothe L, Ebukuro Y, Yamano A, Kakefu M, Oda Y, Mitsuzuka K, Momota S, Itoh T, Okita S, Yoshiwatari S, Kobayashi Y. Expanding the output power of PrimePACK(TM) with RC-IGBT in industrial applications. *International Exhibition and Conference for Power Electronics, Intelligent Motion, Renewable Energy and Energy Management*, Online: VDE; 2021:1-7.
128. Yamano A, Takahashi M, Ichikawa H. 7th-generation "X series" RC-IGBT module for industrial applications. *Fuji Elect Rev*. 2017;62:241-245.
129. *The 5th Generation [CSTBT™] IGBT Chip use 12NF/24NF/24-A Series* (Technical Report). Tokyo, Japan: Mitsubishi Electric; 2014.
130. Majumbar G. Power Devices indispensable for Advancing Power Electronics—Keynote Presentation. *IEEE PEAC Plenary Session*; Hannover, Germany; 2018.
131. Chen W, Cheng J, Chen XB. A novel IGBT with high-k dielectric modulation achieving ultralow turn-off loss. *IEEE Trans Electron Devices*. 2020;67:1066-1070.
132. Soneda S, Nitta T, Narazaki A. 1200V RC-IGBT based on CSTBT™ with Suppressed Dynamic Cres and Partial Lifetime Control. *International Symposium on Power Semiconductor Devices and ICs (ISPSD)*, Vienna, Austria: IEEE; 2020:474-477.
133. Honda S, Minato T, Shimizu K, et al. Multidirectional development of IGBTs and diodes: low loss and tough but gentle (user-friendly) power devices. *IET Power Electron*. 2019;12:3882-3892.
134. Liu G, Li K, Wang Y, Luo H, Luo H. Recent advances and trend of HEV/EV-oriented power semiconductors—an overview. *IET Power Electron*. 2020;13:394-404.
135. Biela J, Schweizer M, Waffler S, Kolar J. SiC versus Si—evaluation of potentials for performance improvement of inverter and DC-DC converter systems by SiC power semiconductors. *IEEE Trans Ind Electron*. 2011;58:2872-2882.
136. Li H. *SiC technologies adoption is going to accelerate with a tipping point in 2019—Power SiC 2017: Materials, Devices, Modules, And Applications Report* (Technical Report). France: Yole Developpement; 2017.
137. She X, Huang AQ, Lucía O, Ozpineci B. Review of silicon carbide power devices and their applications. *IEEE Trans Ind Electron*. 2017;64:8193-8205.
138. Friedrichs P, Millán J, Harder T, Kaminski N, Lindemann A, Lorenz L, Schindele L, Ward P. *Next Generation Power Electronics based on Wide Bandgap Devices—Challenges and Opportunities for Europe (ECPE Position Paper)* (Technical Report). Nuremberg: ECPE; 2016.
139. Donato N, Rouger N, Pernot J, Longobardi G, Udrea F. Diamond power devices: state of the art, modelling, figures of merit and future perspective. *J Phys D Appl Phys*. 2019;53:93001.
140. Wort CJH, Balmer RS. Diamond as an electronic material. *Mater Today*. 2008;11:22-28.
141. Microsemi PPG. *Gallium Nitride (GaN) versus Silicon Carbide (SiC) In The High Frequency (RF) and Power Switching Applications* (Technical Report). California, USA: Microsemi; 2018.
142. Nie H, Diduck Q, Alvarez B, et al. 1.5-kV and 2.2-mΩ-cm^{2}Vertical GaN transistors on bulk-GaN substrates. *IEEE Electron Device Letters*. 2014;35:939-941.
143. Amano H, Baines Y, Beam E, et al. The GaN power electronics roadmap. *J Phys D Appl Phys*. 2018;51(2018):1-78.
144. Chen KJ, Haberlen O, Lidow A, et al. GaN-on-Si power technology: devices and applications. *IEEE Trans Electron Devices*. 2017;64:779-795.
145. Sheridan DC, Lee DY, Ritenour A, Bondarenko V, Yang J, Coleman C. Ultra-low loss 600V to 1200V GaN power transistors for high efficiency applications. *Proceedings of the International Exhibition and Conference for Power Electronics, Intelligent Motion, Renewable Energy and Energy Management (PCIM)*, Nuremberg, Germany: VDE; 2014:1-7.
146. Wei J, Zhang M, Lyu G, Chen KJ. GaN integrated bridge circuits on bulk silicon substrate: issues and proposed solution. *IEEE J Electron Devices Soc*. 2021;9:545-551.
147. Ryu S, Capell C, Jonas C, Cheng L, O'Loughlin M, Burk A, Agarwal A, Palmour J, Hefner A. Ultra high voltage (>12 kV), high performance 4H-SiC IGBTs. *Proceedings of the International Symposium on Power Semiconductor Devices and ICs (ISPSD)*, Bruges, Belgium: IEEE; 2012:257-260.
148. Soler V, Cabello M, Berthou M, et al. High-voltage 4H-SiC power MOSFETs with boron-doped gate oxide. *IEEE Trans Ind Electron*. 2017;64:8962-8970.
149. Pala V, Van Brunt E, Ryu SH, Hull B, Allen S, Palmour J, Hefner A. Physics of bipolar, unipolar and intermediate conduction modes in Silicon Carbide MOSFET body diodes. *Proceedings of the International Symposium on Power Semiconductor Devices and ICs (ISPSD)*, Prague, Czech Republic: IEEE; 2016:227-230.
150. Mirzaee H, De A, Tripathi A, Bhattacharya S. Design comparison of high-power medium-voltage converters based on a 6.5-kV Si-IGBT/Si-PiN diode, a 6.5-kV Si-IGBT/SiC-JBS diode, and a 10-kV SiC-MOSFET/SiC-JBS diode. *IEEE Trans Ind Appl*. 2014;50:2728-2740.

1099114x, 2022, 15, Downloaded from https://onlinelibrary.wiley.com/doi/10.1002/er.8581 by Universidad Del Pais Vasco, Wiley Online Library on [17/01/2023]. See the Terms and Conditions (https://onlinelibrary.wiley.com/terms-and-conditions) on Wiley Online Library for rules of use; OA articles are governed by the applicable Creative Commons License

151. *Effective Use of Power Devices—Silicon Carbide Power Devices Understanding and Application Examples Utlizing Merits* (Technical Report). Kyoto, Japan: ROHM Semiconductor; 2017.
152. *SiC Power Devices and Modules Application Note* (Technical Report). Kyoto, Japan: ROHM Semiconductor; 2020.
153. *SiC Power Devices* (Technical Report). Tokyo, Japan: Mitsubishi Electric; 2019.
154. Zhang L, Yuan X, Wu X, Shi C, Zhang J, Zhang Y. Performance evaluation of high-power SiC MOSFET modules in comparison to Si IGBT modules. *IEEE Trans Power Electron*. 2019;34:1181-1196.
155. Santi E, Peng K, Mantooth HA, Hudgins JL. Modeling of wide-bandgap power semiconductor devices - part II. *IEEE Trans Electron Devices*. 2015;62:434-442.
156. Kim HS, Han SW, Jang WH, et al. Normally-off GaN-on-Si MOSFET using PECVD SiON gate dielectric. *IEEE Electron Device Lett*. 2017;38:1090-1093.
157. Uemoto Y, Hikita M, Ueno H, Matsuo H, Ishida H, Yanagihara M, Ueda T, Tanaka T, Ueda D. A normally-off AlGaN/GaN power transistor using conductivity modulation. *IEEE Trans Electron Devices*. 2007;54:3393-3399.
158. He J, Cheng WC, Wang Q, Cheng K, Yu H, Chai Y. Recent advances in GaN-based power HEMT devices. *Adv Electron Mater*. 2021;7:1-24.
159. Roccaforte F, Greco G, Fiorenza P, Iucolano F. An overview of normally-off GaN-based high electron mobility transistors. *Materials*. 2019;12:1-18.
160. Meneghini M, Hilt O, Wuerfl J, Meneghesso G. Technology and reliability of normally-off GaN HEMTs with p-type gate. *Energies*. 2017;10:1-15.
161. Zheng Z, Song W, Zhang L, Yang S, Wei J, Chen KJ. High ion and ion/Ioff ratio enhancement-mode buried p-channel GaN MOSFETs on p-GaN gate power HEMT platform. *IEEE Electron Device Lett*. 2020;41:26-29.
162. Benakaprasad B, Eblabla AM, Li X, Crawford KG, Elgaid K. Optimization of Ohmic contact for AlGaN/GaN HEMT on Low-resistivity silicon. *IEEE Trans Electron Devices*. 2020;67:863-868.
163. Uesugi T, Kachi T. Which are the future GaN power devices for automotive applications, lateral structures or vertical structures? *Proceedings of the International Conference on Compound Semiconductor Manufacturing Technology (CS MANTECH)*, Mantech, United States; 2011:307-310.
164. Zanoni E, Meneghini M, Chini A, Marcon D, Meneghesso G. AlGaN/GaN-based HEMTs failure physics and reliability: mechanisms affecting gate edge and Schottky junction. *IEEE Trans Electron Devices*. 2013;60:3119-3131.
165. Shirabe K, Swamy MM, Kang JK, et al. Efficiency comparison between Si-IGBT-based drive and GaN-based drive. *IEEE Trans Ind Appl*. 2014;50:566-572.
166. Sun R, Lai J, Chen W, Zhang B. GaN power integration for high frequency and high efficiency power applications: a review. *IEEE Access*. 2020;8:15529-15542.
167. Su M, Chen C, Rajan S. Prospects for the application of GaN power devices in hybrid electric vehicle drive systems. *Semicond Sci Technol*. 2013;28:1-9.
168. Lidow A, Strydom J, Rooij MD, Reusch D. *GaN Transistors for Efficient Power Conversion*. 2nd ed., United States: Wiley; 2014.
169. Li H, Yao C, Fu L, Zhang X, Wang J. Evaluations and applications of GaN HEMTs for power electronics. *Proceedings of the International Power Electronics and Motion Control Conference (EPE/PEMC)*, Hefei: IEEE; 2016:563-569.
170. Jordá X, Perpina X, Vellvehi M, Sánchez D, García A, Ávila A. Analysis of Natural Convection Cooling Solutions for GaN HEMT Transistors. *Proceedings of the European Conference on Power Electronics and Applications (EPE ECCE Europe)*, Riga, Latvia: IEEE; 2018:1-9.
171. Okamoto N, Sato M, Nishimori M, Kumazaki Y, Ohki T, Hara N, Watanabe K. *Thermal Design of GaN-on-GaN HEMT Power Amplifier for a Selective Heating Microwave Oven*. United States: IEEE Transactions on Components, Packaging and Manufacturing Technology; 2021:1-9.
172. Han S, Yang S, Sheng K. High-voltage and high- ion/Ioff vertical GaN-on-GaN Schottky barrier diode with Nitridation-based termination. *IEEE Electron Device Lett*. 2018;39:572-575.
173. Chatterjee B, Ji D, Agarwal A, Chan SH, Chowdhury S, Choi S. Electro-thermal investigation of GaN vertical trench MOSFETs. *IEEE Electron Device Lett*. 2021;42:723-726.
174. Farzana E, Wang J, Monavarian M, et al. Over 1 kV vertical GaN-on-GaN p-n diodes with Low on-resistance using ammonia molecular beam epitaxy. *IEEE Electron Device Lett*. 2020;41:1806-1809.
175. Huang AQ. Power semiconductor devices for smart grid and renewable energy systems. *Proc IEEE*. 2017;105:2019-2047.
176. White RV. GaN: the challenges ahead [white hot]. *IEEE Power Electron Mag*. 2014;1:56-54.
177. Millán J. A review of WBG power semiconductor devices. *Proceedings of the International Semiconductor Conference (CAS)*, Sinaia, Romania: IEEE; 2012:57-66.
178. Fodorean D. Study of a high-speed motorization with improved performances dedicated for an electric vehicle. *IEEE Trans Magnet*. 2014;50:921-924.
179. Reusch D, Strydom J. Understanding the effect of PCB layout on circuit performance in a high-frequency gallium-nitride-based point of load converter. *IEEE Trans Power Electron*. 2014;29:2008-2015.
180. Wang K, Wang L, Yang X, Zeng X, Chen W, Li H. A multi-loop method for minimization of parasitic inductance in GaN-based high-frequency DC–DC converter. *IEEE Trans Power Electron*. 2017;32:4728-4740.
181. Aikawa K, Shiida T, Matsumoto R, Umetani K, Hiraki E. Measurement of the common source inductance of typical switching device packages. *Proceedings of the International Future Energy Electronics Conference and ECCE Asia (IFEEC - ECCE Asia)*, Kaohsiung, Taiwan: IEEE; 2017:1172-1177.
182. Letellier A, Dubois MR, Trovão JPF, Maher H. Calculation of printed circuit board power-loop stray inductance in GaN or high di/dt applications. *IEEE Trans Power Electron*. 2019;34:612-623.
183. Tong Z, Gu L, Ye Z, Surakitbovorn K, Rivas-Davila J. On the techniques to utilize sic power devices in high- and very high-frequency power converters. *IEEE Trans Power Electron*. 2019;34:12181-12192.
184. Wang Z, Wu Y, Mahmud MH, Yuan Z, Zhao Y, Mantooth HA. Busbar design and optimization for voltage overshoot mitigation of a silicon carbide high-power three-

1099114x, 2022, 15, Downloaded from https://onlinelibrary.wiley.com/doi/10.1002/er.8581 by Universidad Del Pais Vasco, Wiley Online Library on [17/01/2023]. See the Terms and Conditions (https://onlinelibrary.wiley.com/terms-and-conditions) on Wiley Online Library for rules of use; OA articles are governed by the applicable Creative Commons License

phase T-type inverter. *IEEE Trans Power Electron*. 2021;36: 204-214.
185. Lidow A, de Rooij M. *eGaN FET Electrical Characteristics: White Paper WP007* (Technical Report). California, United States: Efficient Power Conversion Corporation (EPC); 2012.
186. Strydom J, Reusch D, Colino S, Nakata A. *Using Enhancement Mode GaN-on-Silicon Power FETs (eGaN FETs): AN003* (Technical Report). California, United States: Efficient Power Conversion Corporation (EPC); 2017.
187. Anderson TJ, Chowdhury S, Aktas O, Bockowski M, Hite JK. GaN power devices—current status and future directions. *Electrochem Soc Inter*. 2018;27:43-47.
188. Roccaforte F, Fiorenza P, Greco G, et al. Emerging trends in wide band gap semiconductors SiC and GaN technology for power devices. *Microelectron Eng*. 2018;187-188:66-77.
189. Longobardi G, Efthymiou L, Arnold M. GaN power devices for Electric Vehicles State-of-the-art and future perspective. *Proceedings of the IEEE International Conference on Electrical Systems for Aircraft, Railway, Ship Propulsion and Road Vehicles International Transportation Electrification Conference (ESARS-ITEC)*, Nottingham, UK: IEEE; 2018:1-6.
190. Yadlapalli RT, Kotapati A, Kandipati R, Balusu SR, Koritala CS. Advancements in energy efficient Gan power devices and power modules for electric vehicle applications: a review. *Int J Energy Res*. 2021;45:12638-12664.
191. *GS-EVx-3PH-650V300A-SM1 650V 300A 3-Phase GaN Power Module External Driver Board Evaluation Kit Technical Manual* (Technical Report). Ontario, Canada: GaN Systems; 2021.
192. White C. *Hitachi Suijin Series of Power Modules for Electric Vehicles* (Technical Report). Boise, United States: EEPOWER, 2018. https://eepower.com/technical-articles/hitachi-suijin-series-of-power-modules-for-electric-vehicles/
193. *Datasheet—HybridPAC™ Drive Module FS820R08A6P2B* (Technical Report). Neubiberg, Germany: Infineon; 2019.
194. *APTMC120TAM12CTPAG Rev0 Datasheet* (Technical Report). California, United States: Microsemi; 2014.
195. *J1-Series for Automotive Applications—New Lightweight Compact Power Modules for xEV InvertersEnhancing Efficiency and Reliability* (Technical Report). Tokyo, Japan: Mitsubishii Electric; 2021.
196. *Datasheet—SKiM459GD12E4* (Technical Report). Nuremberg, Germany: Semikron; 2017.
197. *CAB011M12FM3 Datasheet—1200 V, 11 mΩ All-Silicon Carbide Half-Bridge Module* (Technical Report). North Carolina, United States: Wolfspeed; 2021.
198. *AB450M12XM3 Datasheet—1200V, 450A All-Silicon Carbide Conduction Optimized, Half-Bridge Module* (Technical Report). North Carolina, United States: Wolfspeed; 2019.
199. *CAB760M12HM3 Datasheet—1200 V, 760 A All-Silicon Carbide High Performance, Switching Optimized, Half-Bridge Module* (Technical Report). North Carolina, United States: Wolfspeed; 2020.
200. *Datasheet—Double Side Cooled Module FF450R08A03P2* (Technical Report). Neubiberg, Germany: Infineon; 2020.
201. *APTGTQ200A65T3G Datasheet—Microsemi SP3F Module* (Technical Report). Arizona, United States: Microchip; 2020.
202. *Public Relations Division No. 2902—Mitsubishi Electric to Release Sample J-Series T-PM Extra Compact Type* (Technical Report). Tokyo, Japan: Mitsubishi Electric Corporation, 2015. https://www.mitsubishielectric.com/news/2015/pdf/0212-c.pdf
203. Note A. *SiC Power Devices and Modules—Rev.003* (Technical Report). Kyoto, Japan: ROHM; 2020.
204. *SKM200GB12T4SiC2 Datasheet—Semikron Semitrans 3* (Technical Report). Nuremberg, Germany: Semikron; 2008.
205. Consulting SP. *Tesla Model 3 Inverter with SiC Power Module from STMicroelectronics* (Technical Report). Geneva, Switzerland: STMicroelectronics; 2018.
206. Lee H, Smet V, Tummala R. A review of sic power module packaging technologies: challenges, advances, and emerging issues. *IEEE Trans Emerg Sel Topics Power Electron*. 2020;8: 239-255.
207. Yang F, Wang Z, Liang Z, Wang F. Electrical performance advancement in sic power module package design with kelvin drain connection and low parasitic inductance. *IEEE Trans Emerg Sel Topics Power Electron*. 2019;7:84-98.
208. Schulz-Harder J. Advantages and new development of direct bonded copper substrates. *Microelectron Reliab*. 2003;43: 359-365.
209. Aranzabal I, de Alegría IM, Delmonte N, Cova P, Kortabarria I. Comparison of the heat transfer capabilities of conventional single- and two-phase cooling systems for an electric vehicle igbt power module. *IEEE Trans Power Electron*. 2019;34:4185-4194.
210. Karami M, Li T, Tallam R, Cuzner R. Thermal characterization of sic modules for variable frequency drives. *IEEE Open J Power Electron*. 2021;2:336-345.
211. Jung CC, Silber C, Scheible J. Heat generation in bond wires. *IEEE Trans Compon Packag Manuf Technol*. 2015;5:1465-1476.
212. Fabian B, Thomas S, Kalajica M, Hinrich A, Wolf A, Gunst S. Simulation and verification of a lifetime model based on front side metal degradation of sintered die top systems (DTS). *Power Cycling Tests*, Nuremberg, Germany; 2020:1-5.
213. Dietrich P. Trends in automotive power semiconductor packaging. *Microelectron Reliab*. 2013;53:1681-1686.
214. Navarro LA, Perpina X, Godignon P, et al. Thermomechanical assessment of die-attach materials for wide bandgap semiconductor devices and harsh environment applications. *IEEE Trans Power Electron*. 2014;29:2261-2271.
215. Guo X, Xun Q, Li Z, Du S. Silicon carbide converters and mems devices for high-temperature power electronics: a critical review. *Micromachines*. 2019;10:1-26.
216. Akbari M, Bahman A, Bina M, Eskandari B, Iannuzzo F, Blaabjerg F. A multi-layer rc thermal model for power modules adaptable to different operating conditions and aging. *Proceedings of the European Conference on Power Electronics and Applications (ECCE Europe)*, Riga, Latvia: IEEE; 2018:1-10.
217. Palmer MJ, Johnson RW, Autry T, Aguirre R, Lee V, Scofield JD. Silicon carbide power modules for high-temperature applications. *IEEE Trans Compon Packag Manuf Technol*. 2012;2:208-216.
218. Yan H, Liang P, Mei Y, Feng Z. Brief review of silver sinter-bonding processing for packaging high-temperature power devices. *Chin J Electr Eng*. 2020;6:25-34.
219. Zhao Y, Mumby-Croft P, Jones S, Dai A, Dou Z, Wang Y, Qin F. Silver sintering die attach process for igbt power module production. *Proceedings of the IEEE Applied Power Electronics*

1099114x, 2022, 15, Downloaded from https://onlinelibrary.wiley.com/doi/10.1002/er.8581 by Universidad Del Pais Vasco, Wiley Online Library on [17/01/2023]. See the Terms and Conditions (https://onlinelibrary.wiley.com/terms-and-conditions) on Wiley Online Library for rules of use; OA articles are governed by the applicable Creative Commons License

Conference and Exposition (APEC), Tampa, FL, USA: IEEE; 2017:3091-3094.

220. An BN, Ishikawa D, Blank T, Wurst H, Demattio H, Leyrer B, Kolb J, Scherer T, Simon A, Weber M. A highly integrated copper sintered sic power module for fast switching operation. *Proceedings of the International Conference on Electronics Packaging and iMAPS All Asia Conference (ICEP-IAAC)*, Mie, Japan: IEEE; 2018:375-380.
221. Anton Miric PD. *Inorganic Substrates for Power Electronics Appliations* (Technical Report). Hanau, Germany: Heraeus Deutscland GmbH; 2015.
222. Terasaki N, Nagatomo Y, Nagase T, Kuromitsu Y. New power-module structures consisting of both cu and al bonded to aln substrates with an al base plate. *Proceedings of the International Conference on Integrated Power Electronics Systems (CIPS)*, Nuremberg, Germany: VDE; 2014:1-5.
223. Chen C, Luo F, Kang Y. A review of SiC power module packaging: layout, material system and integration. *CPSS Trans Power Electron Appl*. 2017;2:170-186.
224. Gurpinar E, Chowdhury S, Ozpineci B, Fan W. Graphite-embedded high-performance insulated metal substrate for wide-bandgap power modules. *IEEE Trans Power Electron*. 2021;36:114-128.
225. Tokuyama T, Mima A, Takagi Y, Matsushita A. Low-inductance double-sided cooling power module with branched lead frame terminals for ev traction inverter. *Proceedings of the IEEE Energy Conversion Congress and Exposition (ECCE)*, Detroit, MI, USA: IEEE; 2020:3987-3991.
226. Wai LC, Yamamoto K, Boon SLS, Yue TG. Power module on copper lead frame with novel sintering paste and snsb solder. *Proceedings of the IEEE Electronics Packaging Technology Conference (EPTC)*, Singapore: IEEE; 2020:302-306.
227. Soldati A, Pietrini G, Dalboni M, Concari C. Electric-vehicle power converters model-based design-for-reliability. *CPSS Trans Power Electron Appl*. 2018;3:102-110.
228. Matallana A, Robles E, Ibarra E, Andreu J, Delmonte N, Cova P. A methodology to determine reliability issues in automotive SiC power modules combining 1D and 3D thermal simulations under driving cycle profiles. *Microelectron Reliab*. 2019;102:1-9.
229. Reigosa PD, Wang H, Yang Y, Blaabjerg F. Prediction of bond wire fatigue of IGBTs in a PV inverter under a long-term operation. *IEEE Trans Power Electron*. 2016;31:7171-7182.
230. Passmore BS, Lostetter AB. A review of SiC power module packaging technologies: attaches, interconnections, and advanced heat transfer. *Proceedings of the International Workshop On Integrated Power Packaging (IWIPP)*, Delft, Netherlands: IEEE; 2017:1-5.
231. Seal S, Mantooth HA. High performance silicon carbide power packaging—past trends, present practices, and future directions. *Energies*. 2017;10:1-30.
232. Abramushkina E, Zhaksylyk A, Geury T, El Baghdadi M, Hegazy O. A thorough review of cooling concepts and thermal management techniques for automotive WBG inverters: topology, technology and integration level. *Energies*. 2021;14:1-21.
233. Aranzabal I. *Aportaciones a la mejora de los sistemas de refrigeración de los convertidores de potencia del vehículo eléctrico* (Ph.D. thesis). Bilbao, Spain: University of The Basque Country (UPV/EHU); 2019.
234. Zhang Z, Wang X, Yan Y. A review of the state-of-the-art in electronic cooling, e-prime - advances in electrical engineering. *Electron Energy*. 2021;1:100009.
235. Jinbum K, Noquil J A, Teik keng T, Chung-Lin W, Seung-Yong C. Multi-flip chip on lead frame overmolded ic package: a novel packaging design to achieve high performance and cost effective module package. *Proceedings of the Electronic Components and Technology (ECTC)*, Lake Buena Vista, FL, USA: IEEE; 2005:1819-1821.
236. Wang M, Mei Y, Liu W, et al. Reliability improvement of a double-sided igbt module by lowering stress gradient using molybdenum buffers. *IEEE Trans Emerg Sel Topics Power Electron*. 2019;7:1637-1648.
237. Wang H, Chang C, Liang Z, Wang J, Yi D, Yang D. Structure design and thermal simulation analysis of dbc substrate for high-power igbt module. *Proceedings of the International Conference on Electronic Packaging Technology (ICEPT)*, Guangzhou, China: IEEE; 2020:1-4.
238. Aranzabal I, Matallana A, Oñederra O, Martinez de Alegria I, Cabezuelo D. Status and advances in electric vehicle's power modules packaging technologies. *Proceedings of the International Exhibition and Conference for Power Electronics, Intelligent Motion, Renewable Energy and Energy Management (PCIM)*, Nuremberg, Germany: VDE; 2016:1-9.
239. Watson J, Castro G. A review of high-temperature electronics technology and applications. *J Mater Sci Mater Electron*. 2015;26:9226-9235.
240. Huang Z, Chen C, Xie Y, Yan Y, Kang Y, Luo F. A high-performance embedded SiC power module based on a DBC-stacked hybrid packaging structure. *IEEE Trans Emerg Sel Topics Power Electron*. 2020;8:351-366.
241. Jørgensen AB, Beczkowski S, Uhrenfeldt C, Petersen NH, Jorgensen S, Munk-Nielsen S. A fast-switching integrated full-bridge power module based on GaN eHEMT devices. *IEEE Trans Power Electron*. 2019;34:2494-2504.
242. Yang S, Zhou S, Zhou X, et al. Essential technologies on the direct cooling thermal management system for electric vehicles. *Int J Energy Res*. 2021;45:14436-14464.
243. Schulz-Harder J. Review on highly integrated solutions for power electronic devices. *Proceedings of the International Conference on Integrated Power Electronics Systems (CIPS)*, Nuremberg, Germany: VDE; 2008:1-7.
244. Kang SS, Aavid T. Advanced cooling for power electronics. *Proceedings of the Integrated Power Electronics Systems (CIPS)*, Nuremberg, Germany: IEEE; 2012:1-8.
245. Schulz-Harder J. Efficient cooling of power electronics. *Proceedings of the International Conference on Power Electronics Systems and Applications (PESA)*, Hong Kong, China: IEEE; 2009:1-4.
246. McPherson B, McGee B, Simco D, Olejniczak K, Passmore B. Direct liquid cooling of high performance silicon carbide (SiC) power modules. *IEEE International Workshop on Integrated Power Packaging (IWIPP)*, Delft, Netherlands: IEEE; 2017:1-5.
247. Hitachi T, Gohara H, Naganue F. Direct liguid cooling IGBT module for automotive applications. *Fuji Elect Rev*. 2012;57:55-59.
248. Liang Z, Li L. HybridPACK2—advanced cooling concept and package technology for Hybrid Electric Vehicles. *Proceedings*

1099114x, 2022, 15, Downloaded from https://onlinelibrary.wiley.com/doi/10.1002/er.8581 by Universidad Del Pais Vasco, Wiley Online Library on [17/01/2023]. See the Terms and Conditions (https://onlinelibrary.wiley.com/terms-and-conditions) on Wiley Online Library for rules of use; OA articles are governed by the applicable Creative Commons License

of the Vehicle Power and Propulsion Conference (VPPC), Harbin: IEEE; 2008:1-5.
249. Uhlemann A. Investigation on AlCu-clad base plates and a new by-pass cooler for pin fin power modules. *Proceedings of the Integrated Power Electronics Systems (CIPS)*, Nuremberg, Germany: VDE; 2014:1-4.
250. Marcinkowski J. Dual-sided cooling of power semiconductor modules. *Proceedings of the Power Electronics, Intelligent Motion Renewable Energy and Energy Management (PCIM)*, Nuremberg, Germany: VDE; 2014:1-7.
251. Burns R. Vertical integration power modules for double sided cooling applications using aluminum conductors and thick film dielectrics. *Proceedings of the Power Electronics, Intelligent Motion Renewable Energy and Energy Management (PCIM)*, Nuremberg, Germany: VDE; 2014:1-8.
252. Liu M, Coppola A, Alvi M, Anwar M. Comprehensive review and state of development of double-sided cooled package Technology for Automotive Power Modules. *IEEE Open J Power Electron*. 2022;3:271-289.
253. Bostanci H, van Ee D, Saarloos BA, Rini DP, Chow LC. Thermal management of power inverter modules at high fluxes via two-phase spray cooling. *IEEE Trans Compon Packag Manuf Technol*. 2012;2:1480-1485.
254. Rizvi MJ, Skuriat R, Tilford T, Bailey C, Johnson CM, Lu H. Modelling of jet-impingement cooling for power electronics. *Proce of the International Conference on Thermal, Mechanical and Multi-Physics Simulation and Experiments in Microelectronics and Microsystems (EuroSimE)*, Delft, Netherlands: IEEE; 2009:1-5.
255. Faulkner D, Khotan M, Shekarriz R. Practical design of a 1000 W/cm2 cooling system [high power electronics]. *Proceedings of the Semiconductor Thermal Measurement and Management Symposium (SEMI-THERM)*, San Jose, CA, USA: IEEE; 2003:223-230.
256. Laloya E, Lucía O, Sarnago H, Burdío JM. Heat Management in Power Converters: from state of the art to future ultrahigh efficiency systems. *IEEE Trans Power Electron*. 2016;31:7896-7908.
257. Nazar M, Ibrahim A, KHATIR Z, Degrenne N, Al Masry Z. Wire-bond contact degradation modeling for remaining useful lifetime prognosis of IGBT power modules. *Microelectron Reliab*. 2020;114:1-6
258. Kim D-H, Oh A-S, Park E-Y, Kim K-H, Jeon S-J, Bae H-C. Thermal and electrical reliability analysis of TO-247 for bonding method, substrate structure and heat dissipation bonding material. *Electronic Components and Technology Conference (ECTC)*, San Diego, CA, USA: IEEE; 2021:1950-1956.
259. Sugiura K, Iwashige T, Tsuruta K, et al. Reliability evaluation of SiC power module with sintered ag die attach and stress-relaxation structure. *IEEE Trans Compon Packag Manuf Technol*. 2019;9:609-615.
260. Luo D, Chen M, Lai W, Xia H, Li H, Yu K. A fault detection method for partial Chip failure in multichip IGBT modules based on turn-off delay time. *IEEE Trans Electron Devices*. 2022;69:3319-3327.
261. Hou F, Wang W, Cao L, et al. Review of packaging schemes for power module. *IEEE Trans Emerg Sel Topics Power Electron*. 2020;8:223-238.
262. Yang Y, Zhang P. A novel bond wire fault detection method for IGBT modules based on turn-on gate voltage overshoot. *IEEE Trans Power Electron*. 2021;36:7501-7512.
263. Brincker M, Pedersen KB, Kristensen PK, Popok VN. Comparative study of Al metallization degradation in power diodes under passive and active thermal cycling. *IEEE Trans Compon Packag Manuf Technol*. 2018;8:2073-2080.
264. Yu F, Cui J, Zhou Z, Fang K, Johnson RW, Hamilton MC. Reliability of ag sintering for power semiconductor die attach in high-temperature applications. *IEEE Trans Power Electron*. 2017;32:7083-7095.
265. Shenai K. High-density power conversion and wide-bandgap semiconductor power electronics switching devices. *Proc IEEE*. 2019;107:2308-2326.
266. Singh T, Chaudhary S, Khanna G. *Recent Advancements in Wide Band Semiconductors (SiC and GaN) Technology for Future Devices, Silicon*, Berlin, Germany: Springer;2021.
267. Ren N, Hu H, Lyu X, et al. Investigation on single pulse avalanche failure of SiC MOSFET and Si IGBT. *Solid-State Electron*. 2019;152:33-40.
268. Bai Z, Tang X, He Y, Yuan H, Song Q, Zhang Y. Improving avalanche robustness of SiC MOSFETs by optimizing three-region P-well doping profile. *Microelectron Reliab*. 2021;124:114332.
269. Zhang Y, Duan B, Yang Y. Simulation study on dynamic and static characteristics of novel SiC gate-controlled bipolar-field-effect composite transistor. *IEEE J Electron Devices Soc*. 2020; 8:1082-1088.
270. Zhang Z, Chen C, Suetake A, Hsieh M-c, Iwaki A, Suganuma K. Reliability of ag sinter-joining die attach under harsh thermal cycling and power cycling tests. *J Electron Mater*. 2021;50:6597-6606.
271. New Products. *mAgic PE338—Ag Sinter Paste for Stencil Printing* (Technical Report). Hanau, Germany: Heraeus Electronics; 2018
272. Lu M-C. Enhanced sintered silver for SiC wide bandgap power electronics integrated package module. *J Electron Packag*. 2019;141:1-14.
273. Zhou D, Haseeb ASMA, Andriyana A, et al. A parametric study of thermal stress and analysis of creep strain under thermal cyclic loading in a hybrid quad flat package. *IEEE Trans Compon Packag Manuf Technol*. 2021;11:435-443.
274. Mirone G, Sitta A, D'Arrigo G, Calabretta M. Material characterization and warpage modeling for power devices active metal brazed substrates. *IEEE Trans Device Mater Reliab*. 2019;19:537-542.
275. Mouawad B, Li J, Castellazzi A, Johnson CM. On the reliability of stacked metallized ceramic substrates under thermal cycling. *International Conference on Integrated Power Electronics Systems*, Stuttgart, Germany: VDE; 2018:1-6.
276. Liu B, Li W, Meng D, et al. Low-stray inductance optimized Design for Power Circuit of SiC-MOSFET-based inverter. *IEEE Access*. 2020;8:20749-20758.
277. Lu B, Pickert V, Hu J, et al. Determination of stray inductance of Low-inductive laminated planar multiport Busbars using vector synthesis method. *IEEE Trans Ind Electron*. 2020;67: 1337-1347.
278. Wolski K, Zdanowski M, Rabkowski J. High-frequency SiC-based inverters with input stages based on quasi-Z-source and

1099114x, 2022, 15, Downloaded from https://onlinelibrary.wiley.com/doi/10.1002/er.8581 by Universidad Del Pais Vasco, Wiley Online Library on [17/01/2023]. See the Terms and Conditions (https://onlinelibrary.wiley.com/terms-and-conditions) on Wiley Online Library for rules of use; OA articles are governed by the applicable Creative Commons License

boost topologies-experimental comparison. *IEEE Trans Power Electron*. 2019;34:9471-9478.
279. He N, Chen M, Wu J, Zhu N, Xu D. 20-kW zero-voltage-switching SiC-mosfet grid inverter with 300 kHz switching frequency. *IEEE Trans Power Electron*. 2019;34:5175-5190.
280. Jordán J, Esteve V, Sanchis-Kilders E, Dede EJ, Maset E, Ejea JB, Ferreres A. A comparative performance study of a 1200 v si and sic mosfet intrinsic diode on an induction heating inverter. *IEEE Trans Power Electron*. 2014;29:2550-2562.
281. Luo H, Iannuzzo F, Diaz Reigosa P, Blaabjerg F, Li W, He X. Modern IGBT gate driving methods for enhancing reliability of high-power converters – An overview. *Microelectron Reliab*. 2015;58:141-150.
282. Nayak P, Hatua K. Parasitic inductance and capacitance-assisted active gate driving technique to minimize switching loss of SiC MOSFET. *IEEE Trans Ind Electron*. 2017;64:8288-8298.
283. *TO-247 4pin Package* (Technical Report). Neubiberg, Germany: Infineon Technologies AG; 2013.
284. Li H, Munk-Nielsen S, Wang X, Beczkowski S, Jones SR, Dai X. Effects of auxiliary-source connections in multichip power module. *IEEE Trans Power Electron*. 2017;32:7816-7823.
285. Zhao C, Wang L, Zhang F. Effect of asymmetric layout and unequal junction temperature on current sharing of paralleled SiC MOSFETs with kelvin-source connection. *IEEE Trans Power Electron*. 2020;35:7392-7404.
286. *Design Considerations for Silicon Carbide Power* (Technical Report). Durham, North Carolina, United States: Wolfspeed; 2020.
287. Wang Z, Zhang Y, You S, Xiao H, Cheng M. An integrated power conversion system for electric traction and V2G operation in electric vehicles with a small film capacitor. *IEEE Trans Power Electron*. 2020;35:5066-5077.
288. Krishna Moorthy RS, Aberg B, Olimmah M, Yang L, Rahman D, Lemmon AN, Yu W, Husain I. Estimation, minimization, and validation of commutation loop inductance for a 135-kW SiC EV traction inverter. *IEEE Trans Emerg Sel Topics Power Electron*. 2020;8:286-297.
289. Gui H, Chen R, Zhang Z, et al. Methodology of low inductance busbar design for three-level converters. *IEEE Trans Emerg Sel Topics Power Electron*. 2021;9:3468-3478.
290. Wang K, Yang X, Wang L, Jain P. Instability analysis and oscillation suppression of enhancement-mode GaN devices in half-bridge circuits. *IEEE Trans Power Electron*. 2018;33:1585-1596.
291. Xue P, Maresca L, Riccio M, Breglio G, Irace A. Investigation on the self-sustained oscillation of Superjunction MOSFET intrinsic diode. *IEEE Trans Electron Devices*. 2019;66:605-612.
292. Hazra S, Madhusoodhanan S, Bhattacharya S, Moghaddam GK, Hatua K. Design considerations and performance evaluation of 1200 V, 100 a SiC MOSFET based converter for high power density application. *Proceedings of the IEEE Energy Conversion Congress and Exposition (ECCE)*, Denver, CO, USA: IEEE; 2013:4278-4285.
293. Zhao F, Li Y, Tang Q, Wang L. Analysis of oscillation in bridge structure based on GaN devices and ferrite bead suppression method. *Proceedings of the IEEE Energy Conversion Congress and Exposition (ECCE)*, Cincinnati, OH, USA: IEEE; 2017:391-398.
294. Dymond HCP, Wang J, Liu D, Dalton JJO, McNeill N, Pamunuwa D, Hollis SJ, Stark BH. A 6.7-GHz active gate driver for GaN FETs to combat overshoot, ringing, and EMI. *IEEE Trans Power Electron*. 2018;33:581-594.
295. Shen TZZ, Jiang D, Qu R. Dual-segment three-phase PMSM with dual inverters for leakage current and common-mode EMI reduction. *IEEE Trans Power Electron*. 2019;34:5606-5619.
296. Acosta-Cambranis F, Zaragoza J, Romeral L, Berbel N. Comparative analysis of SVM techniques for a five-phase VSI based on SiC devices. *Energies*. 2020;13:1-30.
297. Fernandez M, Sierra-Gonzalez A, Robles E, Kortabarria I, Ibarra E, Martin J. New modulation technique to mitigate common mode voltage effects in star-connected five-phase AC drives. *Energies*. 2020;13:1-19.
298. Yu B, Song W, Guo Y. A simplified and generalized SVPWM scheme for two-level multiphase inverters with common-mode voltage reduction. *IEEE Trans Ind Electron*. 2022;69:1378-1388.
299. Poorfakhraei A, Narimani M, Emadi A. A review of multilevel inverter topologies in electric vehicles: current status and future trends. *IEEE Open J Power Electron*. 2021;2:155-170.
300. Acosta-Cambranis F, Zaragoza J, Berbel N, Capella GJ, Romeral Martinez L. Common-mode voltage mitigation strategies using Sigma-Delta modulation in five-phase VSIs. *IEEE Trans Power Electron*. 2022;37:1.
301. Concari L, Barater D, Toscani A, et al. Assessment of efficiency and reliability of wide band-gap based H8 inverter in electric vehicle applications. *Energies*. 2019;12:1-17.
302. Jung W, Choo K, Kim J, Kim W, Won C. H7 inverter using zener diode with model predictive current control for common-mode voltage reduction in PMSM drive system. *Proceedings of the IEEE International Power Electronics and Application Conference and Exposition (PEAC)*, Shenzhen, China: IEEE; 2018:1-6.
303. Vijeh M, Rezanejad M, Samadaei E, Bertilsson K. A general review of multilevel inverters based on main submodules: structural point of view. *IEEE Trans Power Electron*. 2019;34:9479-9502.
304. Du S, Wu B, Zargari NR. Common-mode voltage elimination for variable-speed motor drive based on flying-capacitor modular multilevel converter. *IEEE Trans Power Electron*. 2018;33:5621-5628.
305. Robles E, Fernandez M, Zaragoza J, Aretxabaleta I, De Alegria IM, Andreu J. Common-mode voltage elimination in multilevel power inverter-based motor drive applications. *IEEE Access*. 2022;10:2117-2139.
306. Ye D, Li J, Chen J, Qu R, Xiao L. Study on steady-state errors for asymmetrical six-phase permanent magnet synchronous machine fault-tolerant predictive current control. *IEEE Trans Power Electron*. 2020;35:640-651.

How to cite this article: Robles E, Matallana A, Aretxabaleta I, Andreu J, Fernández M, Martín JL. The role of power device technology in the electric vehicle powertrain. *Int J Energy Res*. 2022;46(15): 22222-22265. doi:10.1002/er.8581

1099114x, 2022, 15, Downloaded from https://onlinelibrary.wiley.com/doi/10.1002/er.8581 by Universidad Del Pais Vasco, Wiley Online Library on [17/01/2023]. See the Terms and Conditions (https://onlinelibrary.wiley.com/terms-and-conditions) on Wiley Online Library for rules of use; OA articles are governed by the applicable Creative Commons License